ELECTROMAGNETIC WAVE SCATTERING BY MANY-SPHERE SYSTEMS WITH APPLICATION TO SIMULATION OF THREE-DIMENSIONAL BODIES

BY

ABDUL-KADIR M. HAMID

A thesis

Submitted to the Faculty of Graduate Studies
in Partial Fulfillment of the Requirements
for the Degree of

DOCTOR OF PHILOSOPHY

Department of Electrical and Computer Engineering
University of Manitoba
Winnipeg, Manitoba, Canada

ISBN 0-315-76774-X

ELECTROMAGNETIC WAVE SCATTERING BY MANY-SPHERE SYSTEMS WITH APPLICATION TO SIMULATION OF THREE-DIMENSIONAL BODIES

BY

ABDUL-KADIR M. HAMID

A thesis submitted to the Faculty of Graduate Studies of
the University of Manitoba in partial fulfillment of the requirements
of the degree of

DOCTOR OF PHILOSOPHY

TO MY PARENTS, MOHAMMAD AND MUNIRA HAMID

ABSTRACT

The problem of multiple scattering of a uniform electromagnetic plane wave incident on an arbitrary configuration of N dielectric spheres of different permittivities is formulated by expanding the incident, scattered, and transmitted fields in terms of an appropriate set of vector spherical wave functions. Three methods are employed to solve this problem: the first two methods are exact analytical while the third is an approximate analytical method. The exact analytical methods require the use of the translation addition theorem for the vector spherical wave functions in order to express the scattered fields by one sphere in terms of the coordinate systems of the other spheres for the application of the boundary conditions at the surface of the spheres. In the first method, the boundary conditions are satisfied simultaneously at the surface of each sphere. The total scattered field by each sphere is due to the incident field plus the scattered fields from the remaining N-1 spheres. The resulting system of linear equations is written in a matrix form and solved by matrix inversion for the unknown scattered field coefficients. In the second method, an iterative procedure is employed and the boundary conditions are satisfied independently for each order of scattered fields or iteration. The first order scattered field results from the excitation of each sphere by the incident field only, while the second order scattered field results from the excitation of each sphere by the sum of all first order scattered fields, and hence this process continues to infinity. The third method is approximate and based on the assumptions that the spheres radii are electrically small. The interaction fields (usually spherical waves) between the spheres are approximated for

larger electrical separation by plane waves of unknown magnitudes. The latter method is shown to be simpler and has computational advantages over the exact solutions, since it does not require computation of the series resulting from applying the vector spherical addition theorem. The agreement between the approximate and exact solutions is excellent for the presented numerical results of the backscattering and bistatic cross section patterns. The formulation is reduced to the special case of N perfectly conducting spheres, and the numerical results show a reduction in the normalized backscattering and bistatic cross sections for certain choices of permittivity relative to conducting arrays of spheres of same dimensions and separations. Results for the scattering by a conducting or dielectric spheroid are given by simulating these bodies with an appropriate system of spheres. Exact numerical results are also presented for arrays of dielectric coated conducting spheres.

ACKNOWLEDGEMENTS

I wish to express my sincere gratitude to Professors I. R. Ciric and M. Hamid for their advice, continuous encouragement and helpful discussion throughout the course of this research.

The author wishes to acknowledge the financial assistance of the Natural Science and Engineering Research Council of Canada and the Faculty of Graduate studies of the University of Manitoba, which made this research possible.

TABLE OF CONTENTS

LIST OF FIGURES

LIST OF TABLES

LIST OF PRINCIPAL SYMBOLS

j	$\sqrt{-1}$
$\overline{E}^i$	incident electric field
$\overline{H}^i$	incident magnetic field
$\overline{E}_p^s$	scattered electric field from the pth sphere
$\overline{H}_p^s$	scattered magnetic field from the pth sphere
$\overline{E}_p^t$	transmitted electric field into the pth sphere
$\overline{H}_p^t$	transmitted magnetic field into the pth sphere
e	base of the natural logarithm (2.71828...)
$e^{-j\omega t}$	time dependence
λ	wavelength
k	wave number
π	3.141592653
ε_n	Neumann's number (1 for $n=0$ and 2 for $n\geq 1$)
$j_n(x)$	spherical Bessel function of order n and argument x
$h_n(x)$	spherical Hankel function of order n and argument x
$P_n^m(x)$	associated Legendre function of order n and argument x
$\hat{n}_p$	outward unit vector normal to the surface of the pth sphere
$\hat{r}_p$	unit vector in the r direction
$\hat{\theta}_p$	unit vector in the θ direction
$\hat{\phi}_p$	unit vector in the ϕ direction
η	intrinsic impedance of free space

η_p	intrinsic impedance of the pth sphere
a_p	radius of the pth sphere
ε_r	relative permittivity of a dielectric sphere
d_{pq}	separation distance between the pth and qth sphere
(x_p, y_p, z_p)	Cartesian coordinate system of the pth sphere
(r_p, θ_p, ϕ_p)	spherical coordinate system of the pth sphere
A_{pE}^s	scattered field coefficients due to TM waves
A_{pM}^s	scattered field coefficients due to TE waves
A_{pE}^t	transmitted field coefficients due to TM waves
A_{pM}^t	transmitted field coefficients due to TE waves
$\overline{A}$	vector contains the scattered field coefficients
$\overline{L}$	vector whose elements represent the excitation to N spheres
T	square matrix represent the coupling between the spheres
A^{pq}	submatrices associated with the translation addition coefficients
σ	scattering cross section
$\delta(x)$	Dirac delta function
$\overline{k}$	incident propagation vector
$\overline{k_s}$	scattered propagation vector

CHAPTER 1

INTRODUCTION

The problem of multiple scattering of a uniform plane electromagnetic wave incident on an arbitrary configuration of N dielectric spheres or a mixture of conducting and dielectric spheres is considered. The investigation is carried out on this specific shape since the sphere is a three dimensional body with a simple geometry for which an exact solution is available.

The scattering by an arbitrary configuration of spheres has numerous applications ranging from the propagation of electromagnetic waves through rain or hail, modeling of complex bodies by a collection of spheres, as shown in Figs. 1-1 and 1-2, such as cylinders capped with half spheres, finite cones, spheroids, scanning of buried objects to the simulation of human or animal bodies by using inhomogeneous dielectric spheres. A novel application is that of loading the aperture of an antenna by a linear array of dielectric spheres (Fig. 1-3) to enhance the gain along preferred directions.

Early investigations of the scattering by a single sphere by Mie led to the so called the Mie series solution [1]. For spheres with large radii (greater than three wavelenghts) the Mie series solution converges slowly. Therefore, to overcome this problem, an asymptotic solution was derived by the application of the Watson's transformation to the Mie series solution [2]. The scattered field is then expressed in terms of a sum of geometrical optics and creeping wave terms. For the case of small spheres ($ka \ll 1$) one can use the Rayleigh approximation, where only the first term in

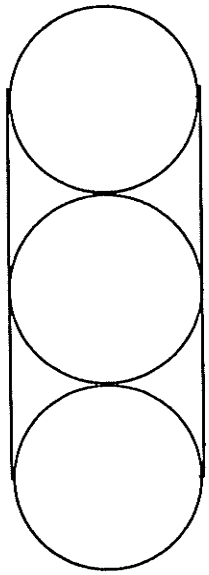

Cylinder capped with half spheres

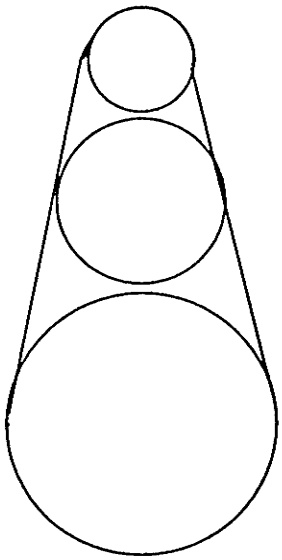

Finite cone

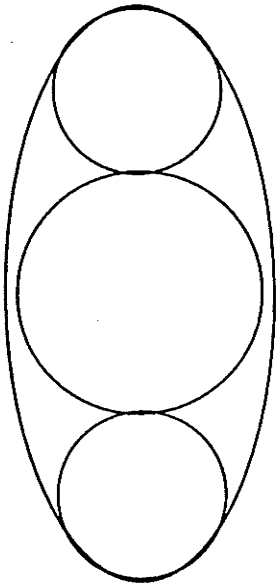

Spheroid

Fig.1-1 Simulation of complex bodies.

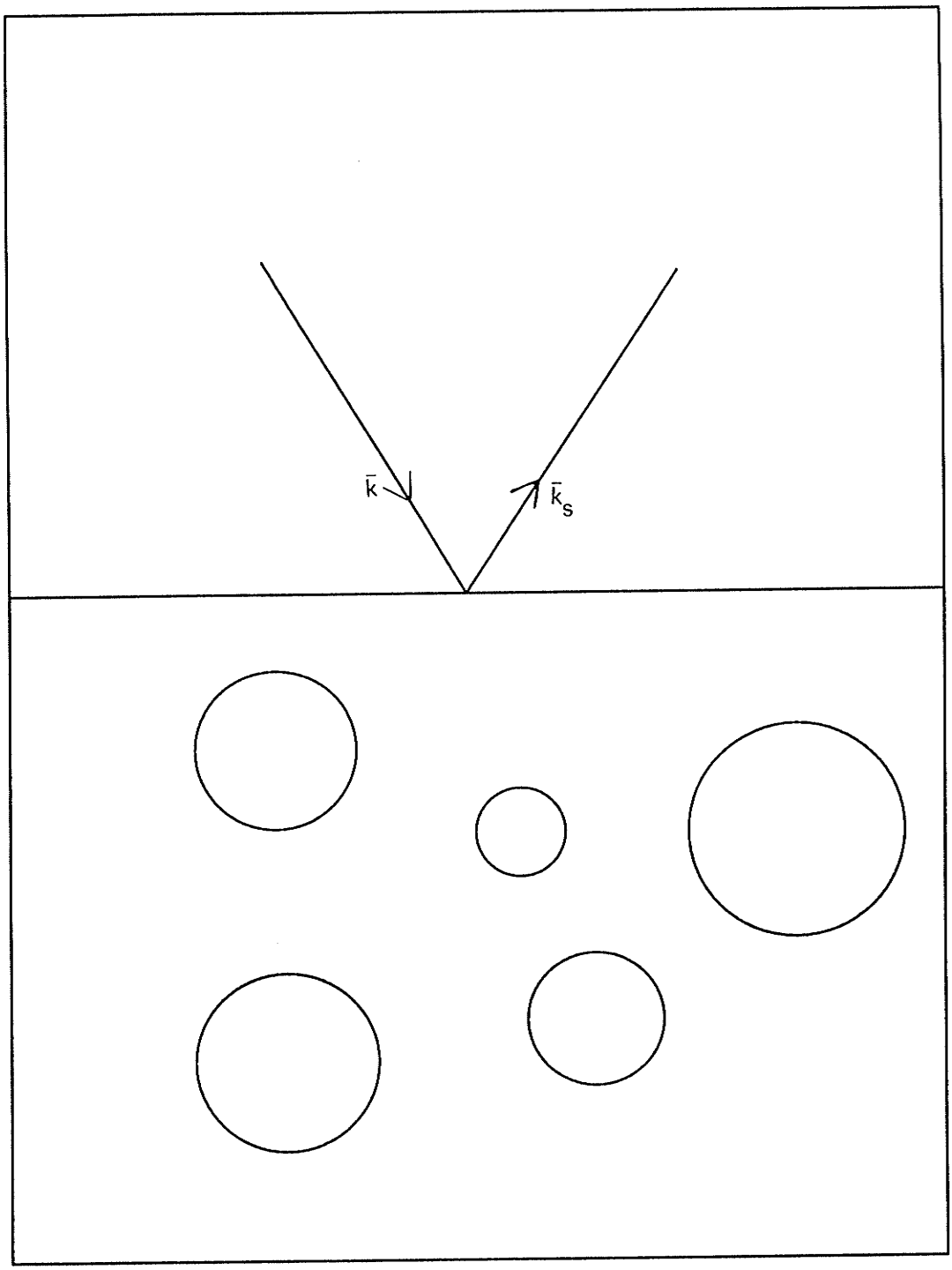

Fig.1-2 Plane wave incident on a half space of densely packed spheres.

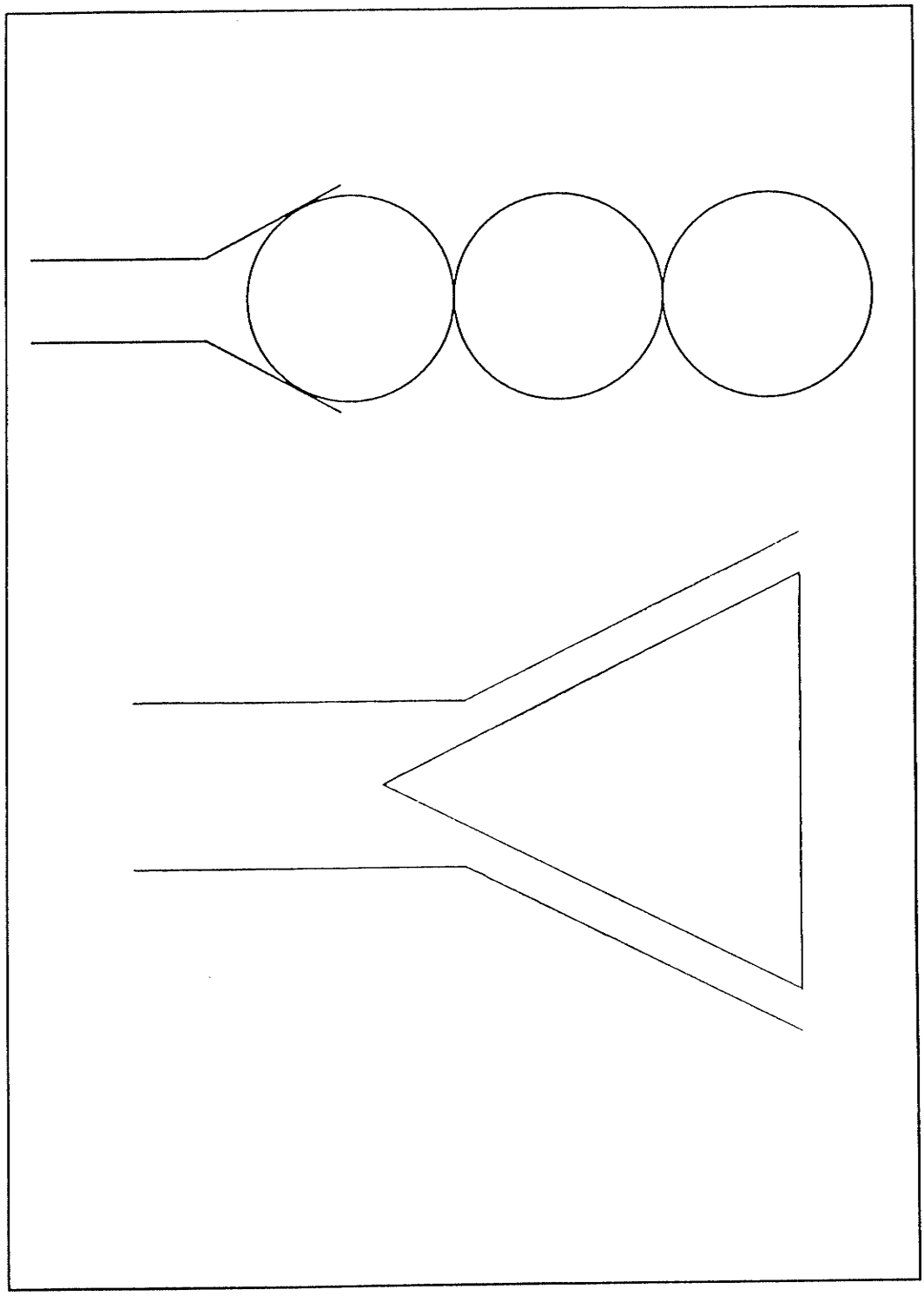

Fig.1-3 Aperture antennas loaded with dielectric spheres.

the series is retained.

Investigations on two-dimensional bodies such as the scattering by two circular cylinders [3] or diffraction by two wedges [4], as well as the scattering by N parallel cylinders [5-6], were carried out extensively. For systems of parallel cylinders two analytic approaches have been used, both requiring the application of the scalar addition theorem for cylindrical functions [7] to impose the boundary conditions on the surface of each body.

The first approach considers the total scattered field from each scatterer is due to incident (primary) field plus scattered (secondary) fields from the remaining scatterers [8-9]. Application of the boundary condition on the surface of each scatterer leads to a system of linear equations for the unknown scattered field coefficients. The system of equations is then solved by direct matrix inversion or by successive iterations. The second is an iterative scattering approach which requires an infinite order of scattered fields [10]. The first order of scattered field results from the excitation of each scatterer by only the incident field (single scattering). The second order scattered field is due to the excitation of each scatterer by the sum of all first order scattered fields from the remaining scatterers, and so on to an infinite order of scattered fields. This approach does not require matrix inversion and therefore the scattered field coefficients are obtained after each iteration and used in the subsequent iteration until the solution converges.

For three-dimensional configurations, the first approach has been previously applied only to the scattering by two conducting or dielectric spheres [11-12]. Investigations regarding systems of an arbitrary number of conducting or dielectric spheres

randomly located were initiated within the frame of the present doctoral thesis [13-14].

Trinks [15] formulated long ago the problem of scattering from two identical spheres of small radii (Rayleigh approximation) and with broadside incidence. Later, Germogenova [16] extended the analysis to two unequal small spheres and an arbitrary angle of incidence. Zitron and Karp [17-18] studied the scattering by two- and three-dimensional (scalar case) bodies of arbitrary shape, while Twersky [19] used the dyadic Green's function formulation to study the multiple scattering of electromagnetic waves by an arbitrary configuration of scatterers. Angelakos and Kumagai [20] made use of geometrical optics to obtain the backscattering cross section of arrays of three identical spheres and compared their results with experimental values. On the other hand, Bhartia *et al* [21] applied the geometrical theory of diffraction to the scattering by two large spheres. Tsang and Kong [22] presented an approximate solution to the scattering of a plane wave obliquely incident on a half space of densely distributed spherical dielectric scatterers. Hunka and Mie [23] employed a modified unimoment technique to generate the system transfer matrix for the scattering by two arbitrarily oriented bodies of revolution. Numerical solutions based on the moment method were presented by Mautz and Harrington [24] to solve for the scattering by a conducting or dielectric body of revolution in terms of equivalent electric and magnetic current sheets over the surface of the body. Later, Kishk and Shafai [25] extended the analysis to the scattering by two bodies of revolution excited by a plane wave or infinitesimal electric dipole. Such numerical solutions require very large computer storage and hence limit the usefulness of these techniques. An analytic solution to the scattering by two spheres was obtained by

Liang and Lo [11] using the translational addition theorem for vector spherical wave functions given by Stein [26] and Cruzan [27]. The obtained system of equations was solved by successive iterations after neglecting the higher order scattered fields. Bruning and Lo [12] pursued the analysis to the scattering by two dielectric spheres and obtained more general numerical results for systems of two spheres. Analytical solutions to the scattering by systems of two spheroids were derived by Sinha and MacPhie [28] for parallel spheroids, and, more recently, by Cooray and Ciric [29] for spheroids of arbitrary orientation.

This thesis presents a general solution to the problem of scattering of a plane electromagnetic wave by an arbitrary configuration of N dielectric spheres using analytic and approximate solutions based on the multipole expansion method. Numerical results are computed and plotted for the normalized backscattering and bistatic cross section patterns for one and two-dimensional arrays of conducting or dielectric spheres.

In chapter 2 the multipole expansion method is used to express the incident, transmitted, and scattered fields in terms of the vector spherical wave functions of the first and third types, respectively. The general translation addition theorem for the vector spherical wave functions is employed to transform the outgoing scattered fields from one sphere in terms of incoming fields on the remaining spheres. This is followed by the application of the boundary conditions which require that the tangential electric and magnetic field components must be continuous at the surface of each sphere. Use of the orthogonality properties of the spherical wave functions leads to a system of linear equations. The system of equations is written in a matrix form and

solved by matrix inversion for the unknown scattered field coefficients.

The novel iterative solution is formulated in chapter 3. This technique requires the solution of the field scattered by each sphere, assumed to be alone in the incident field, and which acts as an incident field on the other spheres. Thus, the first order scattered field (first iteration) results from the excitation of each sphere by the incident field only. The second order scattered field results from the excitation of each sphere by the sum of all first order scattered fields from the remaining N-1 spheres. This process of iteration continues until the solution converges. In order to compute the higher order terms of scattered fields, the translation addition is employed. Coefficients for the various order scattered fields are obtained and written in a matrix form. One of the main advantages of using this iterative solution is to show the significance of the computed higher order scattered fields on the total scattered field patterns.

Once the scattered electric field coefficients are determined, expressions for the normalized backscattering and bistatic cross sections are obtained in chapter 4 for both methods after employing the asymptotic values of the vector spherical wave functions. In addition, we compare the numerical results of both methods, and show the effect of the number, size and location of spheres on the numerical results.

The approximate method is derived in chapter 5 for small and non contacting spheres. The total scattered field by each sphere is due to the incident field plus the scattered fields from the remaining N-1 spheres which are approximated by plane waves of unknown magnitudes. The purpose of presenting the approximate solution is to show that such a solution reduces computational time and computer storage

since it does not require computation of the series resulting from applying the addition theorem. Finally, the formulation is extended to the scattering by dielectric coated conducting spheres in chapter 6 to show the effect of the coating on the back-scattering cross section, while the discussion and outline of future research are given in chapter 7.

CHAPTER 2

SCATTERING OF ELECTROMAGNETIC WAVES BY AN ARBITRARY CONFIGURATION OF CONDUCTING OR DIELECTRIC SPHERES

The scattering by an arbitrary configuration of N dielectric spheres is formulated in this chapter using the modal expansion method. For example, the solution can be used to simulate human bodies using inhomogeneous dielectric spheres to treat various diseases, and for the simulation of dielectric complex bodies. As already mentioned, a novel engineering application is that of loading the aperture of an antenna by dielectric spheres to enhance the gain along preferred directions. To support this, experimental results to improve the gain of antennas loaded with a single dielectric sphere have been reported [30-31].

To date, there are no analytical, approximate or purely numerical solutions available in the literature for the scattering by more than two dielectric spheres due to the complexity of computing the coefficients of the translation addition theorem. Therefore, the goal of this chapter is to present analytic solution for the scattering by N dielectric spheres [32-33], since purely numerical techniques require very large computer storage and hence tend to limit the usefulness of these techniques.

Early studies of the problem of a plane electromagnetic wave scattering by an imperfectly conducting, dielectric, or plasma sphere were given by King and Harrison [34]. Later, tabulated results for the backscattering cross section of a conducting or dielectric sphere were obtained by Adler and Johnson [35]. Analytical and experimental results to the scattering by two dielectric spheres were presented by [12], while numerical results were given by [25,36].

It is perhaps worthwhile to mention that the scattering by N two-dimensional bodies is a scalar problem and therefore can be solved independently for *TE* and *TM* waves [6]. On the other hand, the case of scattering by three-dimensional bodies is a vector problem and hence the *TE* and *TM* waves are coupled regardless of whether the excitation is by *TE* or *TM* waves.

The multipole expansion method is employed to express the incident and transmitted fields in terms of the spherical wave functions of the first type $(\overline{M}_{mn}^{(1)}, \overline{N}_{mn}^{(1)})$ that are associated with the spherical Bessel function, so that the fields will be finite at the origin [37]. Then, the incident field expansion coefficients of the pth spheres (p=1,2,...,N) are obtained using the orthogonality properties of the vector spherical wave functions. Moreover, The scattered electric and magnetic fields are also expanded in terms of the vector spherical wave functions of the third type $(\overline{M}_{mn}^{(3)}, \overline{N}_{mn}^{(3)})$ that are associated with the spherical Hankel function to satisfy the radiation condition.

The general translation addition theorem is employed to transform the outgoing scattered fields from one sphere in terms of incoming fields on the remaining N-1 spheres [26-27]. Application of the boundary conditions require the tangential electric and magnetic field components must be continuous at $r = a_p$ (p=1,2,...,N). Using the orthogonality properties of the vector wave functions leads to a system of linear equations for the unknown scattered field coefficients. The system of linear equations is written in a matrix form and the desired scattered field coefficients are obtained by direct matrix inversion.

The special case of a linear array of N dielectric spheres is deduced by spacing

the spheres along the z-axis. This allows the azimuthal modes to decouple and therefore enables us to solve the system of equations for each mode independently. The scattered fields are then obtained by summing the required azimuthal modes.

Finally, the scattering by an arbitrary configuration of N perfectly conducting spheres is presented by letting the permittivity of each dielectric sphere become very high (theoretically infinite).

2.1 Expansion of the incident field

Consider a plane electromagnetic wave incident on an arbitrary configuration of dielectric spheres as shown in Fig. 2-1, where the radius of the pth sphere is a_p and the permittivity is ε_p (p=1,2,...,N). The spheres are centered at d_p with local cartesian coordinates (x_p, y_p, z_p). The separation distance between the centers of the pth and qth spheres is denoted by d_{pq}. The incident plane wave has a unit electric field intensity whose propagation vector $\bar{k}$ lies in the xz plane and makes an angle α with the positive z-axis. The incident electric field is considered to be in the $\hat{y}$ direction. The incident electric and magnetic fields are expressed by

$$\bar{E}^i = e^{j\bar{k}\cdot\bar{r}}\hat{y} \tag{2-1}$$

$$\bar{H}^i = -\frac{1}{\eta}e^{j\bar{k}\cdot\bar{r}}(\cos\alpha\hat{x} - \sin\alpha\hat{z}) \tag{2-2}$$

η is the intrinsic impedance of the surrounding medium. Considering the relationship $\bar{r} = \bar{d}_p + \bar{r}_p$, one can write

$$e^{j\bar{k}\cdot\bar{r}} = e^{j\bar{k}\cdot\bar{d}_p}\, e^{j\bar{k}\cdot\bar{r}_p} \tag{2-3}$$

Therefore, the incident plane wave is expressed with reference to the spherical coordinates of the pth sphere as

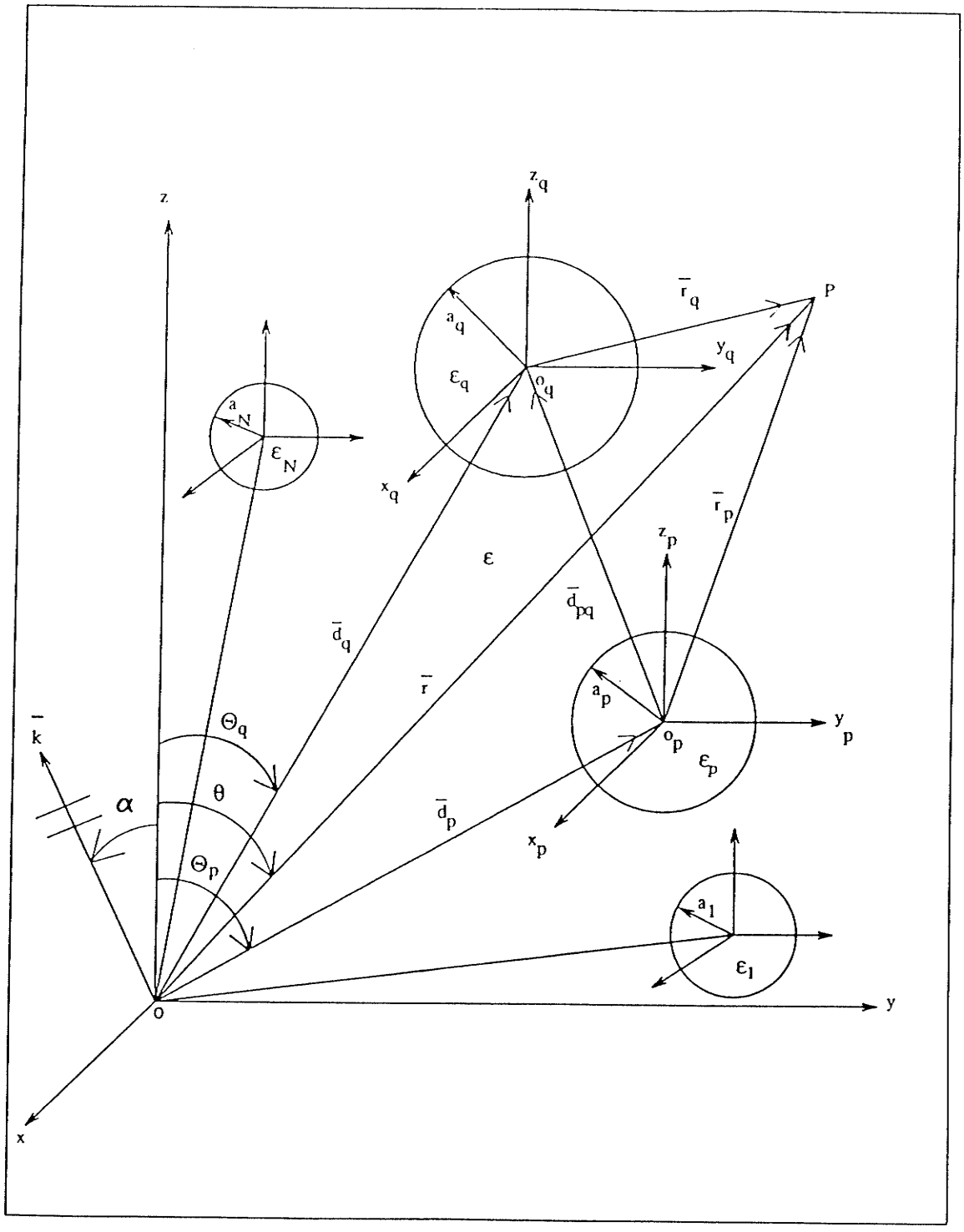

Fig.2-1. Arbitrary configuration of dielectric spheres.

$$e^{j\bar{k}\cdot(\bar{r}_p+\bar{d}_p)}=e^{jkd_p\zeta_i}\sum_{n=0}^{\infty}\sum_{m=-n}^{m=n}j^n(2n+1)\frac{(n-m)!}{(n+m)!}P_n^m(\cos\alpha)\,P_n^m(\cos\theta_p)\,j_n(kr_p)\,e^{jm\phi_p} \quad (2\text{-}4)$$

where j_n is the spherical Bessel function, P_n^m is the associated Legendre function of the first kind with order n and

$$\zeta_i=\sin\Theta_p\cos\Phi_p\sin\alpha+\cos\Theta_p\cos\alpha$$

For the special case of a linear array of N dielectric spheres spaced along the z-axis, as shown in Fig. 2-2, we have $\Theta_p=0$ (p=1,2,...,N).

Expanding the incident electric and magnetic fields in terms of the spherical vector wave functions of the first kind, with the $e^{-j\omega t}$ time dependence suppressed throughout, we obtain [38-39]

$$\bar{E}^i(r_p,\theta_p,\phi_p)=\sum_{n=1}^{\infty}\sum_{m=-n}^{m=n}[P_p(m,n)\bar{N}_{mn}^{(1)}(r_p,\theta_p,\phi_p)+Q_p(m,n)\bar{M}_{mn}^{(1)}(r_p,\theta_p,\phi_p)] \quad (2\text{-}5)$$

$$\eta\bar{H}^i(r_p,\theta_p,\phi_p)=j\sum_{n=1}^{\infty}\sum_{m=-n}^{m=n}[P_p(m,n)\bar{M}_{mn}^{(1)}(r_p,\theta_p,\phi_p)+Q_p(m,n)\bar{N}_{mn}^{(1)}(r_p,\theta_p,\phi_p)] \quad (2\text{-}6)$$

where p takes integer values from 1 to N, P_p and Q_p are the unknown field expansion coefficients, while $\bar{M}_{mn}^{(1)}$ and $\bar{N}_{mn}^{(1)}$ are the spherical vector wave functions of the first type which represent incoming waves and are given by

$$\bar{M}_{mn}^{(1)}(r_p,\theta_p,\phi_p)=\nabla\times[u_{mn}(r_p,\theta_p,\phi_p)\,\bar{r}_p] \quad (2\text{-}7)$$

$$\bar{N}_{mn}^{(1)}(r_p,\theta_p,\phi_p)=\frac{1}{k}\nabla\times\bar{M}_{mn}^{(1)}(r_p,\theta_p,\phi_p) \quad (2\text{-}8)$$

with

$$u_{mn}(r_p,\theta_p,\phi_p)=j_n(kr_p)\,P_n^m(\cos\theta_p)\,e^{jm\phi_p}\ , \qquad 0\le n\le\infty,\ -n\le m\le n$$

Taking the curl of equations (2-7) and (2-8), we obtain

$$\bar{M}_{mn}^{(1)}(r_p,\theta_p,\phi_p)=\hat{\theta}_p\,\{j_n(kr_p)\frac{jm}{\sin\theta_p}P_n^m(\cos\theta_p)e^{jm\phi_p}\}$$

$$-\hat{\phi}_p \{ j_n(kr_p) \frac{\partial}{\partial \theta_p} P_n^m(\cos\theta_p) e^{jm\phi_p} \} \qquad (2\text{-}9)$$

and

$$\begin{aligned} \overline{N}_{mn}^{(1)}(r_p,\theta_p,\phi_p) = \hat{r}_p \{ & \frac{1}{kr_p} j_n(kr_p)\, n(n+1) P_n^m(\cos\theta_p) e^{jm\phi_p} \} \\ & + \hat{\theta}_p \{ \frac{1}{kr_p} \frac{\partial}{\partial r_p} [r_p j_n(kr_p)] \frac{\partial}{\partial \theta_p} P_n^m(\cos\theta_p) e^{jm\phi_p} \} \\ & + \hat{\phi}_p \{ \frac{1}{kr_p} \frac{\partial}{\partial r_p} [r_p j_n(kr_p)] \frac{jm}{\sin\theta_p} P_n^m(\cos\theta_p) e^{jm\phi_p} \} \end{aligned} \qquad (2\text{-}10)$$

where it can be seen that the radial components are contained in $\overline{N}_{mn}^{(1)}$. Thus, for H waves (TE), $\overline{H}$ is represented by $\overline{N}_{mn}^{(1)}$ and $\overline{E}$ by $\overline{M}_{mn}^{(1)}$, while in the case of E waves (TM) the opposite is true. Using the orthogonality properties of the vector wave functions (Appendix A) in equations (2-5) and (2-6), we obtain the incident field expansion coefficients as

$$P_p(m,n) = -j^n e^{jkd_p\zeta_i} \frac{(2n+1)}{n(n+1)} \frac{(n-m)!}{(n+m)!} \frac{m}{\sin\alpha} P_n^m(\cos\alpha) \qquad (2\text{-}11)$$

$$Q_p(m,n) = -j^n e^{jkd_p\zeta_i} \frac{(2n+1)}{n(n+1)} \frac{(n-m)!}{(n+m)!} \frac{\partial}{\partial \alpha} P_n^m(\cos\alpha) \qquad (2\text{-}12)$$

while in the case of a linear array of spheres, equations (2-11) and (2-12) reduce to the following forms, *i.e.*,

$$P_p(m,n) = -j^n e^{jkd_p\cos\alpha} \frac{(2n+1)}{n(n+1)} \frac{(n-m)!}{(n+m)!} \frac{m}{\sin\alpha} P_n^m(\cos\alpha) \qquad (2\text{-}13)$$

$$Q_p(m,n) = -j^n e^{jkd_p\cos\alpha} \frac{(2n+1)}{n(n+1)} \frac{(n-m)!}{(n+m)!} \frac{\partial}{\partial \alpha} P_n^m(\cos\alpha) \qquad (2\text{-}14)$$

For the limiting case where the direction of the incident plane wave coincides with the direction of the positive z-axis ($\alpha=0$ in Fig. 2-2), equations (2-13) and (2-14) lead to the simpler form

$$P_p(m,n) = Q_p(m,n) = -j^n \frac{2n+1}{2n(n+1)} \delta_{m,1} e^{jkd_p} \qquad (2\text{-}15)$$

with $\delta_{m,1}$ being the Kronecker delta.

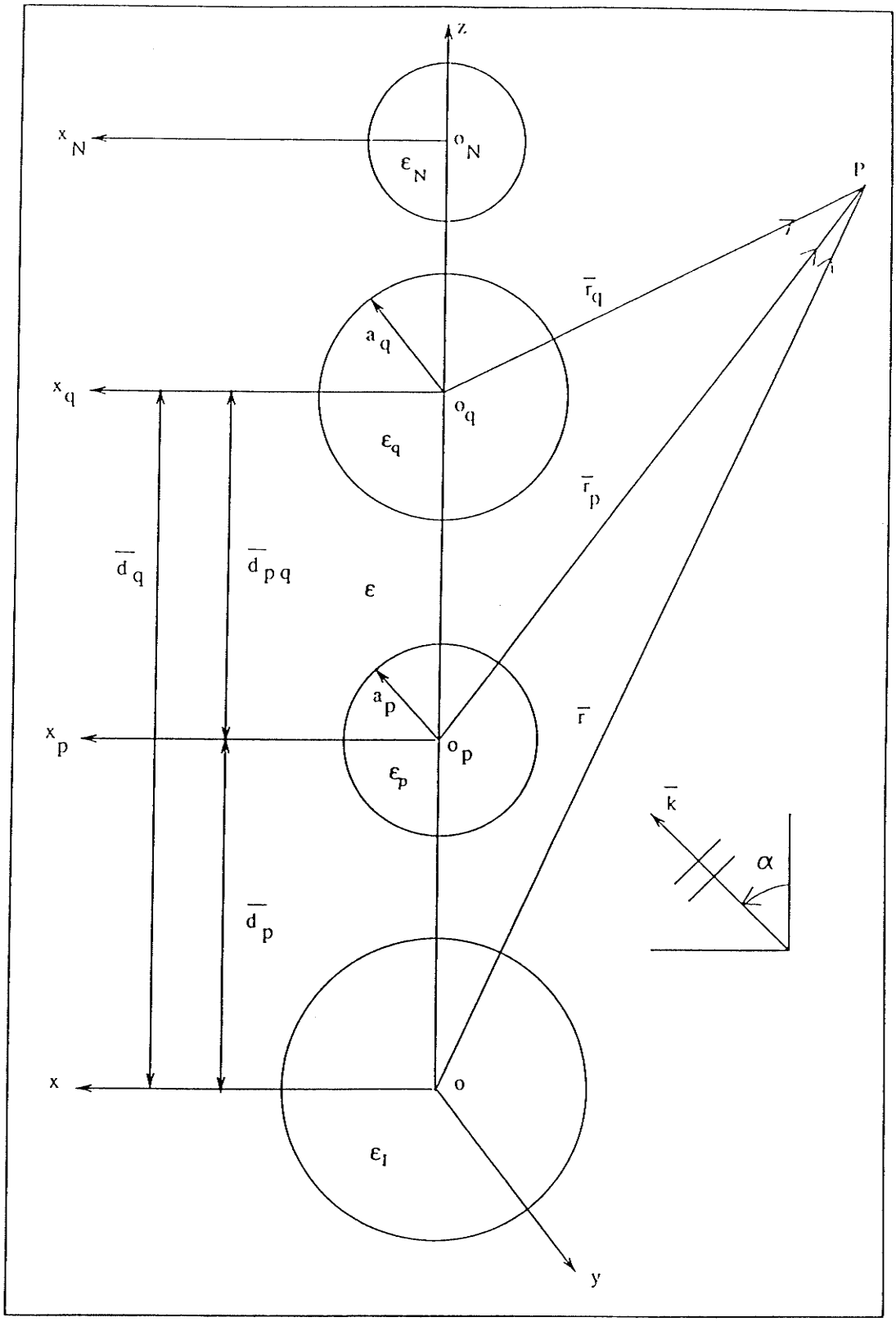

Fig.2-2. Linear array of dielectric spheres.

2.2 Expansion of the scattered and transmitted fields

The scattered fields from the pth dielectric sphere ($r_p > a_p$) can be expanded in terms of spherical wave functions of the third kind as

$$\overline{E}_p^s(r_p,\theta_p,\phi_p) = \sum_{n=1}^{\infty}\sum_{m=-n}^{m=n} [A_{pE}^s(m,n)\overline{N}_{mn}^{(3)}(r_p,\theta_p,\phi_p) + A_{pM}^s(m,n)\overline{M}_{mn}^{(3)}(r_p,\theta_p,\phi_p)] \tag{2-16}$$

$$\eta\,\overline{H}_p^s(r_p,\theta_p,\phi_p) = j\sum_{n=1}^{\infty}\sum_{m=-n}^{m=n} [A_{pE}^s(m,n)\overline{M}_{mn}^{(3)}(r_p,\theta_p,\phi_p) + A_{pM}^s(m,n)\overline{N}_{mn}^{(3)}(r_p,\theta_p,\phi_p)] \tag{2-17}$$

where A_{pE}^s and A_{pM}^s are the unknown scattered field coefficients due to TM and TE waves and will be determined later. $\overline{M}_{mn}^{(3)}$ and $\overline{N}_{mn}^{(3)}$ are the spherical vector wave functions of the third type which represent outgoing waves and which may be obtained by replacing j_n by the spherical Hankel function $h_n^{(1)}$ in equations (2-9) and (2-10). Similarly, the transmitted electric and magnetic fields into the pth sphere ($r_p < a_p$) may be written as

$$\overline{E}_p^t(r_p,\theta_p,\phi_p) = \sum_{n=1}^{\infty}\sum_{m=-n}^{m=n} [A_{pE}^t(m,n)\overline{N}_{mn}^{(1)}(r_p,\theta_p,\phi_p) + A_{pM}^t(m,n)\overline{M}_{mn}^{(1)}(r_p,\theta_p,\phi_p)] \tag{2-18}$$

$$\eta_p\,\overline{H}_p^t(r_p,\theta_p,\phi_p) = j\sum_{n=1}^{\infty}\sum_{m=-n}^{m=n} [A_{pE}^t(m,n)\overline{M}_{mn}^{(1)}(r_p,\theta_p,\phi_p) + A_{pM}^t(m,n)\overline{N}_{mn}^{(1)}(r_p,\theta_p,\phi_p)] \tag{2-19}$$

Here η_p is the medium intrinsic impedance of the pth sphere, while A_{pE}^t and A_{pM}^t are the unknown transmitted field expansion coefficients.

2.3 Translation addition theorem for spherical wave functions

In order to impose the boundary conditions at $r_p = a_p$ (p=1,2,...,N), the outgoing scattered fields from the qth sphere must be transformed in terms of incoming fields

on the pth sphere and vice versa. Hence we apply the translation addition theorem (Appendix B) for the vector spherical wave functions, *i. e.*,

$$\overline{M}_{mn}^{(3)}(r_q,\theta_q,\phi_q) = \sum_{\nu=1}^{\infty}\sum_{\mu=-\nu}^{\mu=\nu}[A_{\mu\nu}^{mn}(d_{pq},\theta_{pq},\phi_{pq})\overline{M}_{\mu\nu}^{(1)}(r_p,\theta_p,\phi_p) + B_{\mu\nu}^{mn}(d_{pq},\theta_{pq},\phi_{pq})\overline{N}_{\mu\nu}^{(1)}(r_p,\theta_p,\phi_p)] \quad (2\text{-}20)$$

$$\overline{N}_{mn}^{(3)}(r_q,\theta_q,\phi_q) = \sum_{\nu=1}^{\infty}\sum_{\mu=-\nu}^{\mu=\nu}[A_{\mu\nu}^{mn}(d_{pq},\theta_{pq},\phi_{pq})\overline{N}_{\mu\nu}^{(1)}(r_p,\theta_p,\phi_p) + B_{\mu\nu}^{mn}(d_{pq},\theta_{pq},\phi_{pq})\overline{M}_{\mu\nu}^{(1)}(r_p,\theta_p,\phi_p)] \quad (2\text{-}21)$$

where $A_{\mu\nu}^{mn}(d_{pq},\theta_{pq},\phi_{pq})$ and $B_{\mu\nu}^{mn}(d_{pq},\theta_{pq},\phi_{pq})$ are the translation coefficients in the addition theorem given in Appendix B and

$$\overline{d}_{pq} = \overline{d}_q - \overline{d}_p \quad (2\text{-}22)$$

$$= (x_q - x_p)\hat{x} + (y_q - y_p)\hat{y} + (z_q - z_p)\hat{z} \quad (2\text{-}23)$$

$$\theta_{pq} = \cos^{-1}\left(\frac{z_q - z_p}{d_{pq}}\right) \quad (2\text{-}24)$$

$$\phi_{pq} = \tan^{-1}\left(\frac{y_q - y_p}{x_q - x_p}\right) \quad (2\text{-}25)$$

$$\overline{M}_{mn}^{(3)}(r_p,\theta_p,\phi_p) = \sum_{\nu=1}^{\infty}\sum_{\mu=-\nu}^{\mu=\nu}(-1)^{n+\nu}[A_{\mu\nu}^{mn}(d_{qp},\theta_{qp},\phi_{qp})\overline{M}_{\mu\nu}^{(1)}(r_q,\theta_q,\phi_q) - B_{\mu\nu}^{mn}(d_{qp},\theta_{qp},\phi_{qp})\overline{N}_{\mu\nu}^{(1)}(r_q,\theta_q,\phi_q)] \quad (2\text{-}26)$$

$$\overline{N}_{mn}^{(3)}(r_p,\theta_p,\phi_p) = \sum_{\nu=1}^{\infty}\sum_{\mu=-\nu}^{\mu=\nu}(-1)^{n+\nu}[A_{\mu\nu}^{mn}(d_{qp},\theta_{qp},\phi_{qp})\overline{N}_{\mu\nu}^{(1)}(r_q,\theta_q,\phi_q) - B_{\mu\nu}^{mn}(d_{qp},\theta_{qp},\phi_{qp})\overline{M}_{\mu\nu}^{(1)}(r_q,\theta_q,\phi_q)] \quad (2\text{-}27)$$

For the special case of a translation along the z-axis, the translation addition theorem takes a simpler form (Appendix C). Therefore, equations (2-20) to (2-27) reduce to the following forms

$$\overline{M}_{mn}^{(3)}(r_q,\theta_q,\phi_q) = \sum_{\nu=1}^{\infty}[A_{m\nu}^{mn}(d_{pq})\overline{M}_{m\nu}^{(1)}(r_p,\theta_p,\phi_p) + B_{m\nu}^{mn}(d_{pq})\overline{N}_{m\nu}^{(1)}(r_p,\theta_p,\phi_p)] \quad (2\text{-}28)$$

$$\overline{N}_{mn}^{(3)}(r_q,\theta_q,\phi_q) = \sum_{\nu=1}^{\infty} [A_{m\nu}^{mn}(d_{pq})\,\overline{N}_{m\nu}^{(1)}(r_p,\theta_p,\phi_p) + B_{m\nu}^{mn}(d_{pq})\,\overline{M}_{m\nu}^{(1)}(r_p,\theta_p,\phi_p)\,] \quad (2\text{-}29)$$

where $A_{m\nu}^{mn}(d_{pq})$ and $B_{m\nu}^{mn}(d_{pq})$ are the translation coefficients in the addition theorem for a translation along the z-axis, and

$$\overline{M}_{mn}^{(3)}(r_p,\theta_p,\phi_p) = \sum_{\nu=1}^{\infty} (-1)^{n+\nu}[A_{m\nu}^{mn}(d_{qp})\,\overline{M}_{m\nu}^{(1)}(r_q,\theta_q,\phi_q) - B_{m\nu}^{mn}(d_{qp})\,\overline{N}_{m\nu}^{(1)}(r_q,\theta_q,\phi_q)\,] \quad (2\text{-}30)$$

$$\overline{N}_{mn}^{(3)}(r_p,\theta_p,\phi_p) = \sum_{\nu=1}^{\infty} (-1)^{n+\nu}[A_{m\nu}^{mn}(d_{qp})\,\overline{N}_{m\nu}^{(1)}(r_q,\theta_q,\phi_q) - B_{m\nu}^{mn}(d_{qp})\,\overline{M}_{m\nu}^{(1)}(r_q,\theta_q,\phi_q)\,] \quad (2\text{-}31)$$

Once the outgoing vector spherical wave functions are transformed into incoming ones, the boundary conditions can easily be applied on the surface of each dielectric sphere.

2.4 Application of the boundary conditions

The boundary conditions on the surface of the pth dielectric sphere require continuity of the tangential electric and magnetic fields, *i.e*,

$$\hat{n}_p \times [\,\overline{E}_p^{out}(r_p,\theta_p,\phi_p) - \overline{E}_p^{t}(r_p,\theta_p,\phi_p)\,] \Big|_{r_p=a_p} = 0\,, \qquad p=1,2,...,N \quad (2\text{-}32)$$

$$\hat{n}_p \times [\,\overline{H}_p^{out}(r_p,\theta_p,\phi_p) - \overline{H}_p^{t}(r_p,\theta_p,\phi_p)\,] \Big|_{r_p=a_p} = 0\,, \qquad p=1,2,...,N \quad (2\text{-}33)$$

where $\hat{n}_p$ is the outward unit normal to the surface of the pth dielectric sphere, and the superscript *out* refers to the region external to the pth sphere ($r_p > a_p$). Hence

$$\overline{E}_p^{out}(r_p,\theta_p,\phi_p) = \overline{E}^{i}(r_p,\theta_p,\phi_p) + \sum_{q=1}^{N} \left\{ \sum_{n=1}^{\infty} \sum_{m=-n}^{m=n} [A_{qE}^{s}(m,n)\,\overline{N}_{mn}^{(3)}(r_q,\theta_q,\phi_q) + A_{qM}^{s}(m,n)\,\overline{M}_{mn}^{(3)}(r_q,\theta_q,\phi_q)\,] \right\} \quad (2\text{-}34)$$

while the magnetic field $\overline{H}_p^{out}(r_p,\theta_p,\phi_p)$ can be written in a similar manner. It should be noted that $\overline{E}_p^{t}$ and $\overline{H}_p^{t}$ are zero for the special case of perfectly conducting spheres. Substituting the appropriate forms of the translation addition theorem (2-20)-(2-27)

into equations (2-32) and (2-33) leads to the following equations in terms of the unknown field expansion coefficients

$$\begin{aligned}
&\overline{r}_p \times \sum_{n=1}^{\infty} \sum_{m=-n}^{m=n} \Big[P_p(m,n)\,\overline{N}_{mn}^{(1)}(a_p,\theta_p,\phi_p) + Q_p(m,n)\,\overline{M}_{mn}^{(1)}(a_p,\theta_p,\phi_p) \\
&+ A_{pE}^{s}(m,n)\,\overline{N}_{mn}^{(3)}(a_p,\theta_p,\phi_p) + A_{pM}^{s}(m,n)\,\overline{M}_{mn}^{(3)}(a_p,\theta_p,\phi_p) \\
&+ \sum_{\substack{q=1 \\ q\neq p}}^{N} \Big\{ A_{qE}^{s}(m,n) \sum_{\nu=1}^{\infty} \sum_{\mu=-\nu}^{\mu=\nu} [A_{\mu\nu}^{mn}(d_{pq},\theta_{pq},\phi_{pq})\,\overline{N}_{\mu\nu}^{(1)}(a_p,\theta_p,\phi_p) \\
&\qquad + B_{\mu\nu}^{mn}(d_{pq},\theta_{pq},\phi_{pq})\,\overline{M}_{\mu\nu}^{(1)}(a_p,\theta_p,\phi_p)\,] \\
&+ A_{pM}^{s}(m,n) \sum_{\nu=1}^{\infty} \sum_{\mu=-\nu}^{\mu=\nu} [A_{\mu\nu}^{mn}(d_{pq},\theta_{pq},\phi_{pq})\,\overline{M}_{\mu\nu}^{(1)}(a_p,\theta_p,\phi_p) \\
&\qquad + B_{\mu\nu}^{mn}(d_{pq},\theta_{pq},\phi_{pq})\,\overline{N}_{\mu\nu}^{(1)}(a_p,\theta_p,\phi_p)\,] \Big\} \\
&- [A_{pE}^{t}(m,n)\,\overline{N}_{mn}^{(1)}(a_p,\theta_p,\phi_p) + A_{pM}^{t}(m,n)\,\overline{M}_{mn}^{(1)}(a_p,\theta_p,\phi_p)\,] \Big] = 0
\end{aligned} \tag{2-35}$$

and

$$\begin{aligned}
&\overline{r}_p \times \frac{1}{\eta} \sum_{n=1}^{\infty} \sum_{m=-n}^{m=n} \Big[P_p(m,n)\,\overline{M}_{mn}^{(1)}(a_p,\theta_p,\phi_p) + Q_p(m,n)\,\overline{N}_{mn}^{(1)}(a_p,\theta_p,\phi_p) \\
&+ A_{pE}^{s}(m,n)\,\overline{M}_{mn}^{(3)}(a_p,\theta_p,\phi_p) + A_{pM}^{s}(m,n)\,\overline{N}_{mn}^{(3)}(a_p,\theta_p,\phi_p) \\
&+ \sum_{\substack{q=1 \\ q\neq p}}^{N} \Big\{ A_{qE}^{s}(m,n) \sum_{\nu=1}^{\infty} \sum_{\mu=-\nu}^{\mu=\nu} [A_{\mu\nu}^{mn}(d_{pq},\theta_{pq},\phi_{pq})\,\overline{M}_{\mu\nu}^{(1)}(a_p,\theta_p,\phi_p) \\
&\qquad + B_{\mu\nu}^{mn}(d_{pq},\theta_{pq},\phi_{pq})\,\overline{N}_{\mu\nu}^{(1)}(a_p,\theta_p,\phi_p)\,] \\
&+ A_{pM}^{s}(m,n) \sum_{\nu=1}^{\infty} \sum_{\mu=-\nu}^{\mu=\nu} [A_{\mu\nu}^{mn}(d_{pq},\theta_{pq},\phi_{pq})\,\overline{N}_{\mu\nu}^{(1)}(a_p,\theta_p,\phi_p) \\
&\qquad + B_{\mu\nu}^{mn}(d_{pq},\theta_{pq},\phi_{pq})\,\overline{M}_{\mu\nu}^{(1)}(a_p,\theta_p,\phi_p)\,] \Big\} \\
&- \frac{\eta}{\eta_p} [A_{pE}^{t}(m,n)\,\overline{M}_{mn}^{(1)}(a_p,\theta_p,\phi_p) + A_{pM}^{t}(m,n)\,\overline{N}_{mn}^{(1)}(a_p,\theta_p,\phi_p)] \Big] = 0
\end{aligned} \tag{2-36}$$

Since our main interest is to obtain the scattered field everywhere, a solution for the unknown scattered field coefficients $A_{pE}^{s}(m,n)$ and $A_{pM}^{s}(m,n)$ will therefore be given here. Applying the orthogonality properties (Appendix A) of the spherical wave functions yields

$$A_{pE}^{s}(m,n)=\mathrm{v}_n(\rho_p)\{P_p(m,n)+\sum_{\substack{q=1\\q\neq p}}^{N}\sum_{\nu=1}^{\infty}\sum_{\mu=-\nu}^{\mu=\nu}[A_{mn}^{\mu\nu}(d_{pq},\theta_{pq},\phi_{pq})A_{qE}^{s}(\mu,\nu)$$

$$+B_{mn}^{\mu\nu}(d_{pq},\theta_{pq},\phi_{pq})A_{qM}^{s}(\mu,\nu)]\} \quad (2\text{-}37)$$

$$A_{pM}^{s}(m,n)=\mathrm{u}_n(\rho_p)\{Q_p(m,n)+\sum_{\substack{q=1\\q\neq p}}^{N}\sum_{\nu=1}^{\infty}\sum_{\mu=-\nu}^{\mu=\nu}[A_{mn}^{\mu\nu}(d_{pq},\theta_{pq},\phi_{pq})A_{qM}^{s}(\mu,\nu)$$

$$+B_{mn}^{\mu\nu}(d_{pq},\theta_{pq},\phi_{pq})A_{qE}^{s}(\mu,\nu)]\} \quad (2\text{-}38)$$

where p=1,2,...,N, while $\mathrm{v}_n(\rho_p)$ and $\mathrm{u}_n(\rho_p)$ are the electric and magnetic scattered field coefficients for a single dielectric sphere [37], which are given by

$$\mathrm{v}_n(\rho_p)=-\frac{j_n(\rho_p)[\xi_p\, j_n(\xi_p)]'-N_p^2 j_n(\xi_p)[\rho_p j_n(\rho_p)]'}{h_n^{(1)}(\rho_p)[\xi_p j_n(\xi_p)]'-N_p^2 j_n(\xi_p)[\rho_p\, h_n^{(1)}(\rho_p)]'} \quad (2\text{-}39)$$

$$\mathrm{u}_n(\rho_p)=-\frac{j_n(\xi_p)[\rho_p j_n(\rho_p)]'-j_n(\rho_p)[\xi_p j_n(\xi_p)]'}{j_n(\xi_p)[\rho_p h_n^{(1)}(\rho_p)]'-h_n^{(1)}(\rho_p)[\xi_p j_n(\xi_p)]'} \quad (2\text{-}40)$$

Here $k_p=N_p k$, $\rho_p = ka_p$, $\xi_p = k_p a_p = N_p \rho_p$, $N_p = \sqrt{\varepsilon_p/\varepsilon}$, while ε_p and ε are the permittivities of the pth sphere and of the surrounding medium, respectively. In the case of N lossy dielectric spheres, N_p is a complex quantity which makes the computations more complicated since the arguments of the radial functions become complex.

Equations (2-37) and (2-38) are a coupled set of linear algebraic equations and should be solved simultaneously in order to yield the unknown scattered field coefficients. In addition, the infinite series must be truncated to a finite number of terms $n=\nu=M$ and $m=\mu=2M+1$ in order to obtain numerical results [32].

For a linear array of N dielectric spheres spaced along the z-axis, equations (2-37) and (2-38) reduce to a simpler form due to the symmetry with respect to the z-axis and hence the summations over μ disappear, *i.e.*,

$$A^s_{pE}(m,n)=\mathrm{v}_n(ka_p)\{P_p(m,n)+\sum_{\substack{q=1\\q\neq p}}^{N}\sum_{\nu=1}^{\infty}[A^{m\nu}_{mn}(d_{pq})A^s_{qE}(m,\nu)+B^{m\nu}_{mn}(d_{pq})A^s_{qM}(m,\nu)]\} \tag{2-41}$$

$$A^s_{pM}(m,n)=\mathrm{u}_n(ka_p)\{Q_p(m,n)+\sum_{\substack{q=1\\q\neq p}}^{N}\sum_{\nu=1}^{\infty}[A^{m\nu}_{mn}(d_{pq})A^s_{qM}(m,\nu)+B^{m\nu}_{mn}(d_{pq})A^s_{qE}(m,\nu)]\} \tag{2-42}$$

It should be noted that the above system is solved for each m independently, since there is no coupling between azimuthal modes, and the scattered field coefficients are obtained by summing over the required azimuthal modes.

2.5 Solution of the resultant system of equations

The obtained system of linear equations can be written in a matrix form as

$$\bar{A}^s_{pE}=[\mathrm{v}_p]\bar{P}_p+[\mathrm{v}_p]\sum_{\substack{q=1\\q\neq p}}^{N}\{[A^{pq}]\bar{A}^s_{qE}+[B^{pq}]\bar{A}^s_{qM}\},\quad p=1,2,...,N \tag{2-43}$$

$$\bar{A}^s_{pM}=[\mathrm{u}_p]\bar{Q}_p+[\mathrm{u}_p]\sum_{\substack{q=1\\q\neq p}}^{N}\{[A^{pq}]\bar{A}^s_{qM}+[B^{pq}]\bar{A}^s_{qE}\},\quad p=1,2,...,N \tag{2-44}$$

where the above column and submatrices are defined in Appendix D. The above system of matrices may be re-written in the following form

$$\begin{bmatrix}\bar{A}^s_{pE}\\ \bar{A}^s_{pM}\end{bmatrix}=\begin{bmatrix}[\mathrm{v}_p] & 0\\ 0 & [\mathrm{u}_p]\end{bmatrix}\begin{bmatrix}\bar{P}_p\\ \bar{Q}_p\end{bmatrix}+\begin{bmatrix}[\mathrm{v}_p] & 0\\ 0 & [\mathrm{u}_p]\end{bmatrix}\sum_{\substack{q=1\\q\neq p}}^{N}\begin{bmatrix}[A^{pq}] & [B^{pq}]\\ [B^{pq}] & [A^{pq}]\end{bmatrix}\begin{bmatrix}\bar{A}^s_{qE}\\ \bar{A}^s_{qM}\end{bmatrix} \tag{2-45}$$

where $\bar{A}^s_{pE}$, $\bar{A}^s_{pM}$ and $\bar{A}^s_{qE}$, $\bar{A}^s_{qM}$ are column matrices of the unknown scattered field coefficients of the pth and qth sphere, respectively. $[\mathrm{v}_p]$ and $[\mathrm{u}_p]$ are diagonal submatrices containing the scattered field coefficients of a single dielectric sphere, while $\bar{P}_p$ and $\bar{Q}_p$ are column matrices for the incident field coefficients. Finally, $[A^{pq}]$ and $[B^{pq}]$ are square submatrices associated with the translation addition coefficients.

Equation (2-45) may be written in a convenient matrix form as

$$A = L + T\,A \tag{2-46}$$

where

$$L = \begin{bmatrix} [v_p] & 0 \\ 0 & [u_p] \end{bmatrix} \begin{bmatrix} \overline{P}_p \\ \overline{Q}_p \end{bmatrix} \tag{2-47}$$

$$T = \begin{bmatrix} [v_p] & 0 \\ 0 & [u_p] \end{bmatrix} \sum_{\substack{q=1 \\ q\neq p}}^{N} \begin{bmatrix} [A^{pq}] & [B^{pq}] \\ [B^{pq}] & [A^{pq}] \end{bmatrix} \tag{2-48}$$

The solution of equation (2-46) by matrix inversion yields the scattered field coefficients in equations (2-16) and (2-17) as

$$A = (I - T)^{-1} L \tag{2-49}$$

Once the scattered coefficients are computed, the total scattered field can be determined everywhere.

2.6 Scattering by perfectly conducting spheres

The special case of scattering by N perfectly conducting spheres is obtained from the dielectric case by letting the permittivity of each dielectric sphere become very large and hence leads to no transmitted fields inside the spheres. The boundary condition requires that the tangential electric field components ($\overline{E}_\theta$ and $\overline{E}_\phi$) must vanish on the surface of the pth sphere. Thus equation (2-32) reduces to

$$\hat{h}_p \times \overline{E}^{total}(r_p,\theta_p,\phi_p)\,|_{\,r_p=a_p} = 0\,, \qquad p = 1,2,...,N \tag{2-50}$$

where

$$\overline{E}^{total}(r_p,\theta_p,\phi_p) = \overline{E}^{i}(r_p,\theta_p,\phi_p) + \sum_{q=1}^{N} \left\{ \sum_{n=1}^{\infty} \sum_{m=-n}^{m=n} [A^{s}_{qE}(m,n)\,\overline{N}^{(3)}_{mn}(r_q,\theta_q,\phi_q) + A^{s}_{qM}(m,n)\,\overline{M}^{(3)}_{mn}(r_q,\theta_q,\phi_q)] \right\} \tag{2-51}$$

Substituting the appropriate forms of the translation addition theorem (2-20)-(20-27)

into equation (2-50) leads to the following equation in terms of the unknown expansion coefficients

$$\begin{aligned}
\overline{r}_p \times \sum_{n=1}^{\infty} \sum_{m=-n}^{m=n} \Big[& P_p(m,n)\,\overline{N}_{mn}^{(1)}(a_p,\theta_p,\phi_p) + Q_p(m,n)\,\overline{M}_{mn}^{(1)}(a_p,\theta_p,\phi_p) \\
& + A_{pE}^{s}(m,n)\,\overline{N}_{mn}^{(3)}(a_p,\theta_p,\phi_p) + A_{pM}^{s}(m,n)\,\overline{M}_{mn}^{(3)}(a_p,\theta_p,\phi_p) \\
& + \sum_{\substack{q=1 \\ q\neq p}}^{N} \Bigg\{ A_{qE}^{s}(m,n) \sum_{\nu=1}^{\infty} \sum_{\mu=-\nu}^{\mu=\nu} [A_{\mu\nu}^{mn}(d_{pq},\theta_{pq},\phi_{pq})\,\overline{N}_{\mu\nu}^{(1)}(a_p,\theta_p,\phi_p) \\
& \qquad + B_{\mu\nu}^{mn}(d_{pq},\theta_{pq},\phi_{pq})\,\overline{M}_{\mu\nu}^{(1)}(a_p,\theta_p,\phi_p)\,] \\
& + A_{pM}^{s}(m,n) \sum_{\nu=1}^{\infty} \sum_{\mu=-\nu}^{\mu=\nu} [A_{\mu\nu}^{mn}(d_{pq},\theta_{pq},\phi_{pq})\,\overline{M}_{\mu\nu}^{(1)}(a_p,\theta_p,\phi_p) \\
& \qquad + B_{\mu\nu}^{mn}(d_{pq},\theta_{pq},\phi_{pq})\,\overline{N}_{\mu\nu}^{(1)}(a_p,\theta_p,\phi_p)\,] \Bigg\} \Big] \qquad (2\text{-}52)
\end{aligned}$$

To determine the unknown scattered field coefficients in the above equation we apply once again the orthogonality properties (Appendix A) of the spherical wave functions, to obtain

$$\begin{aligned}
A_{pE}^{s}(m,n) = \nu_n(\rho_p)\{ & P_p(m,n) + \sum_{\substack{q=1 \\ q\neq p}}^{N} \sum_{\nu=1}^{\infty} \sum_{\mu=-\nu}^{\mu=\nu} [A_{mn}^{\mu\nu}(d_{pq},\theta_{pq},\phi_{pq})\,A_{qE}^{s}(\mu,\nu) \\
& + B_{mn}^{\mu\nu}(d_{pq},\theta_{pq},\phi_{pq})\,A_{qM}^{s}(\mu,\nu)]\} \qquad (2\text{-}53) \\
A_{pM}^{s}(m,n) = u_n(\rho_p)\{ & Q_p(m,n) + \sum_{\substack{q=1 \\ q\neq p}}^{N} \sum_{\nu=1}^{\infty} \sum_{\mu=-\nu}^{\mu=\nu} [A_{mn}^{\mu\nu}(d_{pq},\theta_{pq},\phi_{pq})\,A_{qM}^{s}(\mu,\nu) \\
& + B_{mn}^{\mu\nu}(d_{pq},\theta_{pq},\phi_{pq})\,A_{qE}^{s}(\mu,\nu)]\} \qquad (2\text{-}54)
\end{aligned}$$

Hence $\nu_n(\rho_p)$ and $u_n(\rho_p)$ are the electric and magnetic scattered field coefficients for a single perfectly conducting sphere and are given by

$$\nu_n(\rho_p) = -\frac{[\rho_p\, j(\rho_p)]'}{[\rho_p\, h_n^{(1)}(\rho_p)]'} \qquad (2\text{-}55)$$

$$u_n(\rho_p) = -\frac{j_n(\rho_p)}{h_n^{(1)}(\rho_p)} \qquad (2\text{-}56)$$

It should be pointed out that equations (2-53) and (2-54) for a system of perfectly

conducting spheres are similar to equations (2-37) and (2-38) for dielectric spheres with the coefficients $v_n(\rho_p)$ and $u_n(\rho_p)$ of dielectric spheres replaced by those for perfectly conducting ones.

CHAPTER 3

ITERATIVE SOLUTION TO THE SCATTERING BY AN ARBITRARY CONFIGURATION OF SPHERES

An exact analytic solution of the problem of scattering by a system of N conducting or dielectric spheres has been obtained in chapter 2 by employing the translational addition theorem for the vector spherical wave functions in order to enforce the boundary conditions simultaneously at the surface of each sphere. Thus, the field outside each sphere is expressed in terms of the incident field plus the scattered fields from the remaining spheres.

In this chapter a novel iterative procedure is proposed for the solution of the scattering by an arbitrary configuration of dielectric or perfectly conducting spheres. This approach requires the solution of the field scattered by each sphere, assumed to be alone in the incident field, which acts as an incident field on the other spheres. Therefore, the first order scattered field (first iteration) results from the excitation of each sphere by the incident field only, while the second order scattered field results from the excitation of each sphere by the sum of all first order scattered fields. Hence this iterative process continues until the solution converges. One of the advantages of employing this approach is that the proposed solution does not require matrix inversion and therefore the desired scattered field coefficients are obtained after each iteration and used in the subsequent iteration. The translation addition theorem for the vector spherical wave function is used in order to compute the higher order terms of the scattered fields. Finally, a general expression is derived and written in a matrix form for the ith order scattered field.

3.1 Iterative solution for dielectric spheres

3.1.1 First order field scattered by dielectric spheres

The first order field scattered results form the excitation of the pth dielectric sphere by the incident plane wave alone. The boundary conditions at the surface of the pth dielectric sphere require continuity of the total tangential electric and magnetic fields at $r_p = a_p$, i. e.,

$$\bar{r}_p \times \left\{ \bar{E}^i(r_p,\theta_p,\phi_p) + \bar{E}^s_{p1}(r_p,\theta_p,\phi_p) - \bar{E}^t_{p1}(r_p,\theta_p,\phi_p) \right\} \Big|_{r_p=a_p} = 0 \ , \ p=1,2,...,N \quad (3\text{-}1)$$

$$\bar{r}_p \times \left\{ \bar{H}^i(r_p,\theta_p,\phi_p) + \bar{H}^s_{p1}(r_p,\theta_p,\phi_p) - \bar{H}^t_{p1}(r_p,\theta_p,\phi_p) \right\} \Big|_{r_p=a_p} = 0 \ , p=1,2,...,N \quad (3\text{-}2)$$

Substituting equations (2-5),(2-16) and (2-18) into (3-1) yields the following equation in terms of the first order scattered field coefficients

$$\begin{aligned} \bar{r}_p \times \Bigg\{ & \sum_{n=1}^{\infty} \sum_{m=-n}^{m=n} [P_p(m,n)\bar{N}^{(1)}_{mn}(a_p,\theta_p,\phi_p) + Q_p(m,n)\bar{M}^{(1)}_{mn}(a_p,\theta_p,\phi_p)] \\ & + \sum_{n=1}^{\infty} \sum_{m=-n}^{m=n} [A^s_{pE_1}(m,n)\bar{N}^{(3)}_{mn}(a_p,\theta_p,\phi_p) + A^s_{pM_1}(m,n)\bar{M}^{(3)}_{mn}(a_p,\theta_p,\phi_p)] \\ & - \sum_{n=1}^{\infty} \sum_{m=-n}^{m=n} [A^t_{pE_1}(m,n)\bar{N}^{(1)}_{mn}(a_p,\theta_p,\phi_p) + A^t_{pM_1}(m,n)\bar{M}^{(1)}_{mn}(a_p,\theta_p,\phi_p)] \Bigg\} = 0 \end{aligned} \quad (3\text{-}3)$$

while equation (3-2) can be imposed similarly. In order to obtain the unknown scattered field expansion coefficients, we use the orthogonality properties of the spherical wave functions. This yields

$$A^s_{pE_1}(m,n) = v_n(\rho_p) P_p(m,n) \qquad p=1,2,...,N \quad (3\text{-}4)$$

$$A^s_{pM_1}(m,n) = u_n(\rho_p) Q_p(m,n) \qquad p=1,2,...,N \quad (3\text{-}5)$$

where $v_n(\rho_p)$ and $u_n(\rho_p)$ are given in equations (2-39) and (2-40), respectively. Equations (3-4) and (3-5) can be written in a matrix form as

$$\begin{bmatrix} \overline{A}^{s}_{pE_1} \\ \overline{A}^{s}_{pM_1} \end{bmatrix} = \begin{bmatrix} [v_p] & 0 \\ 0 & [u_p] \end{bmatrix} \begin{bmatrix} \overline{P}_p \\ \overline{Q}_p \end{bmatrix} \tag{3-6}$$

where $\overline{A}^{s}_{pE_1}$, $\overline{A}^{s}_{pM_1}$, $\overline{P}_p$, $\overline{Q}_p$ are column matrices, while $[v_p]$, $[u_p]$ are diagonal submatrices.

3.1.2 Higher order fields scattered by dielectric spheres

The second order scattered field results from the excitation of the pth sphere by the field scattered from the remaining N-1 spheres due to the initial plane wave incident field. The boundary conditions require continuity of the total electric and magnetic fields at $r_p=a_p$, i. e.,

$$\overline{r}_p \times \left\{ \sum_{\substack{q=1 \\ q\neq p}}^{N} \overline{E}^{s}_{q1}(r_q,\theta_q,\phi_q) + \overline{E}^{s}_{p2}(r_p,\theta_p,\phi_p) - \overline{E}^{t}_{p2}(r_p,\theta_p,\phi_p) \right\} \Bigg|_{r_p=a_p} = 0,\ p=1,2,...,N \tag{3-7}$$

$$\overline{r}_p \times \left\{ \sum_{\substack{q=1 \\ q\neq p}}^{N} \overline{H}^{s}_{q1}(r_q,\theta_q,\phi_q) + \overline{H}^{s}_{p2}(r_p,\theta_p,\phi_p) - \overline{H}^{t}_{p2}(r_p,\theta_p,\phi_p) \right\} \Bigg|_{r_p=a_p} = 0,\ p=1,2,...,N \tag{3-8}$$

To enforce the above boundary conditions, we express the outgoing vector wave functions in the coordinates associated with each sphere q into incoming vector wave functions in terms of the coordinates associated with the pth sphere. Hence we apply the translation addition theorem for the vector spherical wave functions [26-27]. Substituting the appropriate forms of the translation addition theorem in equations (2-20)-(2-27) into (3-7) and (3-8), leads to the following equations in terms of the second order scattered field coefficients

$$\overline{r}_p \times \sum_{n=1}^{\infty}\sum_{m=-n}^{m=n}\left[\sum_{\substack{q=1\\q\neq p}}^{N}\left\{A^s_{qE_1}(m,n)\sum_{\nu=1}^{\infty}\sum_{\mu=-\nu}^{\mu=\nu}[A^{mn}_{\mu\nu}(d_{pq},\theta_{pq},\phi_{pq})\overline{N}^{(1)}_{\mu\nu}(a_p,\theta_p,\phi_p)\right.\right.$$

$$+B^{mn}_{\mu\nu}(d_{pq},\theta_{pq},\phi_{pq})\overline{M}^{(1)}_{\mu\nu}(a_p,\theta_p,\phi_p)\,]\;+A^s_{qM_1}(m,n)\sum_{\nu=1}^{\infty}\sum_{\mu=-\nu}^{\mu=\nu}[A^{mn}_{\mu\nu}(d_{pq},\theta_{pq},\phi_{pq})\overline{M}^{(1)}_{\mu\nu}(a_p,\theta_p,\phi_p)$$

$$\left.\left.+B^{mn}_{\mu\nu}(d_{pq},\theta_{pq},\phi_{pq})\overline{N}^{(1)}_{\mu\nu}(a_p,\theta_p,\phi_p)\,]\right\}+[A^s_{pE_2}(m,n)\overline{N}^{(3)}_{mn}(a_p,\theta_p,\phi_p)\right.$$

$$\left.+A^s_{pM_2}(m,n)\overline{M}^{(3)}_{mn}(a_p,\theta_p,\phi_p)\,]-[A^t_{pE_2}(m,n)\overline{N}^{(1)}_{mn}(a_p,\theta_p,\phi_p)+A^t_{pM_2}(m,n)\overline{M}^{(1)}_{mn}(a_p,\theta_p,\phi_p\,]\right]=0 \tag{3-9}$$

and

$$\overline{r}_p \times \sum_{n=1}^{\infty}\sum_{m=-n}^{m=n}\left[\frac{1}{\eta}\sum_{\substack{q=1\\q\neq p}}^{N}\left\{A^s_{qE_1}(m,n)\sum_{\nu=1}^{\infty}\sum_{\mu=-\nu}^{\mu=\nu}[A^{mn}_{\mu\nu}(d_{pq},\theta_{pq},\phi_{pq})\overline{M}^{(1)}_{\mu\nu}(a_p,\theta_p,\phi_p)\right.\right.$$

$$+B^{mn}_{\mu\nu}(d_{pq},\theta_{pq},\phi_{pq})\overline{N}^{(1)}_{\mu\nu}(a_p,\theta_p,\phi_p)\,]\;+A^s_{qM_1}(m,n)\sum_{\nu=1}^{\infty}\sum_{\mu=-\nu}^{\mu=\nu}[A^{mn}_{\mu\nu}(d_{pq},\theta_{pq},\phi_{pq})\overline{N}^{(1)}_{\mu\nu}(a_p,\theta_p,\phi_p)$$

$$\left.\left.+B^{mn}_{\mu\nu}(d_{pq},\theta_{pq},\phi_{pq})\overline{M}^{(1)}_{\mu\nu}(a_p,\theta_p,\phi_p)\,]\right\}+\frac{1}{\eta}[A^s_{pE_2}(m,n)\overline{M}^{(3)}_{mn}(a_p,\theta_p,\phi_p)\;+A^s_{pM_2}(m,n)\right.$$

$$\left.\cdot\overline{N}^{(3)}_{mn}(a_p,\theta_p,\phi_p)]\;-\frac{1}{\eta_p}[A^t_{pE_2}(m,n)\overline{M}^{(1)}_{mn}(a_p,\theta_p,\phi_p)+A^t_{pM_2}(m,n)\overline{N}^{(1)}_{mn}(a_p,\theta_p,\phi_p)]\right]=0 \tag{3-10}$$

Since we are mainly interested in the field outside the spheres, we present here expressions for the scattered field coefficients. Applying the orthogonality properties of the spherical vector wave functions, we obtain

$$A^s_{pE_2}(m,n)=v_n(\rho_p)\sum_{\substack{q=1\\q\neq p}}^{N}\sum_{\nu=1}^{\infty}\sum_{\mu=-\nu}^{\mu=\nu}[A^{\mu\nu}_{mn}(d_{pq},\theta_{pq},\phi_{pq})A^s_{qE_1}(\mu,\nu)$$

$$+B^{\mu\nu}_{mn}(d_{pq},\theta_{pq},\phi_{pq})A^s_{qM_1}(\mu,\nu)] \tag{3-11}$$

$$A^s_{pM_2}(m,n)=u_n(\rho_p)\sum_{\substack{q=1\\q\neq p}}^{N}\sum_{\nu=1}^{\infty}\sum_{\mu=-\nu}^{\mu=\nu}[A^{\mu\nu}_{mn}(d_{pq},\theta_{pq},\phi_{pq})A^s_{qM_1}(\mu,\nu)$$

$$+B^{\mu\nu}_{mn}(d_{pq},\theta_{pq},\phi_{pq})A^s_{qE_1}(\mu,\nu)] \tag{3-12}$$

where $A^s_{qE_1}$, $A^s_{qM_1}$ are known first order scattered field coefficients given by equation

(3-6), and $A^s_{pE_2}$, $A^s_{pM_2}$ are the second order scattered field coefficients. The infinite series in equations (3-11) and (3-12) must be truncated to a finite number of terms $n=\nu=M$ and $m=\mu=M+1$ to obtain numerical results [39].

For the special case of a linear array of N dielectric spheres spaced along the z-axis, equations (3-11) and (3-12) reduce to the simpler form

$$A^s_{pE_2}(m,n)=\nu_n(\rho_p)\sum_{\substack{q=1\\q\neq p}}^{N}\sum_{\nu=1}^{\infty}[A^{m\nu}_{mn}(d_{pq})A^s_{qE_1}(m,\nu)+B^{m\nu}_{mn}(d_{pq})A^s_{qM_1}(m,\nu)] \tag{3-13}$$

$$A^s_{pM_2}(m,n)=u_n(\rho_p)\sum_{\substack{q=1\\q\neq p}}^{N}\sum_{\nu=1}^{\infty}[A^{m\nu}_{mn}(d_{pq})A^s_{qM_1}(m,\nu)+B^{m\nu}_{mn}(d_{pq})A^s_{qE_1}(m,\nu)] \tag{3-14}$$

The above system of equations is solved for each m independently as in chapter 2, since there is no coupling between the azimuthal modes. Hence equations (3-11) and (3-12) may be written in a matrix form as

$$\begin{bmatrix}\bar{A}^s_{pE_2}\\ \bar{A}^s_{pM_2}\end{bmatrix}=\begin{bmatrix}[\nu_p] & 0\\ 0 & [u_p]\end{bmatrix}\sum_{\substack{q=1\\q\neq p}}^{N}\begin{bmatrix}[A^{pq}] & [B^{pq}]\\ [B^{pq}] & [A^{pq}]\end{bmatrix}\begin{bmatrix}\bar{A}^s_{qE_1}\\ \bar{A}^s_{qM_1}\end{bmatrix} \tag{3-15}$$

where $[A^{pq}]$ and $[B^{pq}]$ are square submatrices whose elements are $A^{\mu\nu}_{mn}$ and $B^{\mu\nu}_{mn}$ which depend on the electrical separation between the spheres. Equation (3-15) may be rewritten in the convenient matrix form

$$\bar{A}^s_{p_2}=T\,\bar{A}^s_{q_1}\,,\qquad p\neq q \tag{3-16}$$

with

$$T=\begin{bmatrix}[\nu_p] & 0\\ 0 & [u_p]\end{bmatrix}\sum_{\substack{q=1\\q\neq p}}^{N}\begin{bmatrix}[A^{pq}] & [B^{pq}]\\ [B^{pq}] & [A^{pq}]\end{bmatrix} \tag{3-17}$$

In order to obtain a general solution, we solve for higher order scattered fields which are sensitive to the electrical separation between the spheres and the angle of incidence. This means that if the spheres are located very close to one another or

touching, then the higher order fields are significant and should therefore be included in the solution. However, these decay rapidly as the separation becomes large. The significance of the higher order scattered fields will be verified numerically by comparison with simultaneous boundary conditions solution in chapter 2.

The general expression for the ith order scattered field coefficients can be written as

$$\bar{A}^s_{p_i} = T\ \bar{A}^s_{q_{i-1}}, \quad i = 2,3,..., \ p \neq q \tag{3-18}$$

It should be noted that the translation addition theorem coefficients in equation (3-18) are computed once for the separations considered, and used for the subsequent iterations. Once the scattered field coefficients are determined, the field scattered from the pth sphere due to the ith order scattered field can be written as

$$\bar{E}^s_p = \sum_{n=1}^{\infty} \sum_{m=-n}^{m=n} \sum_{i=1,2,...} [A^s_{pE_i}(m,n)\bar{N}^{(3)}_{mn}(r_p,\theta_p,\phi_p) + A^s_{pM_i}(m,n)\bar{M}^{(3)}_{mn}(r_p,\theta_p,\phi_p)] \tag{3-19}$$

Summing the fields scattered from all spheres, equation (3-19) becomes

$$\bar{E}^s = \sum_{p=1}^{N} \sum_{n=1}^{\infty} \sum_{m=-n}^{m=n} \sum_{i=1,2,...} [A^s_{pE_i}(m,n)\bar{N}^{(3)}_{mn}(r_p,\theta_p,\phi_p) + A^s_{pM_i}(m,n)\bar{M}^{(3)}_{mn}(r_p,\theta_p,\phi_p)] \tag{3-20}$$

3.2 Iterative solution for perfectly conducting spheres

An iterative solution of the special case of N conducting spheres can be obtained from the dielectric solution by letting the permittivity of each dielectric sphere become high as outlined in section 2.6.

3.2.1 First order scattered field by conducting spheres

The boundary condition at the surface of the pth conducting sphere requires that

the total tangential electric field at $r_p=a_p$ must vanish, i. e.,

$$\bar{r}_p \times \left\{ \bar{E}^i(r_p,\theta_p,\phi_p) + \bar{E}^s_{p1}(r_p,\theta_p,\phi_p) \right\}_{|r_p=a_p} = 0 \ , \ p=1,2,...,N \qquad (3\text{-}21)$$

Substituting equations (2-5) and (2-16) into (3-21), we obtain the following equation in terms of the first order scattered field coefficients

$$\bar{r}_p \times \left\{ \sum_{n=1}^{\infty} \sum_{m=-n}^{m=n} [P_p(m,n)\bar{N}^{(1)}_{mn}(a_p,\theta_p,\phi_p) + Q_p(m,n)\bar{M}^{(1)}_{mn}(a_p,\theta_p,\phi_p)\,] \right.$$
$$\left. + \sum_{n=1}^{\infty} \sum_{m=-n}^{m=n} [A^s_{pE_1}(m,n)\bar{N}^{(3)}_{mn}(a_p,\theta_p,\phi_p) + A^s_{pM_1}(m,n)\bar{M}^{(3)}_{mn}(a_p,\theta_p,\phi_p)\,] \right\} = 0 \qquad (3\text{-}22)$$

In order to obtain the unknown scattered field coefficients, we use the orthogonality properties of the spherical wave functions. This yields the first order scattered field coefficients

$$A^s_{pE_1}(m,n) = v_n(\rho_p)P_p(m,n) \qquad p=1,2,...,N \qquad (3\text{-}23)$$

$$A^s_{pM_1}(m,n) = u_n(\rho_p)Q_p(m,n) \qquad p=1,2,...,N \qquad (3\text{-}24)$$

where $v_n(\rho_p)$ and $u_n(\rho_p)$ are given in equations (2-55) and (2-56), respectively.

3.2.2 Higher order scattered fields by conducting spheres

The total electric field at the surface of the pth conducting sphere is equal to the sum of all first order scattered fields from the N-1 remaining spheres plus the second order scattered field from the pth sphere which at $r_p=a_p$ must vanish, i. e.,

$$\bar{r}_p \times \left\{ \sum_{\substack{q=1 \\ q\neq p}}^{N} \bar{E}^s_{q1}(r_q,\theta_q,\phi_q) + \bar{E}^s_{p2}(r_p,\theta_p,\phi_p) \right\} \Bigg|_{r_p=a_p} = 0 \ , \ p=1,2,...,N \qquad (3\text{-}25)$$

Applying the translation addition theorem and the orthogonality properties of the vector wave functions, we obtain

$$A^{s}_{pE_2}(m,n) = \nu_n(\rho_p) \sum_{\substack{q=1 \\ q\neq p}}^{N} \sum_{\nu=1}^{\infty} \sum_{\mu=-\nu}^{\mu=\nu} [A^{\mu\nu}_{mn}(d_{pq},\theta_{pq},\phi_{pq}) A^{s}_{qE_1}(\mu,\nu) + B^{\mu\nu}_{mn}(d_{pq},\theta_{pq},\phi_{pq}) A^{s}_{qM_1}(\mu,\nu)] \quad (3\text{-}26)$$

$$A^{s}_{pM_2}(m,n) = u_n(\rho_p) \sum_{\substack{q=1 \\ q\neq p}}^{N} \sum_{\nu=1}^{\infty} \sum_{\mu=-\nu}^{\mu=\nu} [A^{\mu\nu}_{mn}(d_{pq},\theta_{pq},\phi_{pq}) A^{s}_{qM_1}(\mu,\nu) + B^{\mu\nu}_{mn}(d_{pq},\theta_{pq},\phi_{pq}) A^{s}_{qE_1}(\mu,\nu)] \quad (3\text{-}27)$$

where $A^{s}_{qE_1}$, $A^{s}_{qM_1}$ are known first order scattered field coefficients given by equations (3-23) and equation (3-24). The general solution of the ith order scattered field can be written similarly as in equation (3-18).

CHAPTER 4

RADAR CROSS SECTION CALCULATIONS

In chapters 2 and 3, expressions for the total scattered field at any point in space for an arbitrary configuration of N conducting or dielectric spheres have been obtained by using two different exact methods. Of particular interest is the scattered electric field in the far zone and the radar cross section of the spheres. Asymptotic expressions for the vector spherical wave function $(\overline{M}_{mn}^{(3)}, \overline{N}_{mn}^{(3)})$ are introduced in this chapter by using the asymptotic form of the Hankel function for large argument. In addition, analytic expressions for the normalized backscattering, forward scattering, and bistatic cross sections are derived due to an arbitrary angles of incidence [40].

Numerical results for one- and two-dimensional arrays of spheres based on the two methods are presented graphically for various electrical separations, sphere sizes, and arbitrary angles of incidence. In addition, the normalized bistatic cross section patterns for conducting or dielectric spheroids are obtained by simulating the spheroids by an appropriate system of spheres.

4.1 Far field approximation

In this section, the asymptotic expressions for the spherical wave functions are obtained using the asymptotic forms of the Hankel function for large argument, i.e.,

$$h_n^{(1)}(kr_p) \simeq (-j)^{(n+1)} \frac{e^{jkr_p}}{kr_p} \tag{4-1}$$

$$\frac{[kr_p\, h_n^{(1)}(kr_p)]'}{kr_p} \approx (-j)^n \frac{e^{jkr_p}}{kr_p} \tag{4-2}$$

4.2 Normalized scattering cross sections

Substituting the above relations into equations (2-9) and (2-10) leads to

$$\overline{M}_{mn}^{(3)}(r_p,\theta_p,\phi_p) \approx j^{-n} \frac{e^{jkr_p}}{kr_p} [\, \frac{m}{\sin\theta_p} P_n^m(\cos\theta_p)\, \hat{\theta}_p + j\, \frac{\partial}{\partial\theta_p} P_n^m(\cos\theta_p) \hat{\phi}_p \,]\, e^{jm\phi_p} \tag{4-3}$$

$$\overline{N}_{mn}^{(3)}(r_p,\theta_p,\hat{\phi}) \approx j^{-n} \frac{e^{jkr_p}}{kr_p} [\, \frac{\partial}{\partial\theta_p} P_n^m(\cos\theta_p)\, \hat{\theta}_p + j\, \frac{m}{\sin\theta_p} P_n^m(\cos\theta_p)\, \hat{\phi}_p \,]\, e^{jm\phi_p} \tag{4-4}$$

In addition, we have the following approximate relations (Fig. 4-1),

$$r_p = r - d_p \zeta_s \tag{4-5}$$

$$\theta = \theta_1 = \cdots = \theta_p = \cdots = \theta_N \tag{4-6}$$

where

$$\zeta_s = \sin\Theta_p \cos\Phi_p \sin\theta\cos\phi + \sin\Theta_p \sin\Phi_p \sin\theta\sin\phi + \cos\Theta_p \cos\theta$$

Substituting the above relations with equations (4-3) and (4-4) into equation (2-16), the total scattered electric field of an arbitrary configuration of spheres in the far zone may hence be written as

$$\overline{E}^s = \frac{e^{jkr}}{kr} [F_\theta(\theta,\phi)\hat{\theta} + F_\phi(\theta,\phi)\hat{\phi}] \tag{4-7}$$

where

$$F_\theta(\theta,\phi) = \sum_{p=1}^{N} F_{\theta p}(\theta,\phi) \tag{4-8}$$

$$F_\phi(\theta,\phi) = \sum_{p=1}^{N} F_{\phi p}(\theta,\phi) \tag{4-9}$$

and

$$F_{\theta p}(\theta,\phi) = \sum_{n=1}^{\infty} \sum_{m=-n}^{m=n} j^{-n+1} [A_{pE}^s(m,n) \frac{\partial}{\partial\theta} P_n^m(\cos\theta)$$

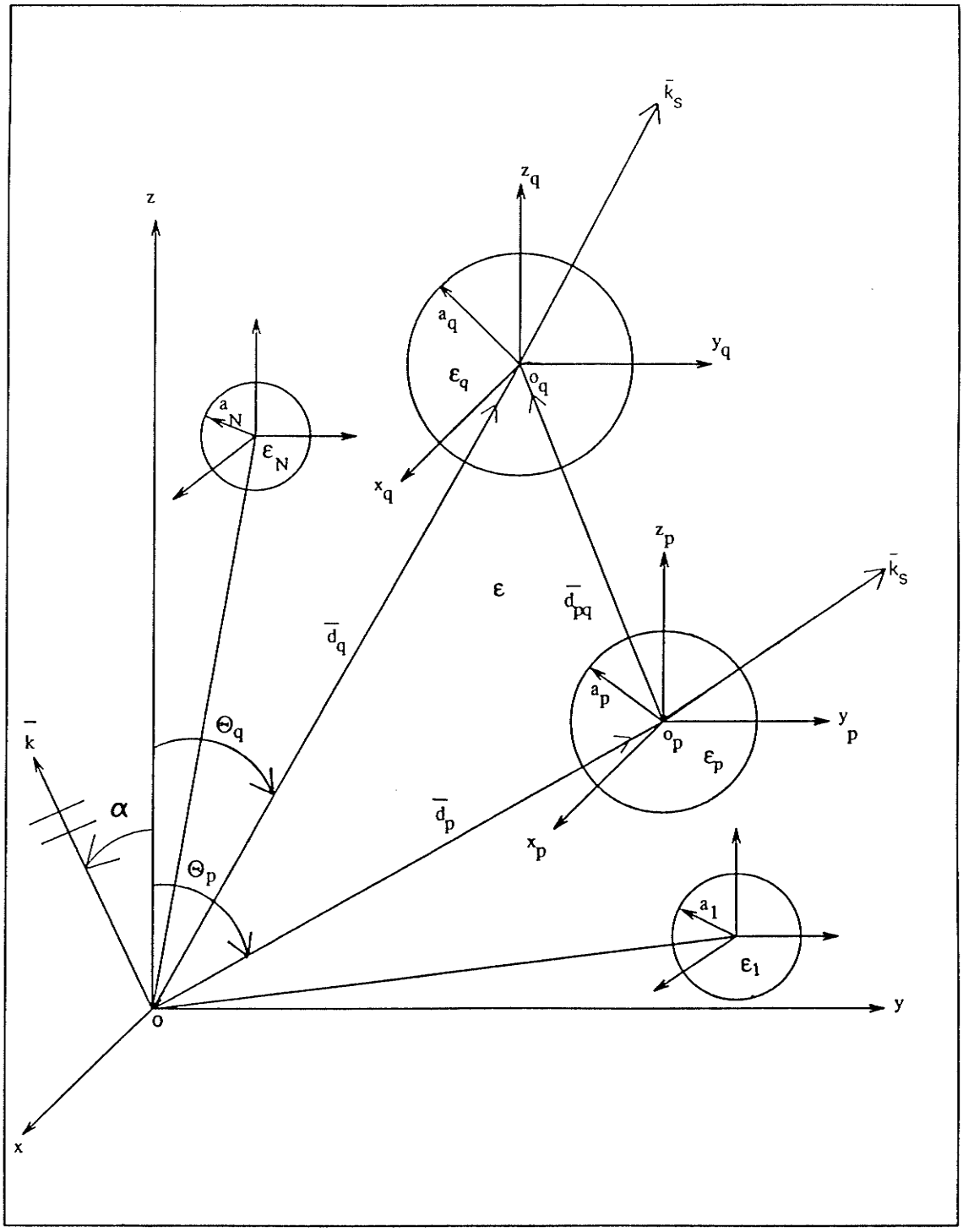

Fig.4-1. Scattering geometry of an arbitrary configuration of dielectric spheres.

$$+A^s_{pM}(m,n)\frac{m}{\sin\theta}P^m_n(\cos\theta)]\sin m\phi\, e^{-jkd_p\zeta_s} \tag{4-10}$$

$$F_{\phi p}(\theta,\phi)=\sum_{n=1}^{\infty}\sum_{m=-n}^{m=n} j^{-n+1}[A^s_{pE}(m,n)\frac{m}{\sin\theta}P^m_n(\cos\theta)$$

$$+A^s_{pM}(m,n)\frac{\partial}{\partial\theta}P^m_n(\cos\theta)]\cos m\phi\, e^{-jkd_p\zeta_s} \tag{4-11}$$

For the special case of a linear array of N spheres, the above expressions reduce to the simpler forms

$$F_{\theta p}(\theta,\phi)=\sum_{n=1}^{\infty}\sum_{m=0}^{m=n} j^{-n+1}\varepsilon_m[A^s_{pE}(m,n)\frac{\partial}{\partial\theta}P^m_n(\cos\theta)$$

$$+A^s_{pM}(m,n)\frac{m}{\sin\theta}P^m_n(\cos\theta)]\sin m\phi\, e^{-jkd_p\cos\theta} \tag{4-12}$$

$$F_{\phi p}(\theta,\phi)=\sum_{n=1}^{\infty}\sum_{m=0}^{m=n} j^{-n+1}\varepsilon_m[A^s_{pE}(m,n)\frac{m}{\sin\theta}P^m_n(\cos\theta)$$

$$+A^s_{pM}(m,n)\frac{\partial}{\partial\theta}P^m_n(\cos\theta)]\cos m\phi\, e^{-jkd_p\cos\theta} \tag{4-13}$$

where ε_m is Neumann's number (1 for $m=0$ and 2 for $m>0$).

In the case of the iterative solution, equations (4-10) and (4-11) take the following forms

$$F_{\theta p}(\theta,\phi)=\sum_{n=1}^{\infty}\sum_{m=-n}^{m=n}\sum_{i=1,2,\ldots} j^{-n+1}\left\{[A^s_{pE_i}(m,n)\frac{\partial}{\partial\theta}P^m_n(\cos\theta)\right.$$

$$\left.+A^s_{pH_i}(m,n)\frac{m}{\sin\theta}P^m_n(\cos\theta)]\sin m\phi\right\}e^{-jk\zeta_s} \tag{4-14}$$

$$F_{\phi p}(\theta,\phi)=\sum_{n=1}^{\infty}\sum_{m=-n}^{m=n}\sum_{i=1,2,\ldots} j^{-n+1}\left\{[A^s_{pE_i}(m,n)\frac{m}{\sin\theta}P^m_n(\cos\theta)\right.$$

$$\left.+A^s_{pH_i}(m,n)\frac{\partial}{\partial\theta}P^m_n(\cos\theta)]\cos m\phi\right\}e^{-jk\zeta_s} \tag{4-15}$$

The bistatic cross section is defined as

$$\sigma(\theta,\phi)=\lim_{r\to\infty} 4\pi r^2\ |\ \bar{E}^s\cdot\hat{t}/E^i\ |^2 \tag{4-16}$$

with the unit vector $\hat{t}$ denoting the direction of the polarization of the field received at the observation point. When $\hat{t}$ has the same direction as $\bar{E}^s$, the normalized bis-

tatic cross section is given by

$$\frac{\sigma(\theta,\phi)}{\pi a_p^2} = \frac{4}{(ka_p)^2}\left[\,|F_\theta(\theta,\phi)|^2 + |F_\phi(\theta,\phi)|^2\right] \tag{4-17}$$

The normalized bistatic cross sections in the E and H planes are obtained by substituting $\phi=\pi/2$ and $\phi=0$, respectively, in equation (4-17).

In the backscatter direction $\theta=\pi-\alpha$ and $\phi=\pi$, the corresponding normalized cross section is

$$\frac{\sigma(\alpha)}{\pi a_p^2} = \frac{4}{(ka_p)^2}\,|F_\phi(\alpha,\pi)|^2 \tag{4-18}$$

where $F_\phi(\alpha,\pi)$ is given by

$$F_{\phi p}(\alpha,\pi)=\sum_{n=1}^{\infty}\sum_{m=0}^{m=n} j^{n+1}\varepsilon_m\left[A_{pE}^s(m,n)\frac{m}{\sin\alpha}P_n^m(\cos\alpha) + A_{pM}^s(m,n)\frac{\partial}{\partial\alpha}P_n^m(\cos\alpha)\right]e^{-jkd_p\cos(\pi-\alpha)} \tag{4-19}$$

For the special case when $\alpha=0$, we obtain from the above equation

$$F_{\phi p}(0,\pi)=-\sum_{n=1}^{\infty} j^{n+1}\,n(n+1)\left[A_{pE}^s(1,n)+A_{pM}^s(1,n)\right]e^{jkd_p} \tag{4-20}$$

4.3 Numerical results

In the computations of the normalized backscattering and bistatic cross sections of one or two-dimensional arrays of spheres, we present numerical results for the normalized backscattering cross section patterns for different systems of spheres of equal and unequal radii versus the separation distance between the spheres in terms of the wavelength and the incidence angle α. The normalized bistatic cross section is presented for systems of identical spheres as a function of the scattering angle θ, corresponding to endfire incidence ($\alpha=0$). The system of matrices in (2-37),(2-38),(3-11) and (3-12) is dimensionally infinite and all series are truncated to an appropriate

finite number in order to generate accurate numerical results. For instance, four digit accuracy is obtained for the computation of the backscattering and bistatic cross sections of three identical spheres (ka=0.5) with kd>3.0 by retaining a number of terms n=5. In the case of endfire incidence on a linear array of spheres, the system of matrices is solved only for $m=1$ due to the rotational symmetry with respect to the z-axis, while in the case of an arbitrary angle of incidence it is sufficient to take $m=0,1,2,3$ for the cases considered.

Figures (4-2) and (4-3) show the normalized bistatic cross section patterns for an equispaced linear array of three and eight conducting spheres. The electrical radius and separation between the successive spheres are ka=0.5 and kd=1.0 (touching), respectively. In addition, these Figures compare the numerical results obtained by the simultaneous boundary conditions solution (SBCS) (chapter 2), with the iterative boundary conditions solution (IBCS) in chapter 3. It can be seen that the agreement between the two methods is not satisfactory for the first order scattered field ($i=1$). This is so, since the first order scattered field does not take into account the interaction fields between the spheres and hence $i=1$ represents the sum of the field scattered by each sphere due to the incident plane wave only. The significance of the multiply scattered fields between the spheres can be seen in the second order term which includes the scattered fields due to the plane wave incidence plus the scattered fields due to first order fields incident on each sphere. However, the process of iteration is terminated after obtaining the fourth order of scattering, where the numerical results converge to the same level of accuracy as the simultaneous boundary conditions solution. The results indicate that the first and second orders are only needed to obtain convergent solutions in the backward scattering cross section, while four

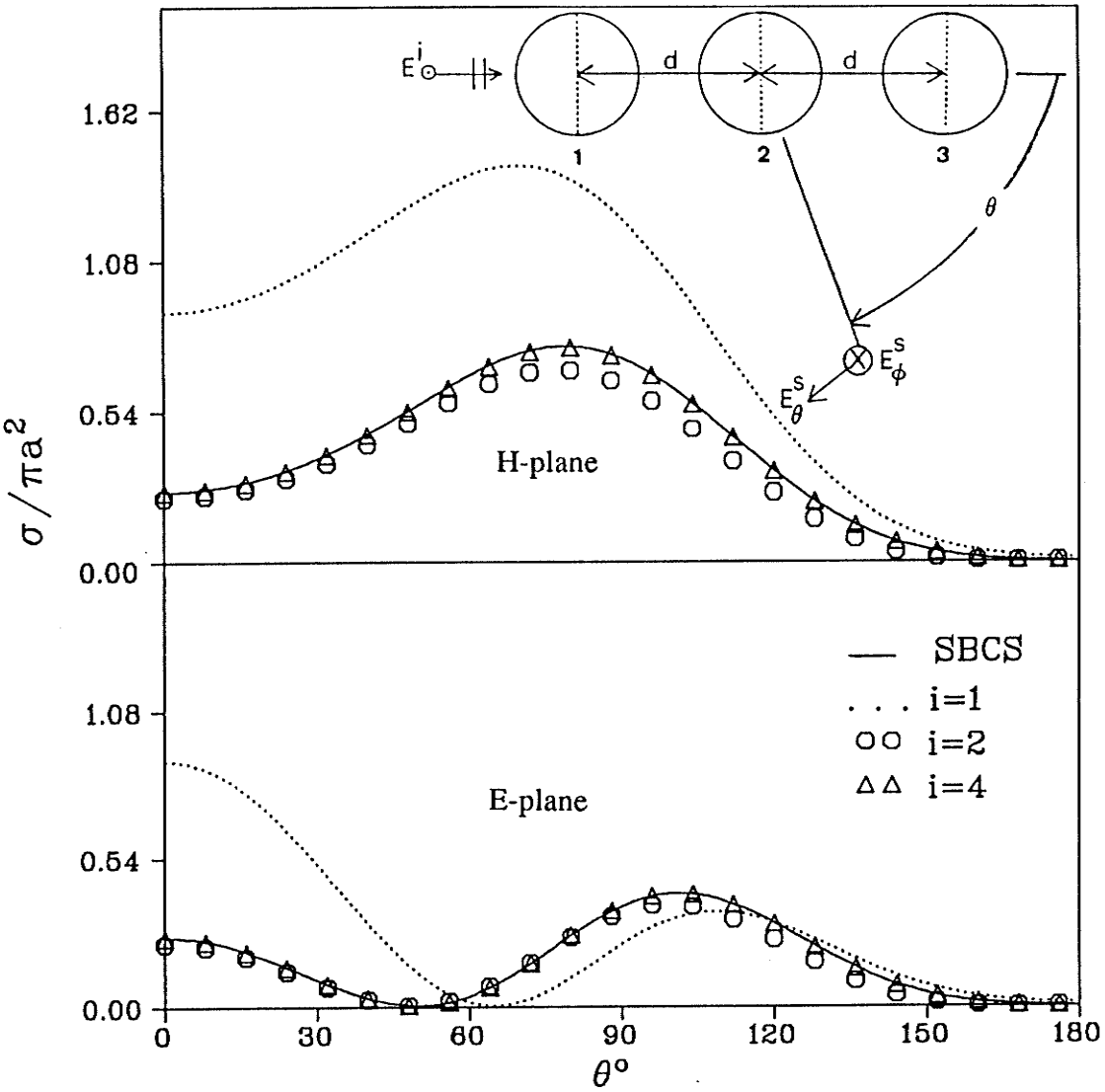

Fig.4-2. Normalized bistatic cross section patterns as a function of scattering angle θ for a system of three identical spheres, with ka=0.5, kd=1.0.

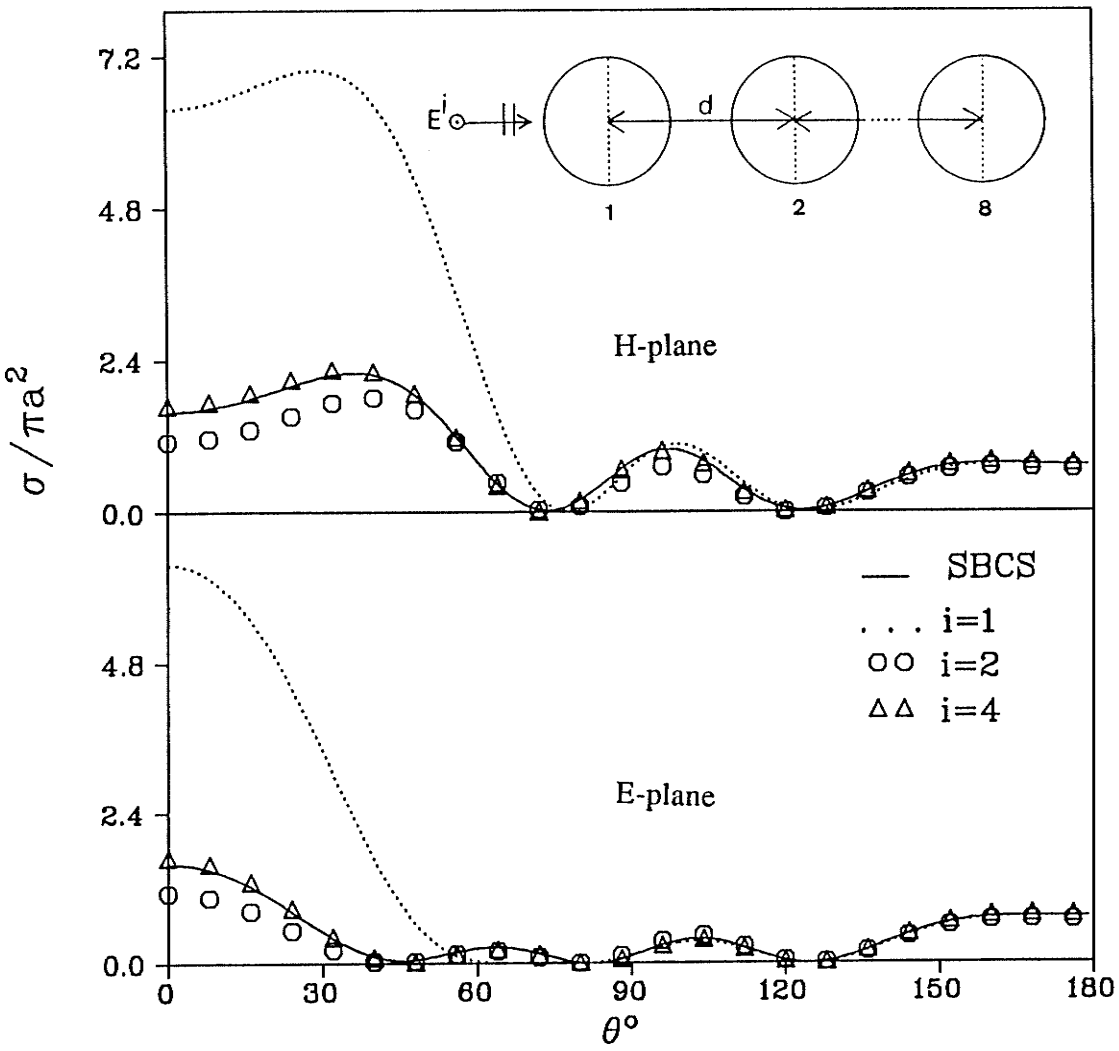

Fig.4-3. Normalized bistatic cross section patterns as a function of scattering angle θ for a system of eight identical spheres, with ka=0.5, kd=1.0.

orders are needed in the forward scattering cross section. In order to terminate the iteration process, the scattered field after each iteration is calculated and divided by the total field scattered from all previous iterations; in most of the cases the process has been terminated when the ratio was smaller than 10^{-4}.

Figures (4-4) and (4-5) present the bistatic cross section patterns for the same geometry and angle of incidence but the electrical separation is increased to kd=2.0. It is interesting to note that the first order solution gives good results in the backward scattering cross section direction namely, $\theta \geq 70^{o}$. However, the process of iteration is terminated after obtaining the first and second orders. We see from these two figures that the higher order scattered fields become weaker as kd increases and can be neglected in this case for $i \geq 2$, since the higher orders have no significant numerical contribution to the total scattered field. It is also interesting to note that by increasing kd from 1 to 2, the magnitude of the forward scattering cross section is increased while the bistatic cross section patterns vanish at certain scattering angles. Figure (4-6) shows the normalized bistatic cross section patterns for a system of five equal spheres with ka=1.5 and kd=4.0. The computer time required to compute the results in the latter example by using the (IBCS) is about 50% less than using the (SBCS).

Figure (4-7) gives the normalized bistatic cross section patterns for three dielectric spheres of the same geometry as in Fig. (4-2) with the dielectric constant ε_r equal to 3.0. It interesting to see that only the first and second orders are needed to achieve the same accuracy by using the (SBCS). This is partly due to the weak coupling between the dielectric spheres.

Figure (4-8) shows the bistatic cross section patterns of a two-dimensional array

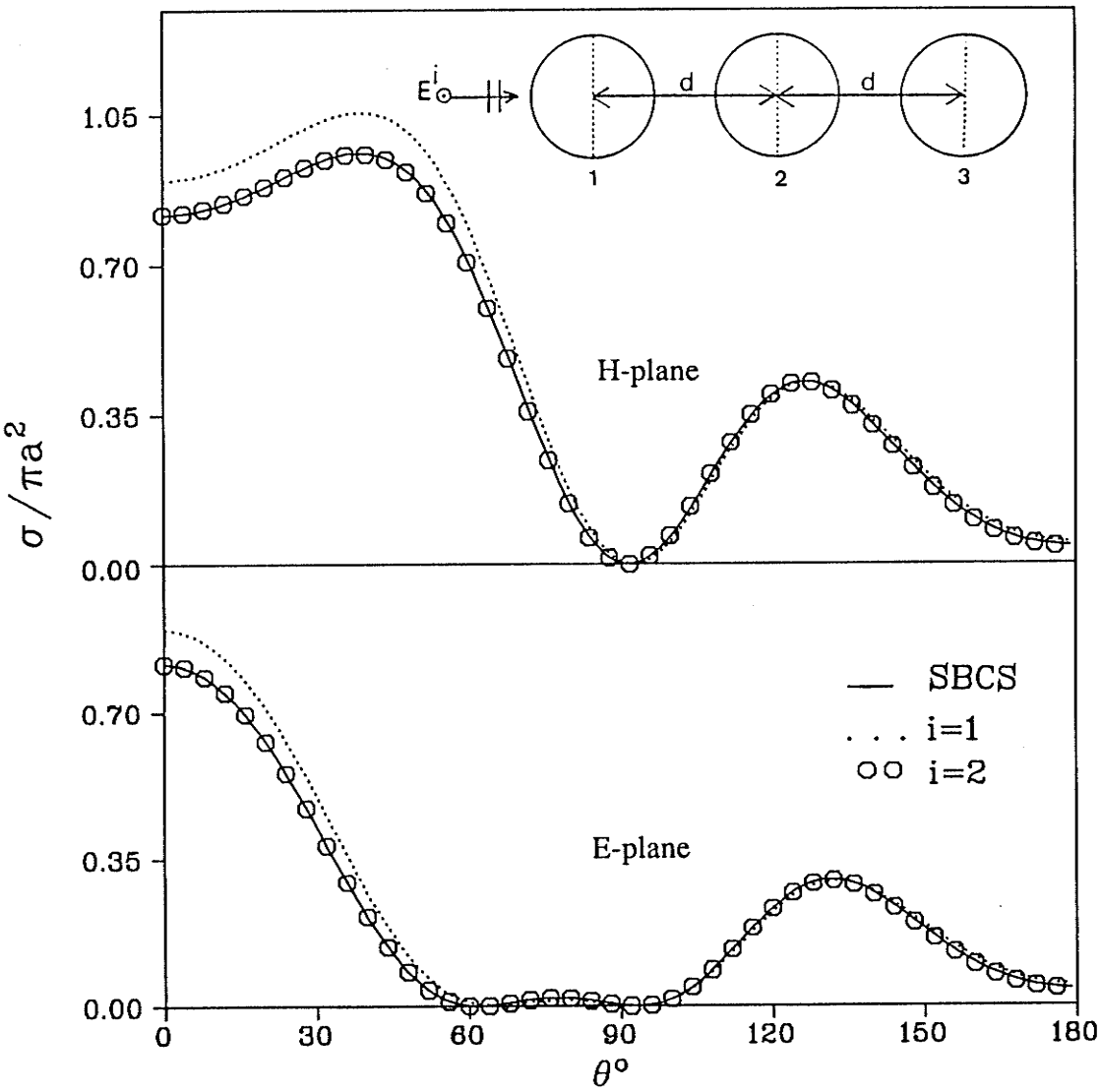

Fig.4-4. Normalized bistatic cross section patterns as a function of scattering angle θ for a system of three identical spheres, with ka=0.5, kd=2.0.

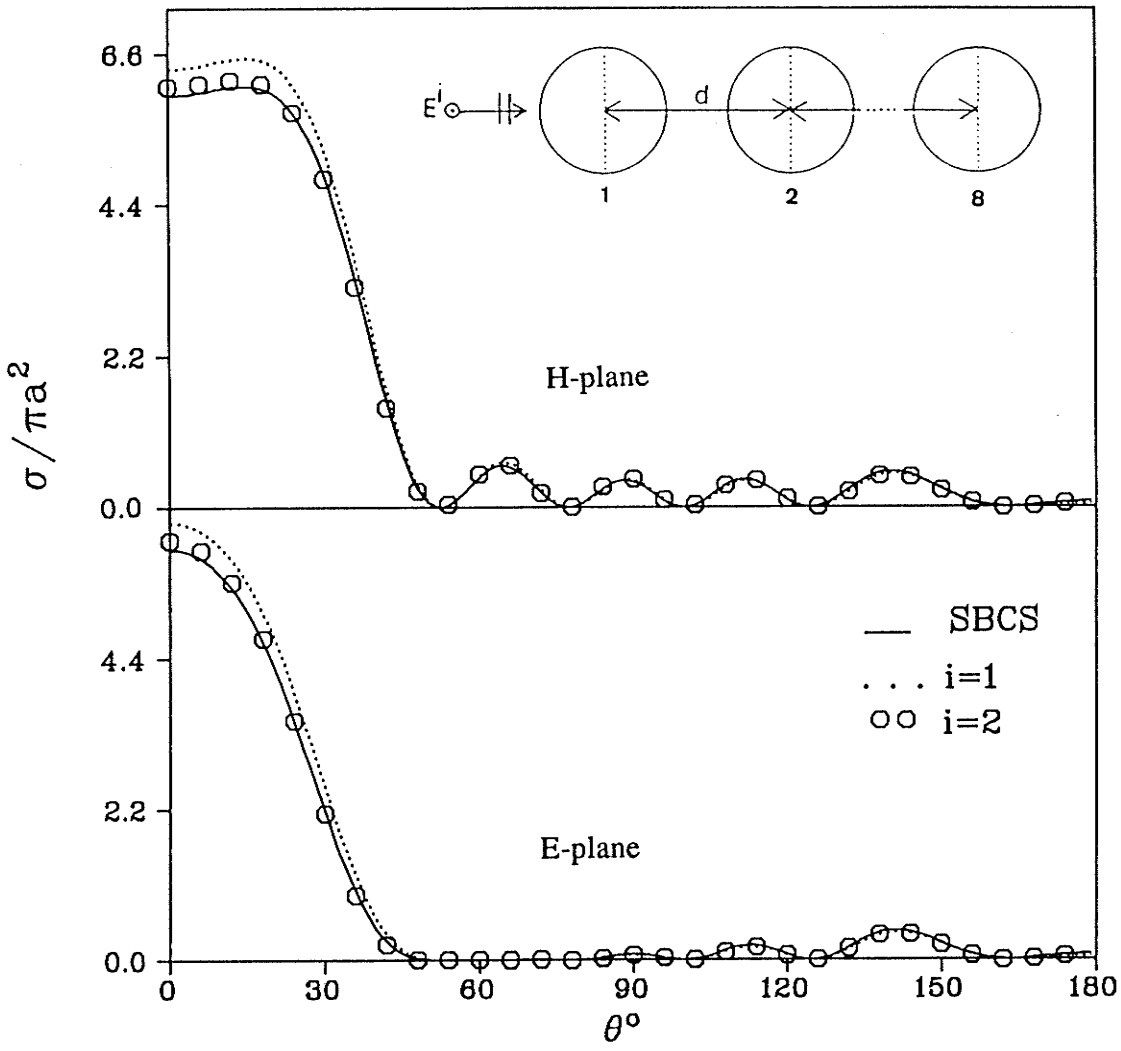

Fig.4-5. Normalized bistatic cross section patterns as a function of scattering angle θ for a system of eight identical spheres, with ka=0.5, kd=2.0.

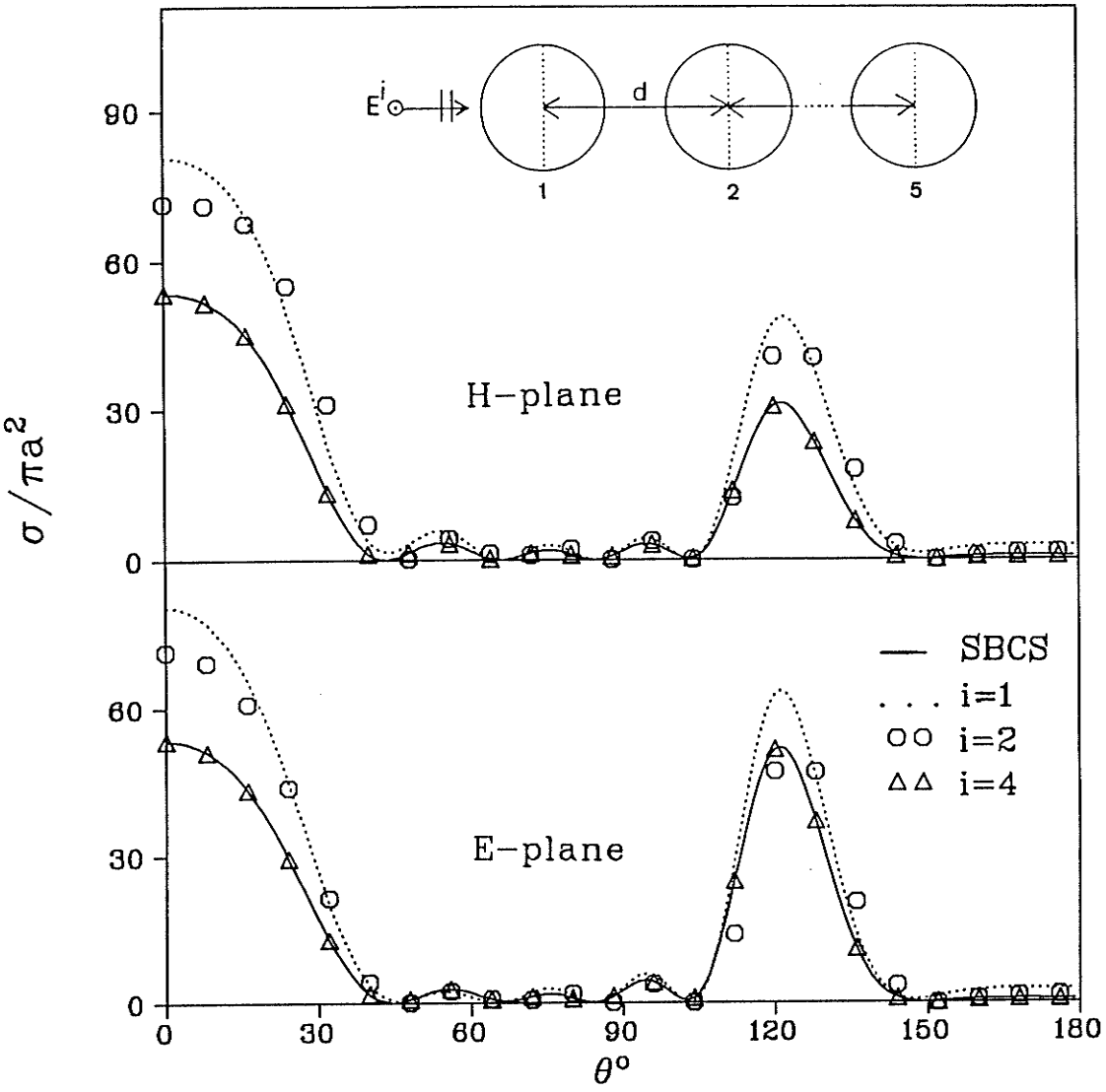

Fig.4-6. Normalized bistatic cross section patterns as a function of scattering angle θ for a system of eight identical spheres, with ka=1.5, kd=4.0.

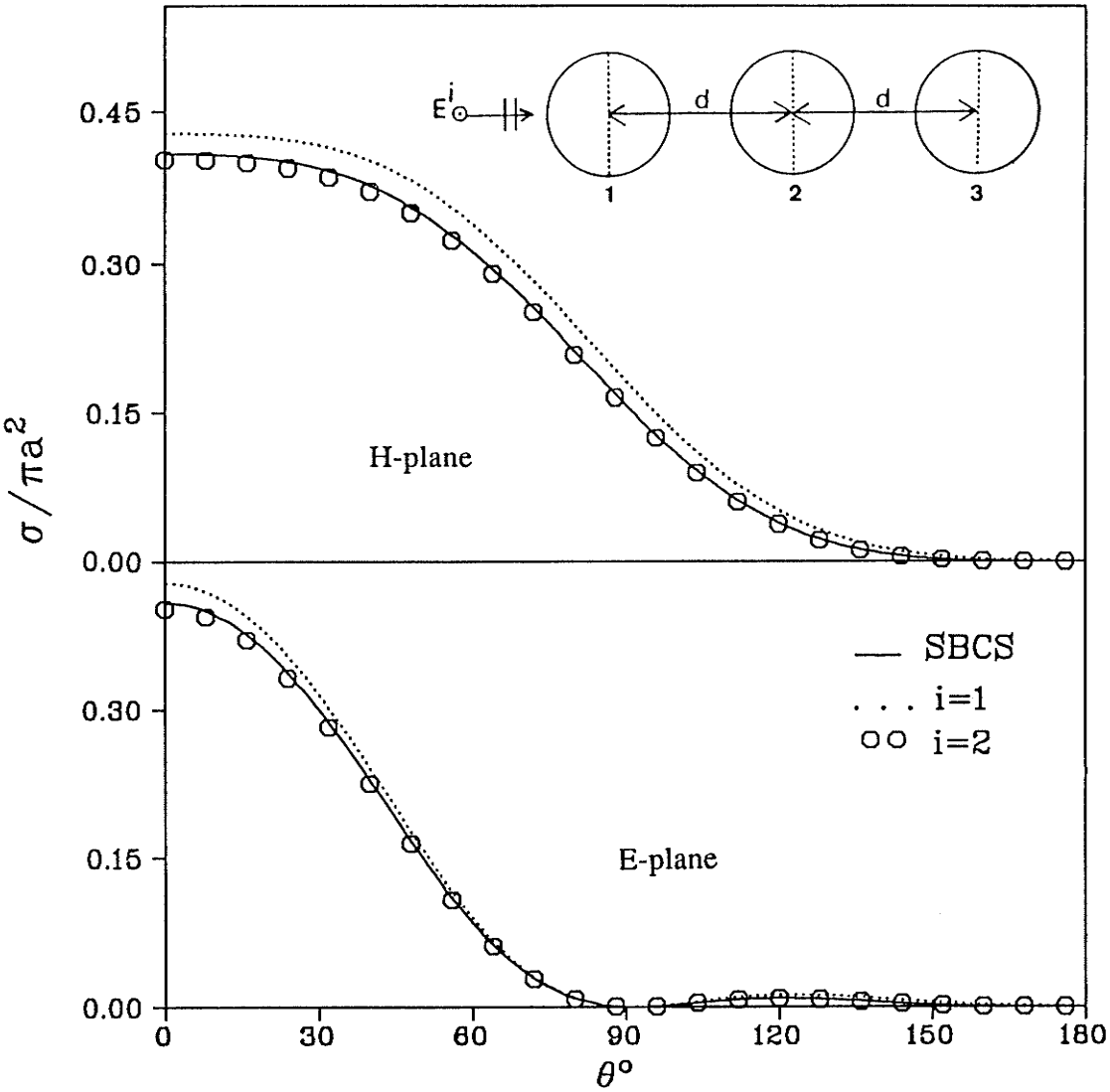

Fig.4-7. Normalized bistatic cross section patterns as a function of the scattering angle θ for a system of three identical spheres with ka=0.5, kd=1.0, ε_r=3.0.

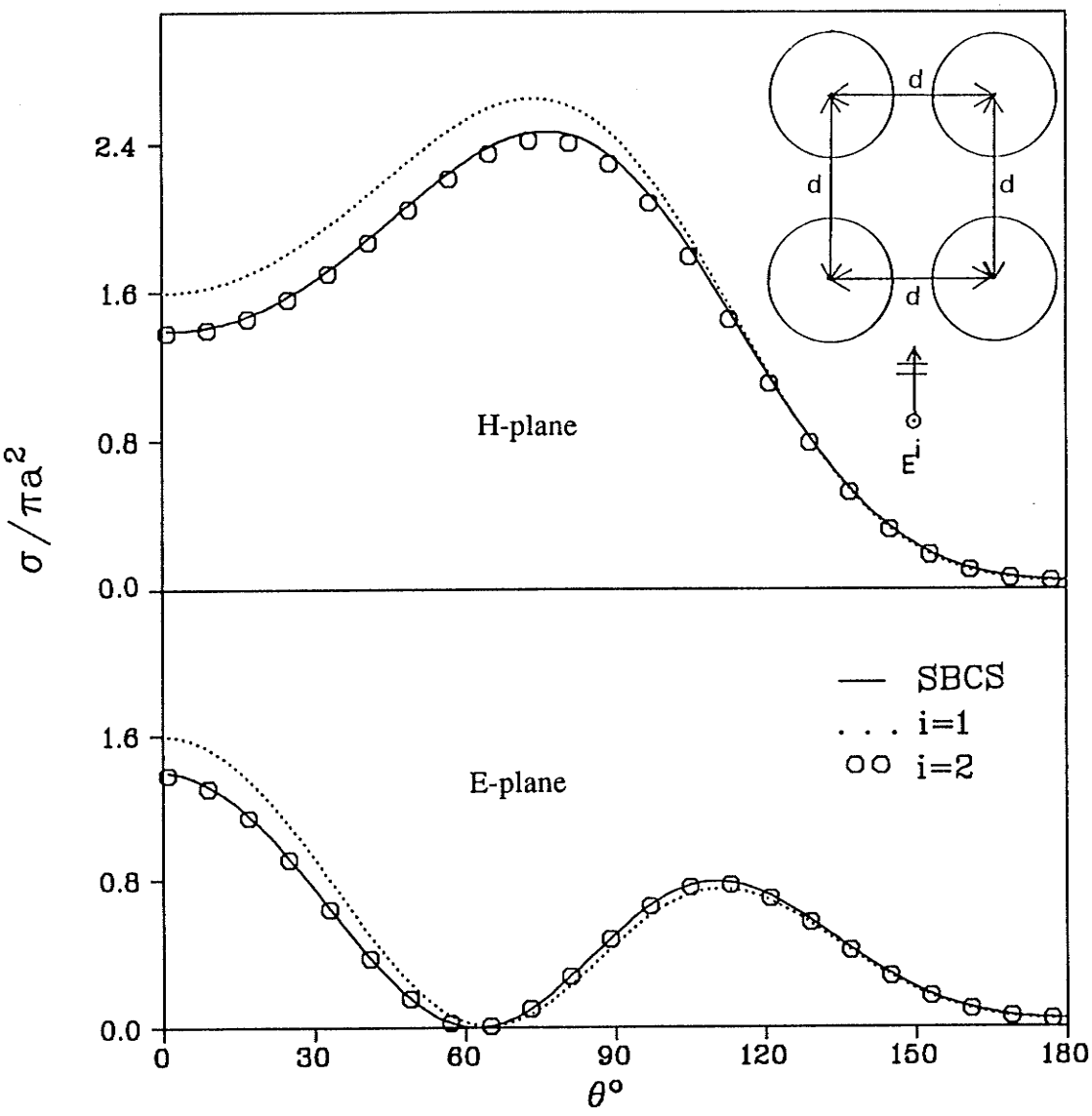

Fig.4-8. Normalized bistatic cross section patterns as a function of the scattering θ for a two-dimensional array of four spheres with ka=0.5, kd=1.5 ,$\varepsilon_r=\infty$.

of four conducting spheres with ka=0.5 located at the vertices of a square which has a side length kd equal to 1.5. Figure (4-9) presents the same geometry for dielectric spheres with ε_r=3.0. We can see from these examples that, contrary to expectation, the number of iterations required for an arbitrary configuration of four dielectric spheres is less than for the same configuration of conducting spheres.

Numerical results are also plotted for the normalized backscattering cross section patterns for different systems of spheres of equal and unequal radii versus the electrical separation between the spheres (kd) and the incidence angle (α).

Figures (4-10) and (4-11) present the normalized backscattering cross section patterns as a function of α for an array of three and five conducting spheres with ka=0.5 and kd=1.0 (touching). The results show a discrepancy between the two methods for the first and second orders, namely for $\alpha \geq 30^o$, and which is significant in the broadside incidence case until i is increased to 4. In addition, the magnitude of the backscattering cross section pattern increases with α, since the fields scattered from the spheres are more in phase while four orders are required to obtain a convergent solution. This is in contrast with the endfire incidence where the results show that the first and second orders are sufficient to obtain a convergent solution. A possible interpretation of this result is that the fields scattered from the remaining spheres are shielded by the front sphere in the illuminated region. On the other hand, Fig. (4-11) illustrates that by increasing the number of spheres from three to five, the magnitude of the backscattering cross section pattern vanishes at $\alpha=54^o$.

In Figures (4-12) and (4-13) we have plotted the normalized backscattering cross section patterns for an array of three and five spheres versus kd with ka=0.5.

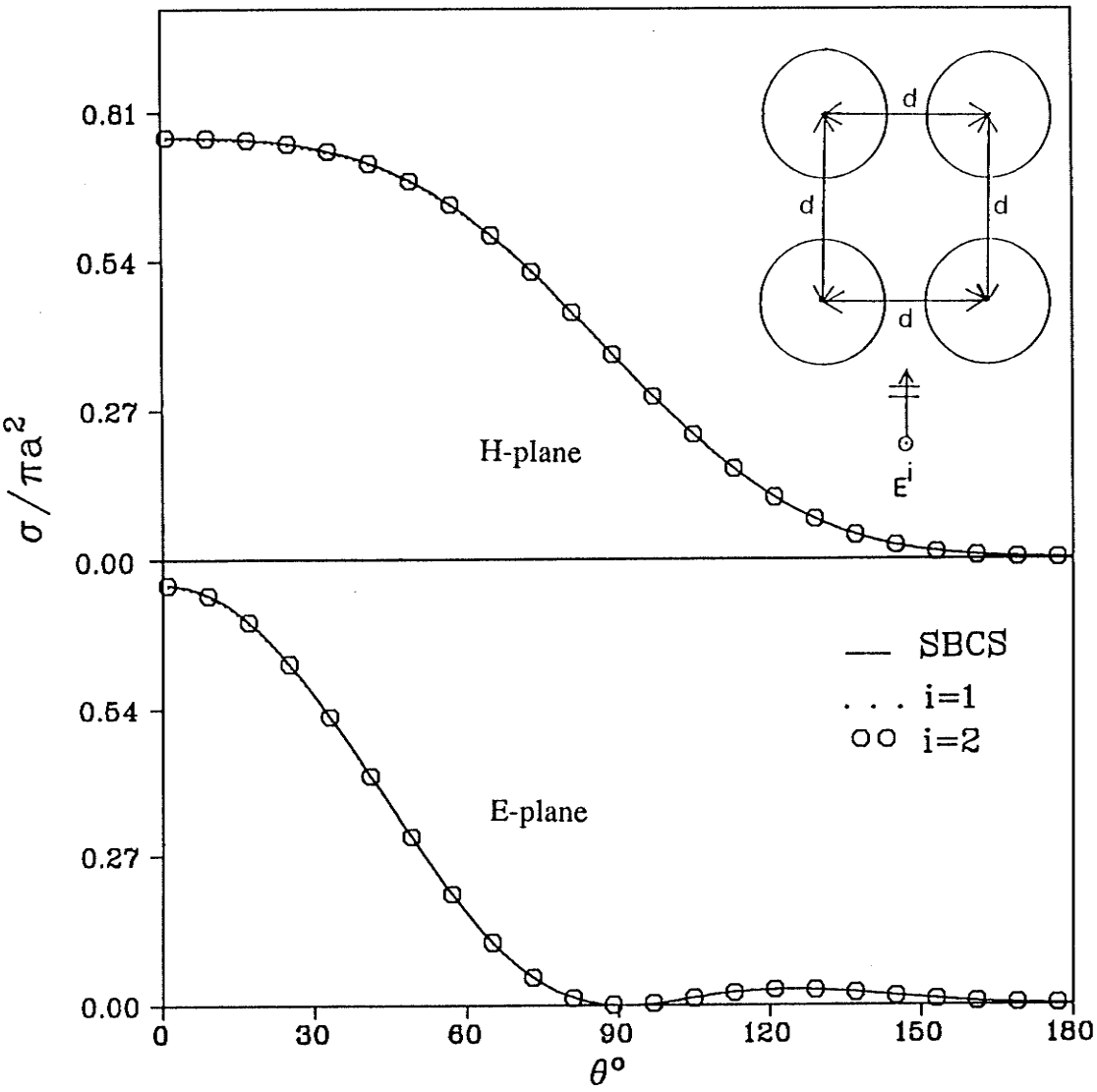

Fig.4-9. Normalized bistatic cross section patterns as a function of the scattering θ for a two-dimensional array of four spheres with ka=0.5, kd=1.5 , ε_r=3.0.

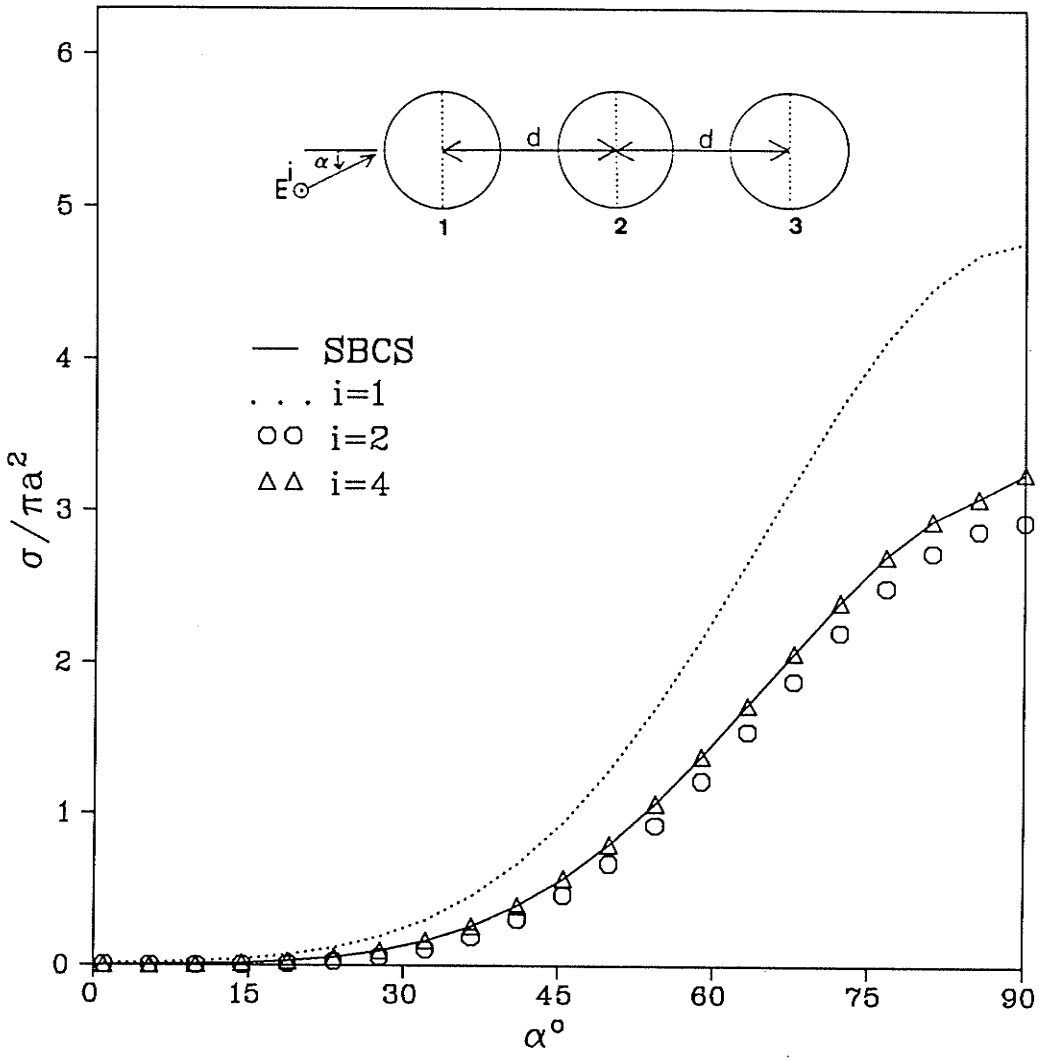

Fig.4-10. Normalized backscattering cross section patterns as a function of incidence angle α for a system of three identical spheres, with ka=0.5, kd=1.0.

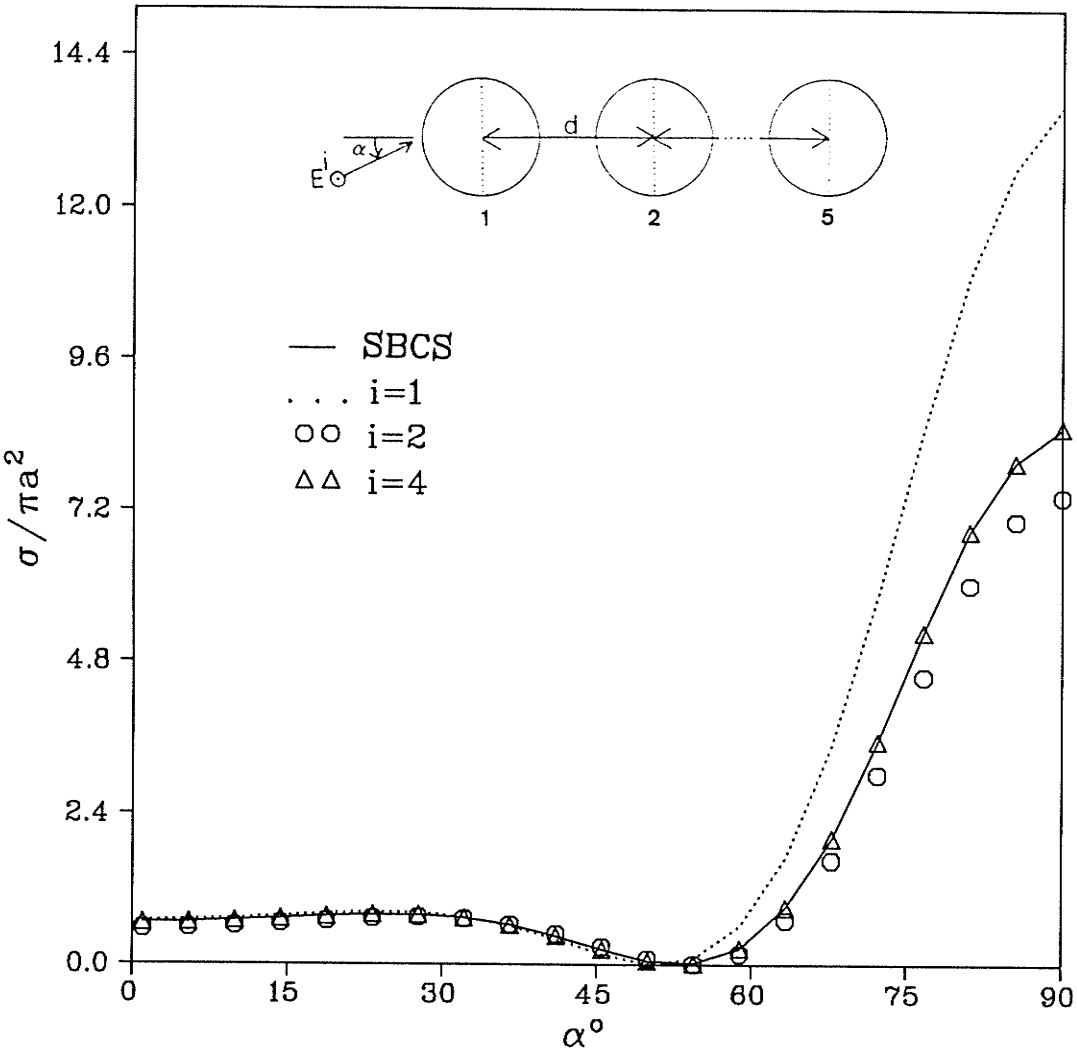

Fig.4-11. Normalized backscattering cross section patterns as a function of incidence angle α for a system of five identical spheres, with ka=0.5, kd=1.0.

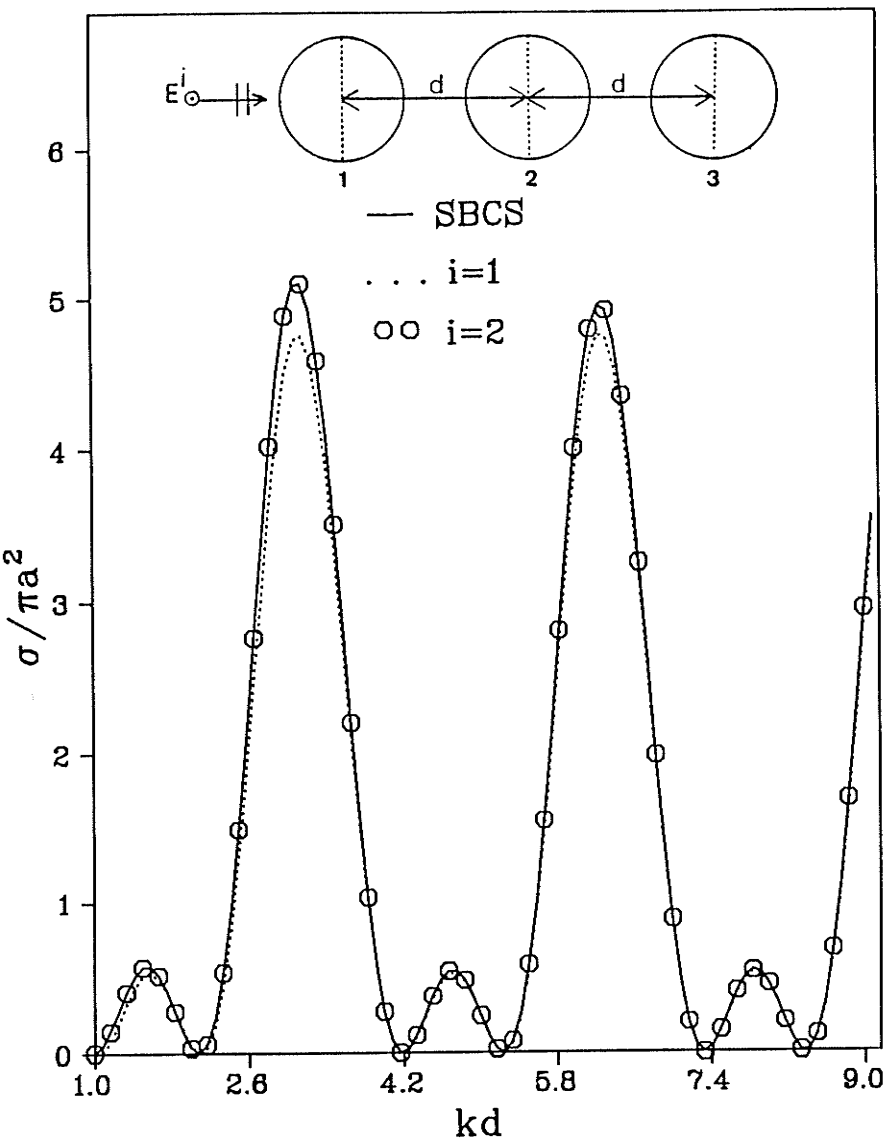

Fig.4-12. Normalized backscattering cross section as a function of kd for a system of three identical spheres, with ka=0.5 and endfire incidence.

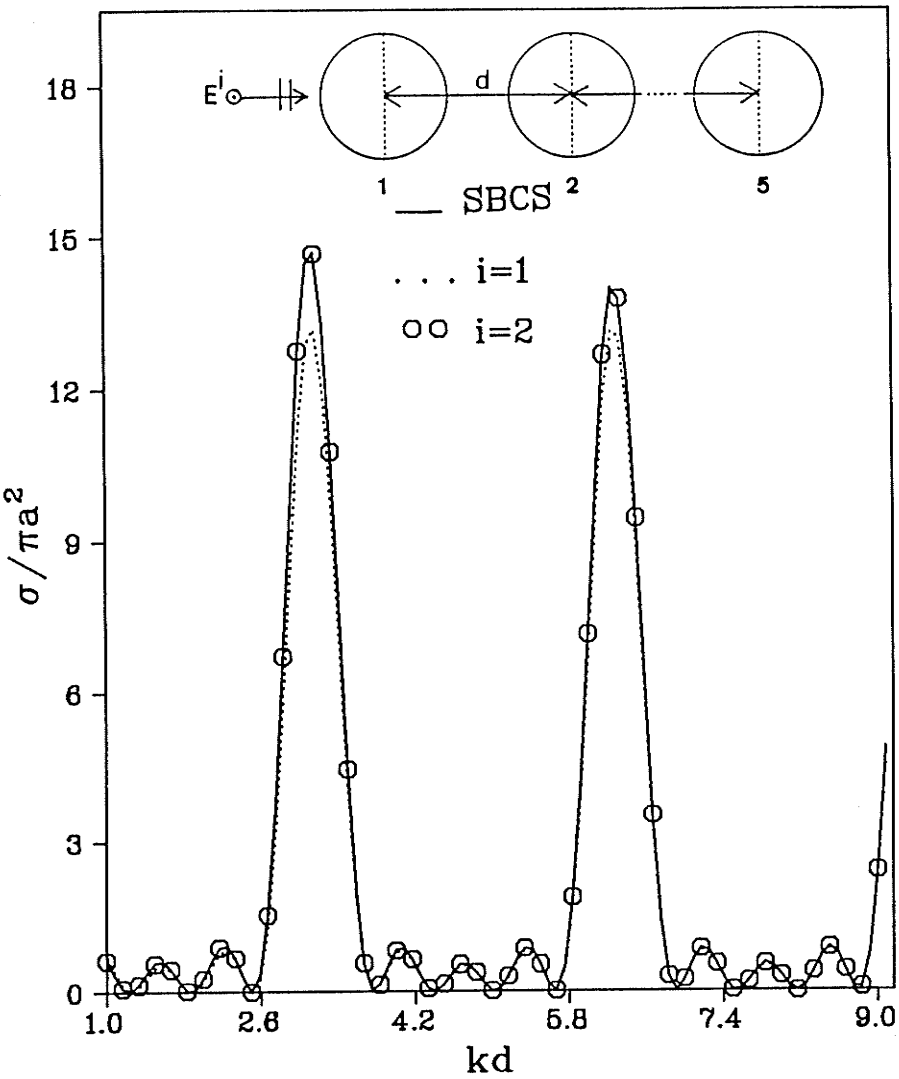

Fig.4-13. Normalized backscattering cross section as a function of kd for a system of five identical spheres, with ka=0.5 and endfire incidence.

The agreement is satisfactory except for a small deviation which occurs approximately every kd=π, due to the resonance between the spheres.

One of the main goals of this thesis is to present some numerical results showing how three-dimensional bodies can be simulated in a scattering sense by a collection of spheres. We select her for our study the scattering by a spheroid due to an axial electromagnetic plane wave incidence, since the spheroid has an exact and numerical solutions available in the literature. Three spheres are needed to simulate the scattering by a spheroid of a major axis ka=1 and with an axial ratio 2. The small spheres have an electrical radii ka=0.25, while the larger sphere in the middle has an electrical radius ka=0.5. The separation distance between the successive spheres is equal to 0.75 (touching). Figure (4-14) shows the normalized bistatic cross section patterns (E-plane) obtained by Sinha and MacPhie [41] using the vector spheroidal wave functions (solid curve) compared with the data obtained using three spheres. It can be seen that the two curves deviate, and the deviation vanishes as the scattering angle increases. Figure (4-15) shows another example of the scattering by a dielectric spheroid with a dielectric constant ε_r=3.0 [24]. Once again, the results show a deviation in the forward scattering while a good agreement is achieved in the backscattering cross section.

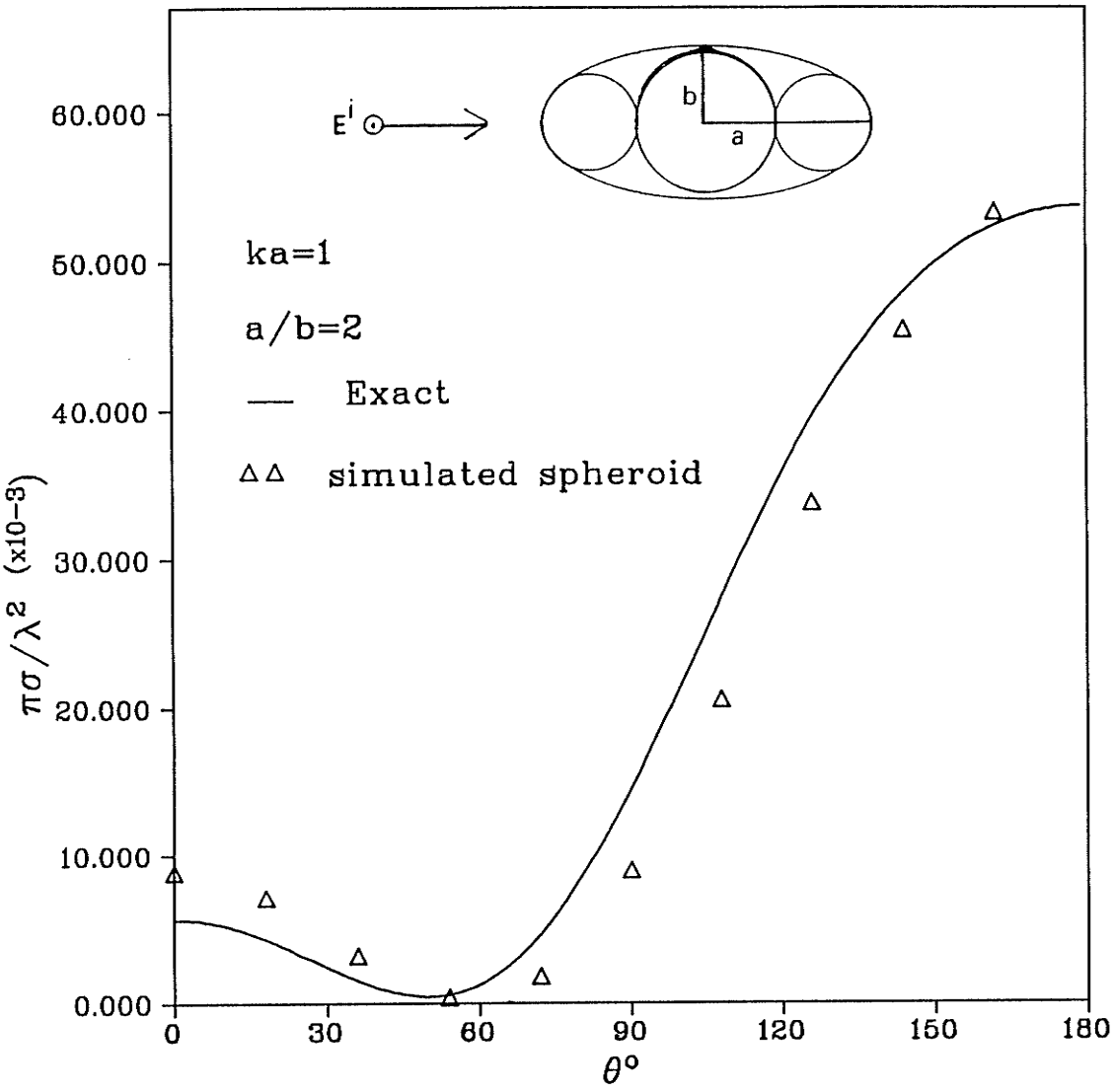

Fig.4-14. Normalized bistatic cross section as a function of the scattering angle θ for a perfectly conducting spheroid.

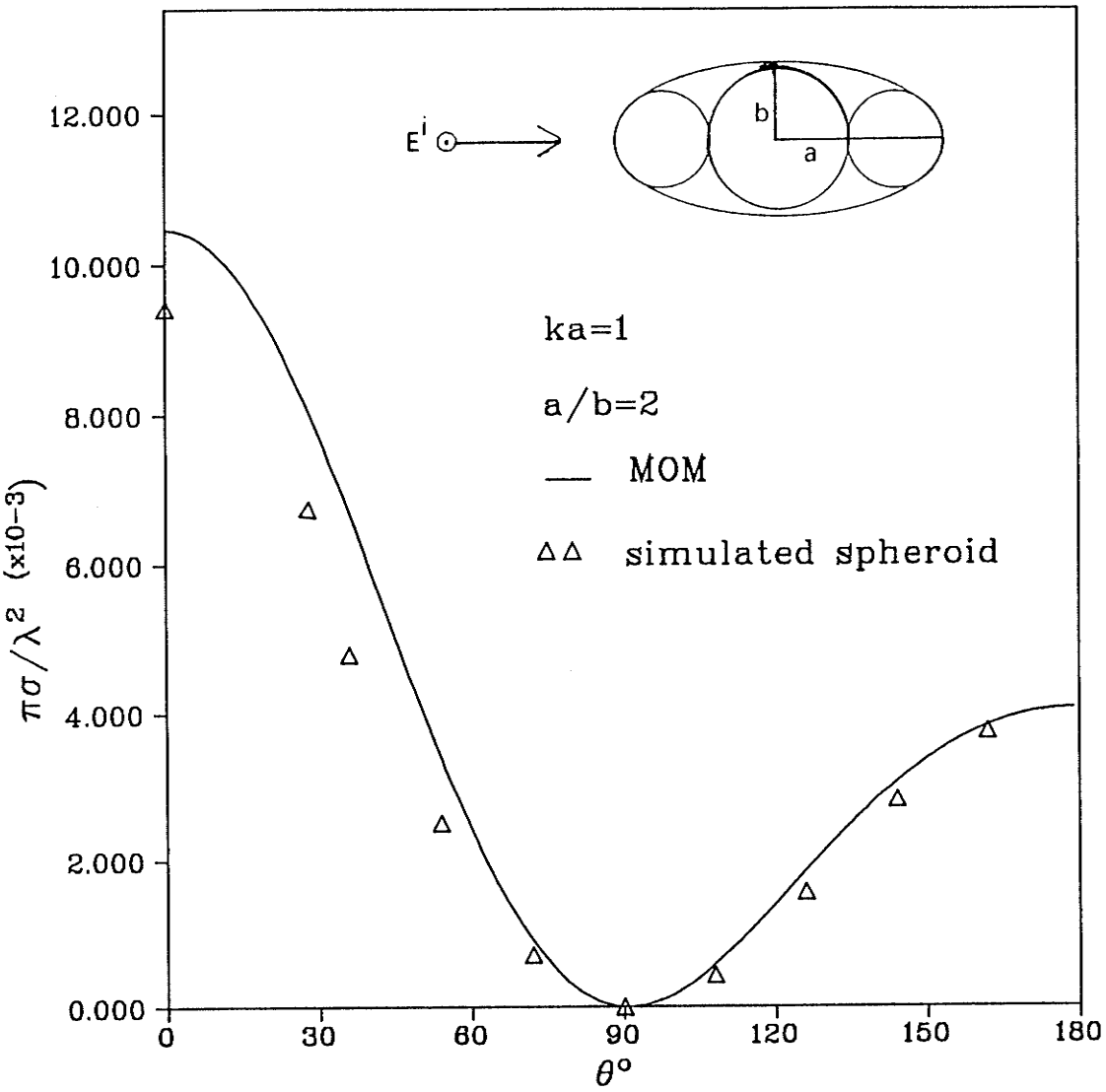

Fig.4-15. Normalized bistatic cross section as a function of the scattering angle θ for a dielectric spheroid, ε_r=3.0.

CHAPTER 5

APPROXIMATE METHOD FOR THE SCATTERING BY A LINEAR ARRAY OF CONDUCTING OR DIELECTRIC SPHERES

In chapters 2 and 3, the scattering by an arbitrary configuration of N conducting or dielectric spheres is formulated analytically using the translation addition theorem in order to impose the boundary conditions at the surface of each sphere. The special case of a linear array of N conducting or dielectric spheres is deduced by spacing the spheres along the z-axis. Although, the analytic solutions are valid for any spheres size and electrical separation distances, it has been established that an efficient approximate solution gives very good numerical results for small spheres when compared with the analytic solutions [32,33,39]. Thus, the purpose of presenting such a solution is to save computer time as well as computer memory by avoiding computation of the series resulting from the application of the translation addition theorem and hence leads to faster convergence.

For the two-dimensional scattering case, Karp and Rusek [42] used fictitious line sources to account for the multiple scattering by two half planes forming a wide slit geometry. Thus, the total scattered field by each half plane is considered due to the incident plane wave and, in addition, to a line source response of unknown magnitude located at the edge of the opposite half plane. Ragheb [9] extended the analysis to the scattering by an arbitrary configuration of N small circular conducting cylinders, while Elsherbeni [43] employed the same technique to the diffraction by two conducting wedges.

In the case of three-dimensional scattering, an approximate solution to the scattering by two identical spheres with large electrical radii was obtained by Bruning and Lo [44] using a ray-optical solution. However, the formulation becomes tedious for the case of more than two spheres because the geometric optics and creeping rays suffer numerous reflections and diffractions which limit the usefulness of the method. On the other hand, Bhartia [45] employed the solution derived by Senior and Goodrich [2] to obtain an asymptotic solution for the scattering by two large spheres as well. This solution involved the application of Watson's transform to the exact Mie series solution where the scattered field by two spheres is expressed as a sum of geometrical optics and creeping waves.

In this chapter a simple approximate method for the case of a linear array of N spheres ($N \geq 2$) is proposed for arbitrary plane wave incidence as shown in Fig. 5-1. For spheres with small electrical radii we make the approximation that the scattered field from each sphere is due to the incident field plus the scattered fields from the remaining spheres approximated by axial plane waves of unknown magnitudes. To evaluate the unknown magnitudes we impose the condition that the far field scattered by each sphere due to an axial plane wave of unknown magnitude representing the interaction with another sphere, be equal to the far field scattered by the sphere considered due to the total field scattered by the second sphere. The accuracy of the far field quantity depends on the radii and separations between the spheres and will be verified numerically by comparison with the analytic solutions.

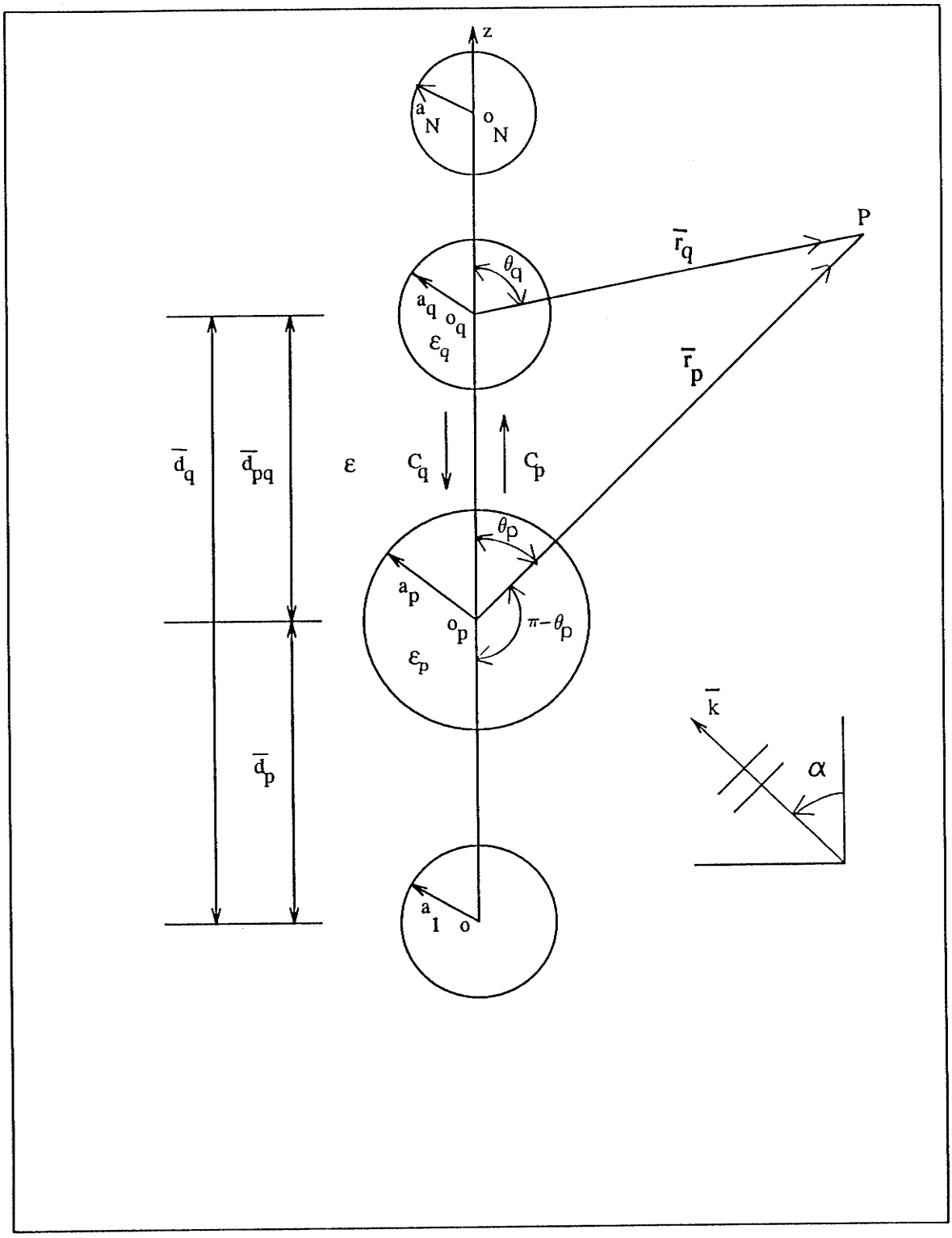

Fig.5-1. Illustration of multiply scattered field of a linear array of dielectric spheres.

5.1 Far scattered field components

The two components of the far scattered electric field from the pth dielectric sphere in the E and H planes due to an arbitrary plane wave incidence can be written as [2,32]

$$f_{\theta p}(\alpha,r_p,\theta_p,\phi_p) = \frac{e^{jkr_p}}{kr_p}\sum_{n=1}^{\infty}\sum_{m=0}^{m=n}\varepsilon_m\, j^{-n+1}[\Psi_{pE}(\alpha,m,n)\,\frac{\partial}{\partial\theta_p}P_n^m(\cos\theta_p) + \Psi_{pM}(\alpha,m,n)\frac{m\,P_n^m(\cos\theta_p)}{\sin\theta_p}]\sin m\phi_p \quad (5\text{-}1)$$

$$f_{\phi p}(\alpha,r_p,\theta_p,\phi_p) = \frac{e^{jkr_p}}{kr_p}\sum_{n=1}^{\infty}\sum_{m=0}^{m=n}\varepsilon_m\, j^{-n+1}[\Psi_{pE}(\alpha,m,n)\,\frac{m\,P_n^m(\cos\theta_p)}{\sin\theta_p} + \Psi_{pM}(\alpha,m,n)\,\frac{\partial}{\partial\theta_p}P_n^m(\cos\theta_p)]\cos m\phi_p \quad (5\text{-}2)$$

where the coefficients $\Psi_{pE}(\alpha,m,n)$ and $\Psi_{pM}(\alpha,m,n)$ are given by

$$\Psi_{pE}(\alpha,m,n) = -j^n\frac{(2n+1)}{n(n+1)}\frac{(n-m)!}{(n+m)!}\frac{mP_n^m(\cos\alpha)}{\sin\alpha}\cdot v_n(\rho_p)\,e^{jkd_p\cos\alpha} \quad (5\text{-}3)$$

$$\Psi_{pM}(\alpha,m,n) = -j^n\frac{(2n+1)}{n(n+1)}\frac{(n-m)!}{(n+m)!}\frac{\partial P_n^m(\cos\alpha)}{\partial\alpha}\cdot u_n(\rho_p)\,e^{jkd_p\cos\alpha} \quad (5\text{-}4)$$

Here $v_n(\rho_p)$ and $u_n(\rho_p)$ are the scattered field coefficients of a single dielectric sphere given in equations (2-39) and (2-40), while in the case of a perfectly conducting sphere the coefficients in equations (2-55) and (2-56) should be used.

For the limiting case where the direction of the incident plane wave coincides with the direction of the z-axis (α=0), equations (5-3) and (5-4) reduce to

$$\Psi_{pE}(0,1,n) = -j^n\frac{2n+1}{2n(n+1)}\cdot v_n(\rho_p)\,e^{jkd_p} \quad (5\text{-}5)$$

$$\Psi_{pM}(0,1,n) = -j^n\frac{2n+1}{2n(n+1)}\cdot u_n(\rho_p)\,e^{jkd_p} \quad (5\text{-}6)$$

In the forward scattering, where $\theta_p=0$, the two components of the scattered electric field in equations (5-1) and (5-2) are singular. Therefore, to overcome this problem,

the following approximations are used

$$\lim_{\theta_p \to 0} \frac{P_n^1(\cos\theta_p)}{\sin\theta_p} = -\frac{n(n+1)}{2} \tag{5-7}$$

$$\lim_{\theta_p \to 0} \frac{\partial}{\partial\theta_p} P_n^1(\cos\theta_p) = -\frac{n(n+1)}{2} \tag{5-8}$$

With the above simplifications, equations (5-1) and (5-2) yield the expressions for the forward scattered field as follows:

$$f_{\theta p}(\alpha, r_p, 0, \phi_p) = -\frac{e^{jkr_p}}{kr_p} \sum_{n=1}^{\infty} j^{-n+1} n(n+1) [\Psi_{pE}(\alpha,1,n) + \Psi_{pM}(\alpha,1,n)] \sin\phi_p \tag{5-9}$$

$$f_{\phi p}(\alpha, r_p, 0, \phi_p) = -\frac{e^{jkr_p}}{kr_p} \sum_{n=1}^{\infty} j^{-n+1} n(n+1) [\Psi_{pE}(\alpha,1,n) + \Psi_{pM}(\alpha,1,n)] \cos\phi_p \tag{5-10}$$

where the coefficients $\Psi_{pE}(\alpha,1,n)$ and $\Psi_{pM}(\alpha,1,n)$ are

$$\Psi_{pE}(\alpha,1,n) = -j^n \frac{(2n+1)}{n(n+1)} \frac{1}{(n+1)} \frac{P_n^1(\cos\alpha)}{\sin\alpha} \cdot v_n(\rho_p) e^{jkd_p\cos\alpha} \tag{5-11}$$

$$\Psi_{pM}(\alpha,1,n) = -j^n \frac{(2n+1)}{n(n+1)} \frac{1}{(n+1)} \frac{\partial P_n^1(\cos\alpha)}{\partial\alpha} \cdot u_n(\rho_p) e^{jkd_p\cos\alpha} \tag{5-12}$$

Adding the two components of the forward scattered field in equations (5-9) and (5-10), we obtain

$$[f_{\theta p}(\alpha, r_p, 0, \phi_p)\hat{\theta} + f_{\phi p}(\alpha, r_p, 0, \phi_p)\hat{\phi}] = -\frac{e^{jkr_p}}{kr_p} \sum_{n=1}^{\infty} j^{-n+1} n(n+1) [\Psi_{pE}(\alpha,1,n) + \Psi_{pM}(\alpha,1,n)] \cdot (\sin\phi_p \hat{\theta} + \cos\phi_p \hat{\phi}) \tag{5-13}$$

When $\theta_p = 0$, we have the following transformation identity:

$$\sin\phi_p \hat{\theta} + \cos\phi_p \hat{\phi} = \hat{y} \tag{5-14}$$

Substituting equation (5-14) into (5-13) yields

$$[f_{\theta p}(\alpha, r_p, 0, \phi_p)\hat{\theta} + f_{\phi p}(\alpha, r_p, 0, \phi_p)\hat{\phi}] = -\frac{e^{jkr_p}}{kr_p} \sum_{n=1}^{\infty} j^{-n+1} n(n+1) \cdot [\Psi_{pE}(\alpha,1,n) + \Psi_{pM}(\alpha,1,n)] \hat{y} \tag{5-15}$$

Equation (5-15) may be written in a more convenient form as

$$[\,f_{\theta p}(\alpha,r_p,0,\phi_p)\,\hat{\theta}+f_{\phi p}(\alpha,r_p,0,\phi_p)\,\hat{\phi}\,]=g_{p1}(\alpha,r_p,0)\,\hat{y} \tag{5-16}$$

where

$$g_{p1}(\alpha,r_p,0)=-\frac{e^{jkr_p}}{kr_p}\sum_{n=1}^{\infty}j^{-n+1}\,n(n+1)\,[\,\Psi_{pE}(\alpha,1,n)+\Psi_{pM}(\alpha,1,n)\,] \tag{5-17}$$

In the backscattering direction, where $\theta=\pi$, the two components of the far scattered electric field are singular as well. Thus, one may employ the following relations

$$\lim_{\theta_p\to\pi}\frac{P_n^1(\cos\theta_p)}{\sin\theta_p}=(-1)^n\,\frac{n(n+1)}{2} \tag{5-18}$$

$$\lim_{\theta_p\to\pi}\frac{\partial}{\partial\theta_p}P_n^1(\cos\theta_p)=-(-1)^n\,\frac{n(n+1)}{2} \tag{5-19}$$

With the above approximations, the two components of the backscattered field are

$$f_{\theta p}(\alpha,r_p,\pi,\phi_p)=-\frac{e^{jkr_p}}{kr_p}\sum_{n=1}^{\infty}j^{-n+1}(-1)^n\,n(n+1)\,[\,\Psi_{pE}(\alpha,1,n)-\Psi_{pM}(\alpha,1,n)\,]\sin\phi_p \tag{5-20}$$

$$f_{\phi p}(\alpha,r_p,\pi,\phi_p)=\frac{e^{jkr_p}}{kr_p}\sum_{n=1}^{\infty}j^{-n+1}(-1)^n\,n(n+1)\,[\,\Psi_{pE}(\alpha,1,n)-\Psi_{pM}(\alpha,1,n)\,]\cos\phi_p \tag{5-21}$$

Adding the above two components of the backscattered fields yields

$$[\,f_{\theta p}(\alpha,r_p,\pi,\phi_p)\,\hat{\theta}+f_{\phi p}(\alpha,r_p,\pi,\phi_p)\,\hat{\phi}\,]=\frac{e^{jkr_p}}{kr_p}\sum_{n=1}^{\infty}j^{-n+1}(-1)^n\,n(n+1)\cdot[\,\Psi_{pE}(\alpha,1,n)-\Psi_{pM}(\alpha,1,n)\,](-\sin\phi_p\,\hat{\theta}+\cos\phi_p\,\hat{\phi}) \tag{5-22}$$

When $\theta_p=\pi$, the transformation takes the following form

$$-\sin\phi_p\,\hat{\theta}+\cos\phi_p\,\hat{\phi}=\hat{y} \tag{5-23}$$

Substituting equation (5-23) into (5-22), one obtains

$$[\,f_{\theta p}(\alpha,r_p,\pi,\phi_p)\,\hat{\theta}+f_{\phi p}(\alpha,r_p,\pi,\phi_p)\,\hat{\phi}\,]=\frac{e^{jkr_p}}{kr_p}\sum_{n=1}^{\infty}j^{-n+1}(-1)^n\,n(n+1)\cdot[\,\Psi_{pE}(\alpha,1,n)-\Psi_{pM}(\alpha,1,n)\,]\hat{y} \tag{5-24}$$

For convenience one can re-write equation (5-24) in the following form

$$[\,f_{\theta p}(\alpha,r_p,\pi,\phi_p)\,\hat{\theta}+f_{\phi p}(\alpha,r_p,\pi,\phi_p)\,\hat{\phi}\,]=g_{p1}(\alpha,r_p,\pi)\,\hat{y} \tag{5-25}$$

where

$$g_{p1}(\alpha,r_p,\pi)=\frac{e^{jkr_p}}{kr_p}\sum_{n=1}^{\infty}j^{-n+1}(-1)^n\,n(n+1)\,[\,\Psi_{pE}(\alpha,1,n)-\Psi_{pM}(\alpha,1,n)\,] \tag{5-26}$$

Equations (5-16) and (5-25) represent the forward and backscattering expressions for a single sphere due to an arbitrary plane wave incidence.

5.2 Total scattered field from the pth sphere

For the case of a linear array of N small spheres illuminated by an arbitrary electromagnetic plane wave of unit amplitude, the total scattered field from the pth sphere at any point is due the incident field (non interaction field) plus the multiply scattered fields from the remaining spheres (interaction field). The total scattered field by the pth sphere may hence be expressed as

$$\begin{aligned}\bar{E}_p^s(r_p,\theta_p,\phi_p)=&[f_{\theta p}(\alpha,r_p,\theta_p,\phi_p)\,\hat{\theta}+f_{\phi p}(\alpha,r_p,\theta_p,\phi_p)\,\hat{\phi}]+\sum_{q=1}^{p-1}C_q e^{-jkd_q}[\,f_{\theta p}(0,r_p,\theta_p,\phi_p)\,\hat{\theta}\\&+f_{\phi p}(0,r_p,\theta_p,\phi_p)\hat{\phi}]+\sum_{q=p+1}^{N}C_q e^{jkd_q}[f_{\theta p}(0,r_p,\pi-\theta_p,\phi_p)\,\hat{\theta}+f_{\phi p}(0,r_p,\pi-\theta_p,\phi_p)\,\hat{\phi}]\end{aligned} \tag{5-27}$$

where the first two terms on the right hand side represent the far scattered field by the pth sphere due to the incident field, while the remaining terms represent the multiple interaction between the pth sphere and the remaining N-1 spheres.

5.3 Evaluation of the unknown coefficients C_q

In order to determine the unknown coefficients C_q, we impose a condition analogous to that used in [42] for the wide slit problem. The partial scattered field from the lth sphere due to the total scattered field from the pth sphere ($\bar{E}_{lp}^s$) can be

determined by considering the magnitude of $\overline{E}_p^s$ at the center of the lth sphere times the response of the far scattered field from the lth sphere, i. e.,

$$\overline{E}_{lp}^s = \begin{cases} E_p^s(d_{pl},0,\phi_p)\, e^{-jkd_l}\,[\mathrm{f}_{\theta l}(0,r_l,\theta_l,\phi_l)\,\hat{\theta} + \mathrm{f}_{\phi l}(0,r_l,\theta_l,\phi_l)\,\hat{\phi}] & \text{for } l>p \\ E_p^s(d_{pl},\pi,\phi_p)\, e^{jkd_l}\,[\mathrm{f}_{\theta l}(0,r_l,\pi-\theta_l,\phi_l)\,\hat{\theta} + \mathrm{f}_{\phi l}(0,r_l,\pi-\theta_l,\phi_l)\,\hat{\phi}] & \text{for } l<p \end{cases} \quad (5\text{-}28)$$

The scattered field $\overline{E}_{lp}^s$ from the lth sphere due to an axial plane wave incidence of unknown magnitude C_p can be expressed as

$$\overline{E}_{lp}^s = \begin{cases} C_p\, e^{-jkd_p}\,[\mathrm{f}_{\theta l}(0,r_l,\theta_l,\phi_l)\,\hat{\theta} + \mathrm{f}_{\phi l}(0,r_l,\theta_l,\phi_l)\,\hat{\phi}] & \text{for } l>p \\ C_p\, e^{jkd_p}\,[\mathrm{f}_{\theta l}(0,r_l,\pi-\theta_l,\phi_l)\,\hat{\theta} + \mathrm{f}_{\phi l}(0,r_l,\pi-\theta_l,\phi_l)\,\hat{\phi}] & \text{for } l<p \\ l=1,2,\cdots,\mathrm{N};\quad l\neq p \end{cases} \quad (5\text{-}29)$$

Comparing expressions in equations (5-28) and (5-29), and summing the partial scattered fields from all spheres due to the total field scattered by the pth sphere yields

$$(\mathrm{N}-1)\, C_p = \sum_{\substack{l=1 \\ l\neq p}}^{\mathrm{N}} e^{-jkd_{pl}} \left\{ g_{p1}(\alpha,d_{pl},\theta_{pl}) + g_{p1}(0,d_{pl},\theta_{pl}) \sum_{q=1}^{p-1} C_q\, e^{-jkd_q} + g_{p2}(0,d_{pl},\theta_{pl}) \sum_{q=p+1}^{\mathrm{N}} C_q\, e^{jkd_q} \right\} \quad (5\text{-}30)$$

where

$$\mathrm{f}_{\theta p}(0,d_{pl},\pi-\theta_{pl},\phi_p)\,\hat{\theta} + \mathrm{f}_{\phi_p}(0,d_{pl},\pi-\theta_{pl},\phi_p)\,\hat{\phi} \equiv g_{p2}(0,d_{pl},\theta_{pl})\,\hat{y} \quad (5\text{-}31)$$

and

$$\theta_{pl} = \begin{cases} 0 & \text{for } l>p \\ \pi & \text{for } l<p \end{cases} \quad (5\text{-}32)$$

Once C_q are known, the total scattered field in the far zone can be expressed as

$$\overline{E}^s = \sum_{p=1}^{\mathrm{N}} \left\{ [\mathrm{f}_{\theta p}(\alpha,r,\theta,\phi)\,\hat{\theta} + \mathrm{f}_{\phi p}(\alpha,r,\theta,\phi)\hat{\phi}] + [\mathrm{f}_{\theta p}(0,r,\theta,\phi)\,\hat{\theta} + \mathrm{f}_{\phi p}(0,r,\theta,\phi)\hat{\phi}] \sum_{q=1}^{p-1} C_q\, e^{-jkd_q} \right.$$

$$+[f_{\theta p}(0,r,\pi-\theta,\phi)\,\hat{\theta}+f_{\phi p}(0,r,\pi-\theta,\phi)\,\hat{\phi}]\sum_{q=p+1}^{N} C_q\, e^{jkd_q}\Bigg\}\, e^{-jkd_p\cos\theta} \qquad (5\text{-}33)$$

5.4 Numerical results

In the computations of the normalized backscattering and bistatic cross sections of a linear array of spheres, we present numerical results for the normalized backscattering cross section for different systems of spheres of equal and unequal radii versus the separation distance between the spheres in terms of the wavelength and the incidence angle α. The normalized bistatic cross section is presented for systems of identical spheres as a function of the scattering angle θ, corresponding to endfire incidence (α=0).

5.4.1 Radar cross section of arrays of conducting spheres

Figure 5-2 presents the backscattering cross section for a linear array of three spheres with different radii, namely ka_1=0.5, ka_2=0.25, and ka_3=0.1, versus the electrical distance between the spheres ($1 \le kd \le 11$) for endfire incidence, and shows a comparison between the exact (solid curve) and approximate (dotted curve) solutions. It can be seen that the two curves deviate at small separation distances ($kd<2.5$), the deviation becoming significant when $kd=\pi/2$. On the other hand, as kd increases, the deviation vanishes. This is so, since the approximate solution is expected to be more valid for larger kd ($kd>2.5$). In addition, the magnitude of the normalized backscattering cross section is small because the larger sphere shields the backscattered field from the smaller spheres, while it varies between a minimum value of 0.4046 and a maximum value which is 1.3217 times the normalized backscattering of a single sphere (Table 5-1), and behaves sinusoidaly with approximately half wavelength

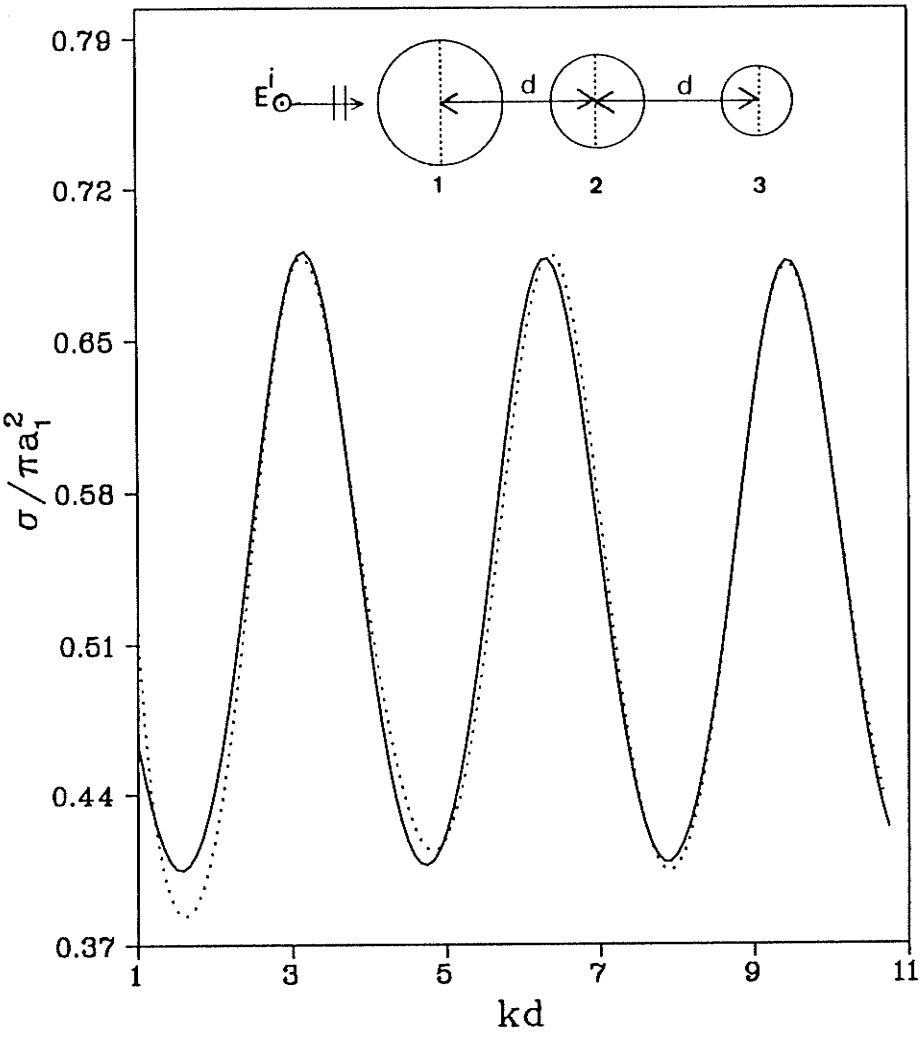

Fig.5-2. Normalized backscattering cross section versus kd for three unequal spheres: ka_1=0.5, k a_2=0.25, ka_3=0.1. (—analytic, ...approximate)

periods. Another example is given in Fig. 5-3 for an array consisting of five spheres of equal radii ka=0.5, while Fig. 5-4 consists of five spheres of unequal radii, where the larger sphere has an electrical radius ka_1=0.5 and the other radii decrease from the largest towards the smallest sphere by an increment of 0.1. It is interesting to note that in the last two cases the approximate solution gives good results at small kd even when the spheres are in contact (Fig. 5-3), while the peaks occur approximately every kd=π.

Figures 5-5 and 5-6 show the normalized bistatic cross section versus the scattering angle (θ) for an equispaced linear array of three and five spheres and endfire incidence. The radius and separation between the successive spheres are ka=0.5 and kd=2.0. The agreement between the exact and approximate solutions does not seem to be satisfactory, since the electrical distances between the successive spheres are small compared to their electrical radii. Figures 5-7 and 5-8 present the bistatic cross section for the same arrays and angle of incidence but the separation between the successive spheres is increased to kd=4.0, and the agreement between the solutions in this case is quite satisfactory. In addition, Fig. 5-9 shows an array consisting of eight spheres with the same size and separation. It can be seen that the magnitude of the normalized bistatic cross section (H-plane) is increased sharply from 3.8 in Fig. 5-7 to approximately 27 in Fig. 5-9 at the particular scattering angle of $\theta=127^o$, while it vanishes at certain scattering angles. Moreover the locations of the maxima are not the same for kd=2.0 and 4.0 and differ from those for a single sphere.

In Figs. 5-10 and 5-11 we have plotted the normalized backscattering cross sec-

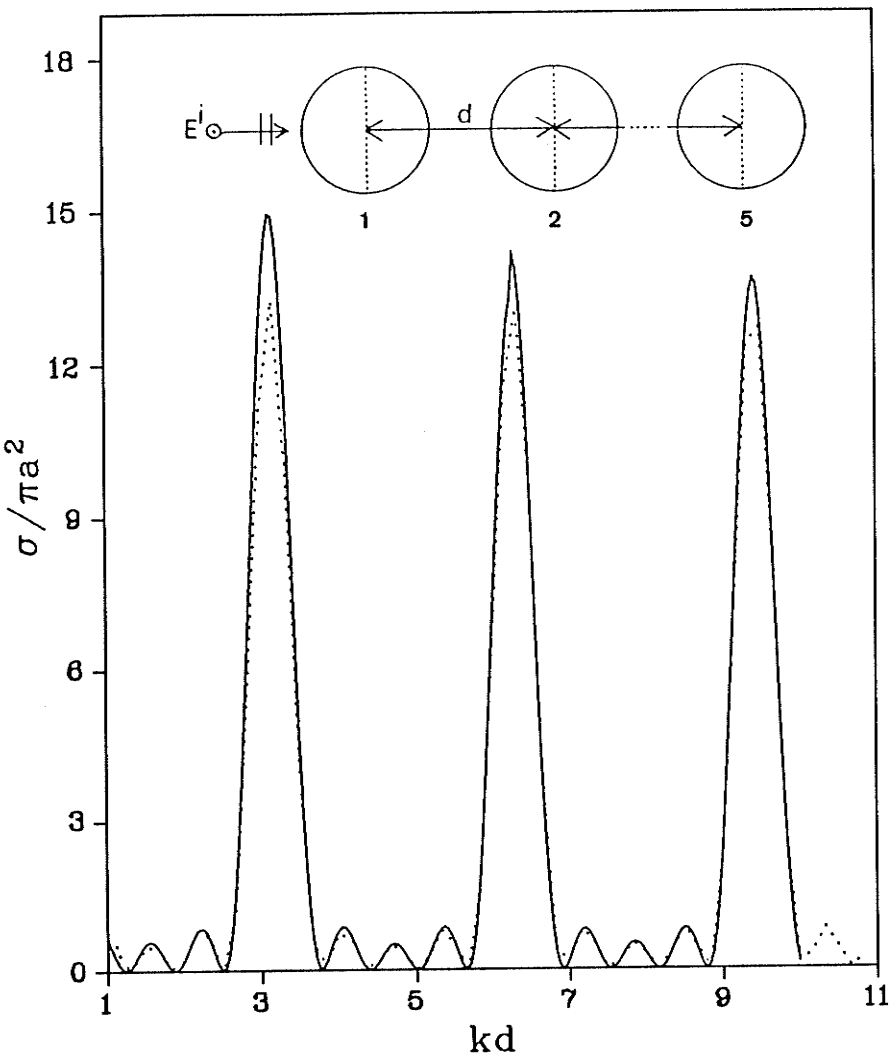

Fig.5-3. Normalized backscattering cross section versus kd for five equal spheres: ka=0.5. (—analytic, ...approximate)

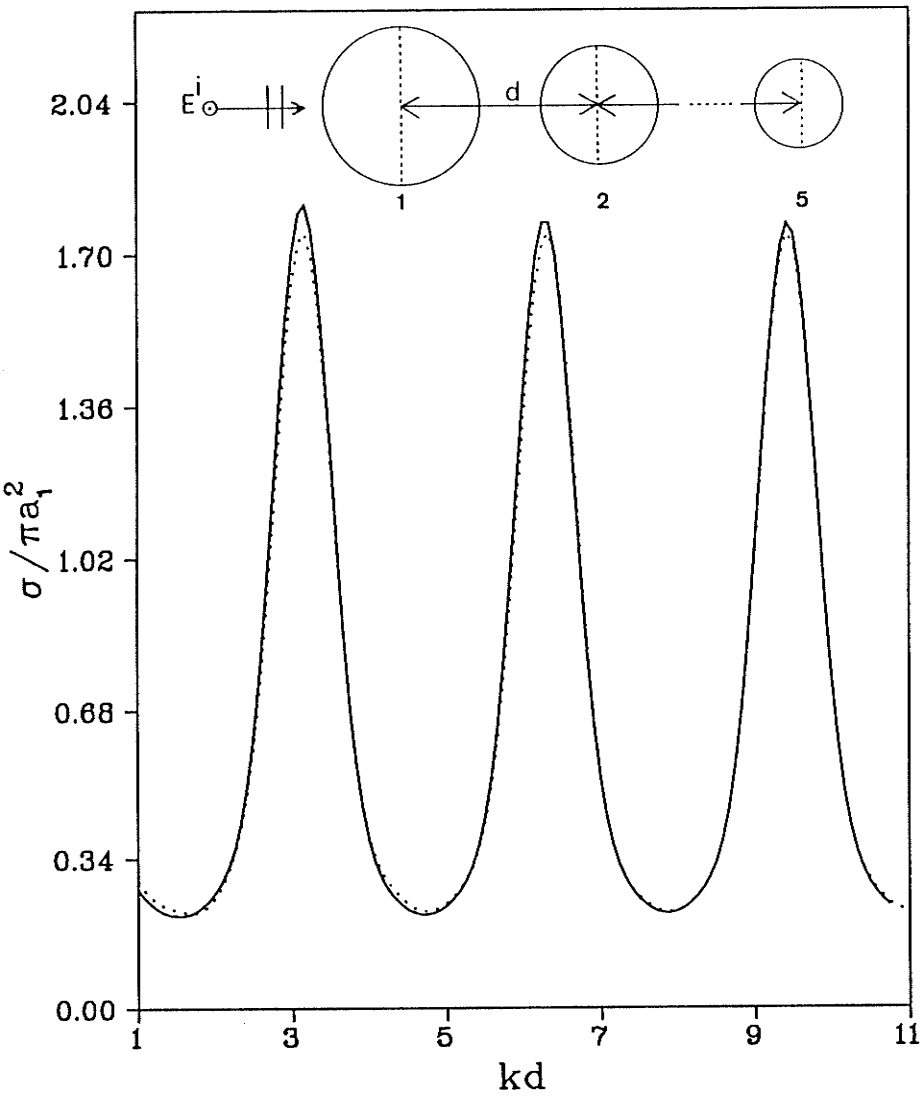

Fig.5-4. Normalized backscattering cross section versus kd for five unequal spheres: ka_1=0.5, ka_2=0.4, ka_3=0.3, ka_4=0.2, ka_5=0.1. (—analytic, ...approximate)

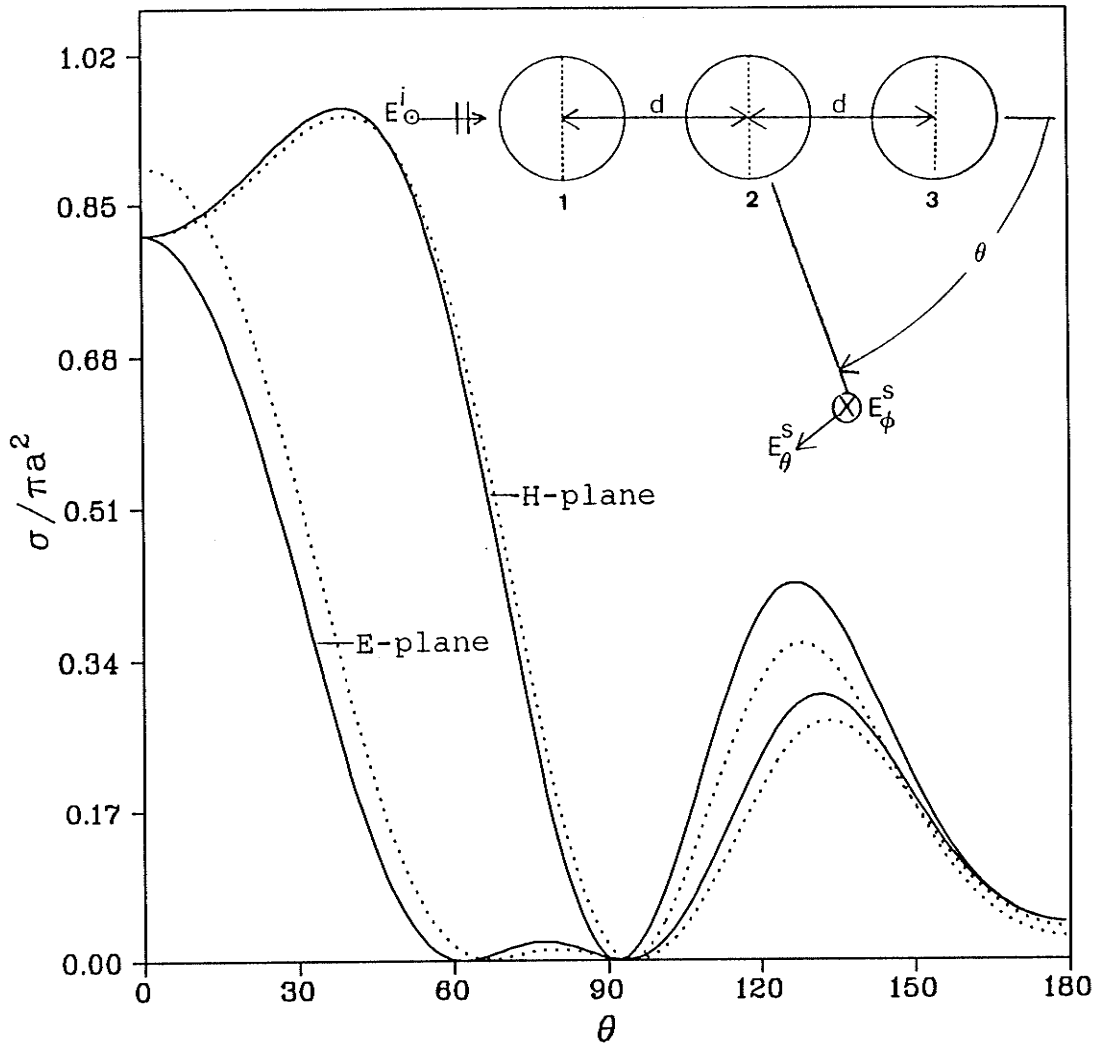

Fig.5-5. Normalized bistatic cross section versus scattering angle θ for a linear array of identical three spheres: ka=0.5, kd=2.0. (—analytic, ...approximate)

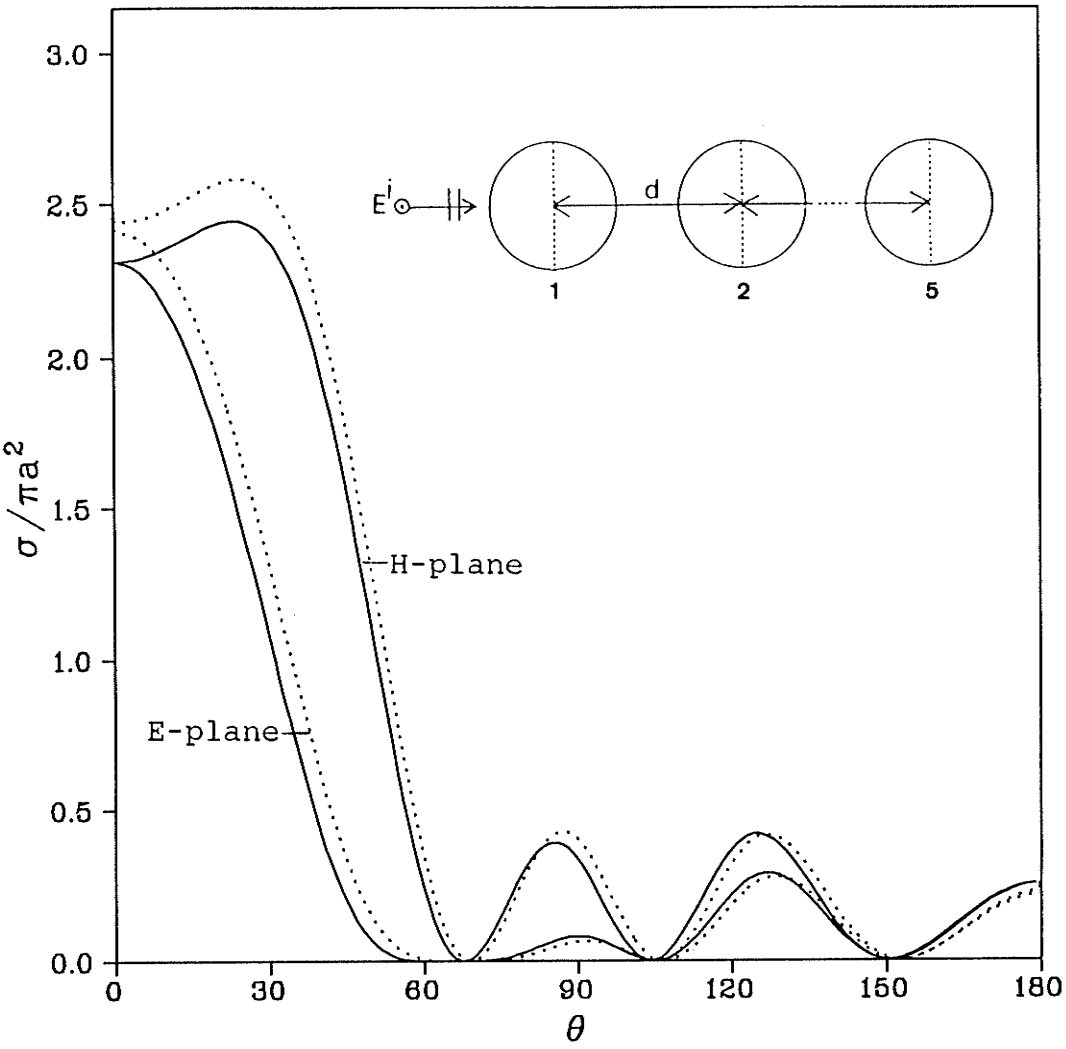

Fig.5-6. Normalized bistatic cross section versus scattering angle θ for a linear array of identical five spheres: ka=0.5, kd=2.0. (—analytic, ...approximate)

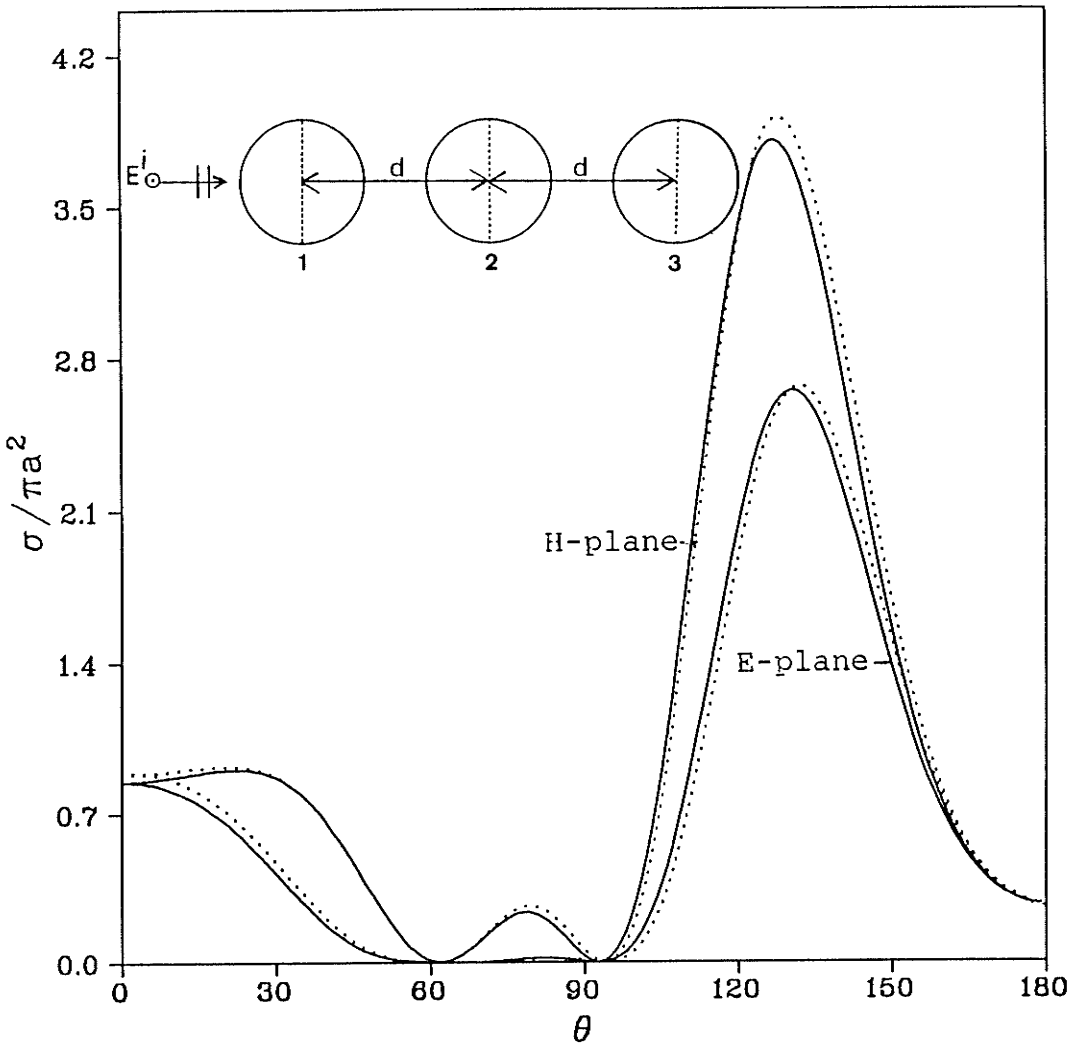

Fig.5-7. Normalized bistatic cross section versus scattering angle θ for a linear array of identical three spheres: ka=0.5, kd=4.0. (—analytic, ...approximate)

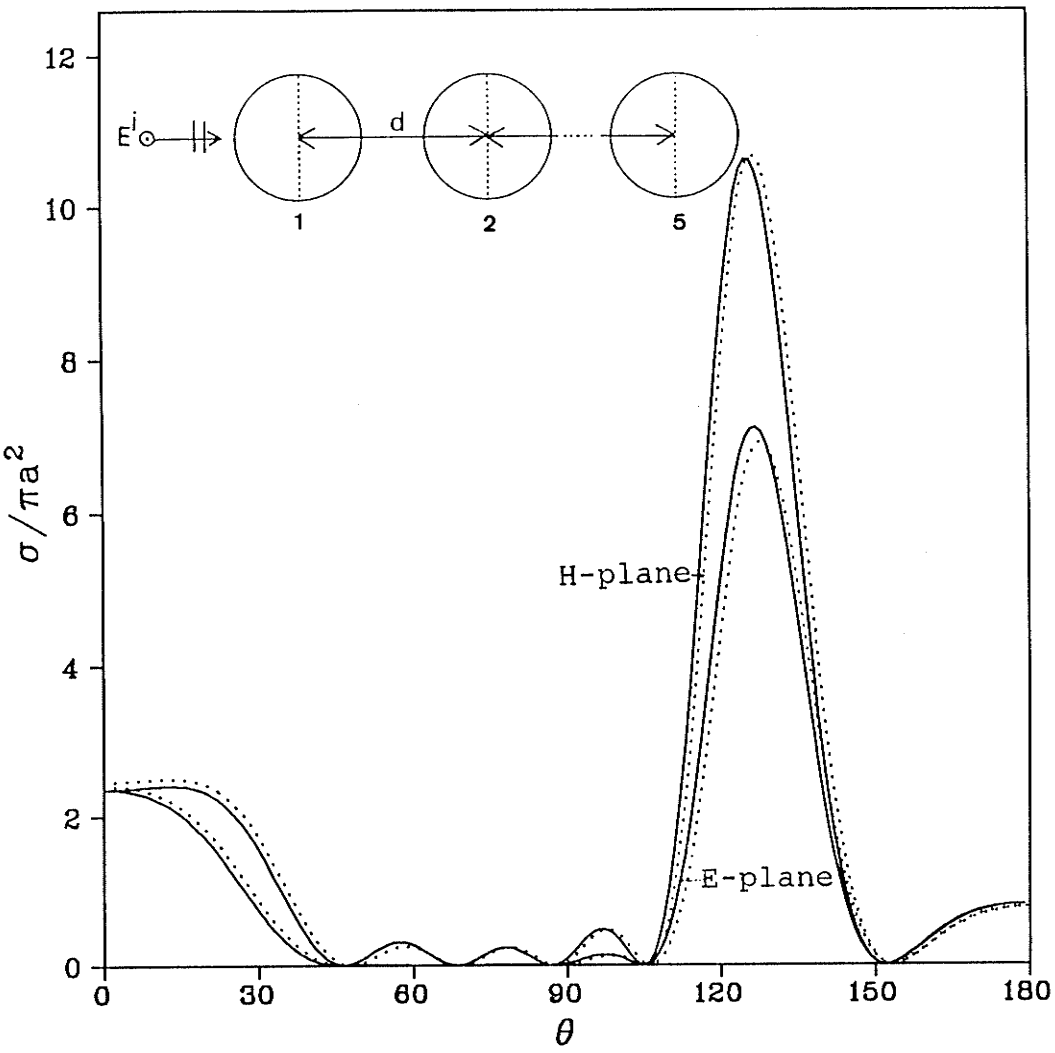

Fig.5-8. Normalized bistatic cross section versus scattering angle θ for a linear array of identical five spheres: ka=0.5, kd=4.0. (—analytic, ...approximate)

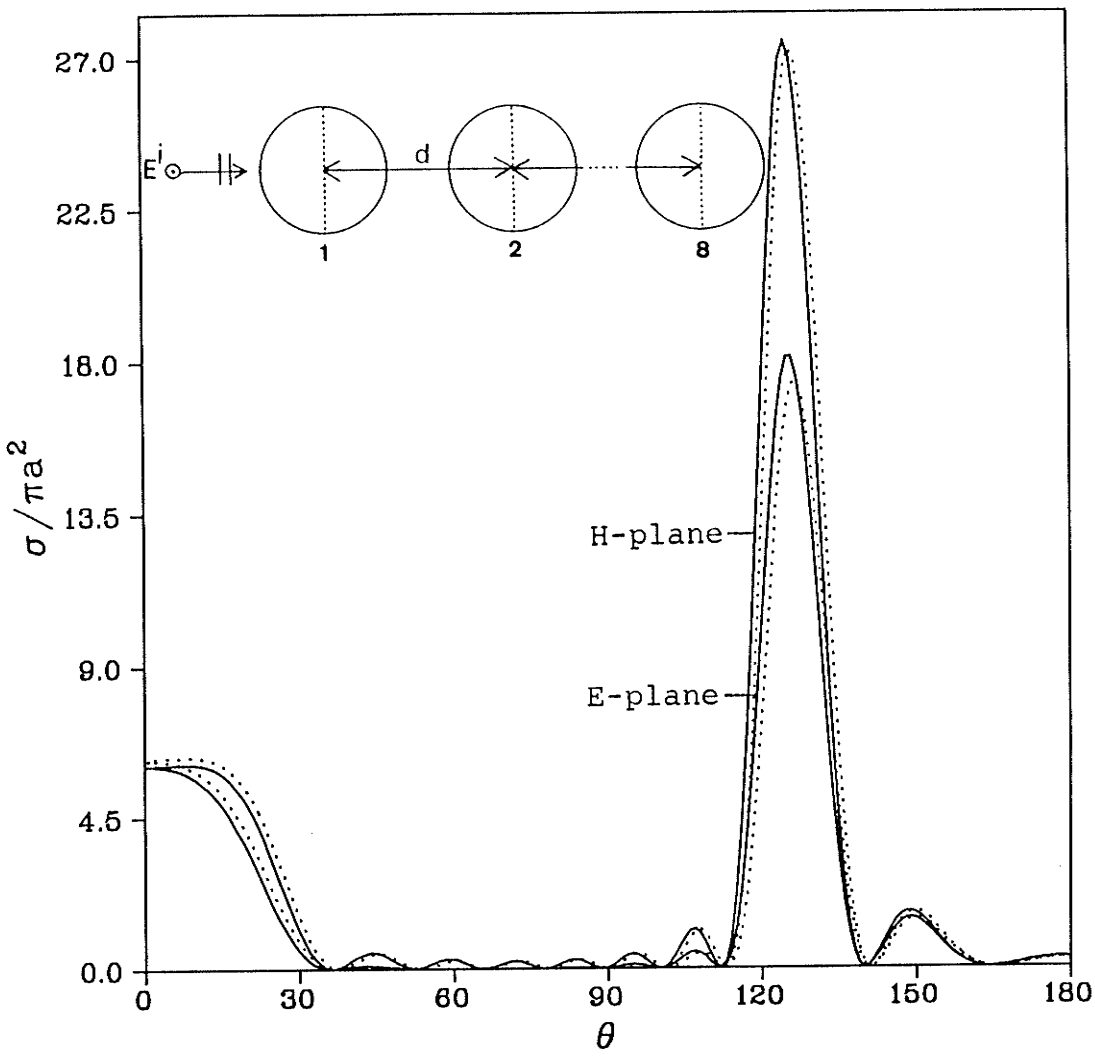

Fig.5-9. Normalized bistatic cross section versus scattering angle θ for a linear array of identical eight spheres: ka=0.5, kd=4.0. (—analytic, ...approximate)

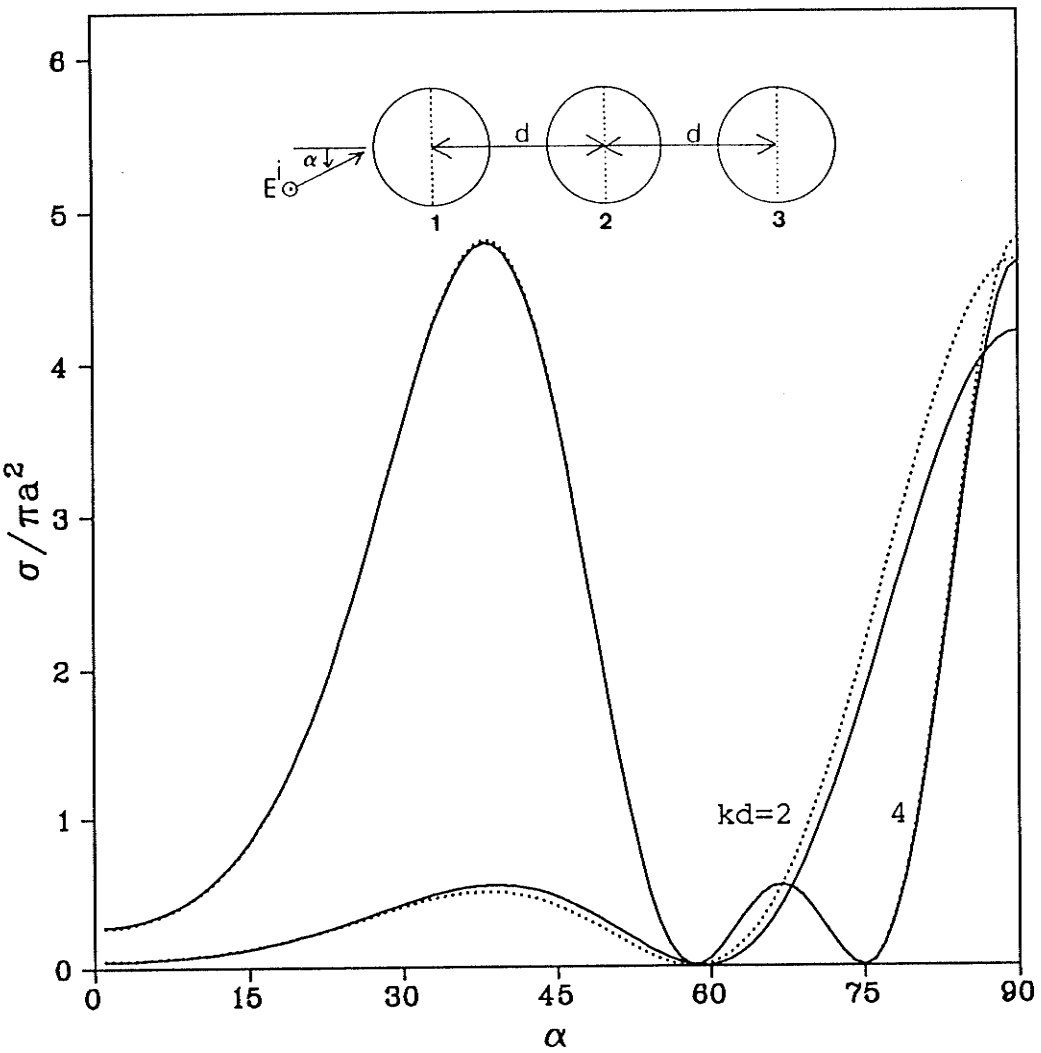

Fig.5-10. Normalized backscattering cross section versus aspect angle α for a linear array of three spheres with ka=0.5. (—analytic, ...approximate)

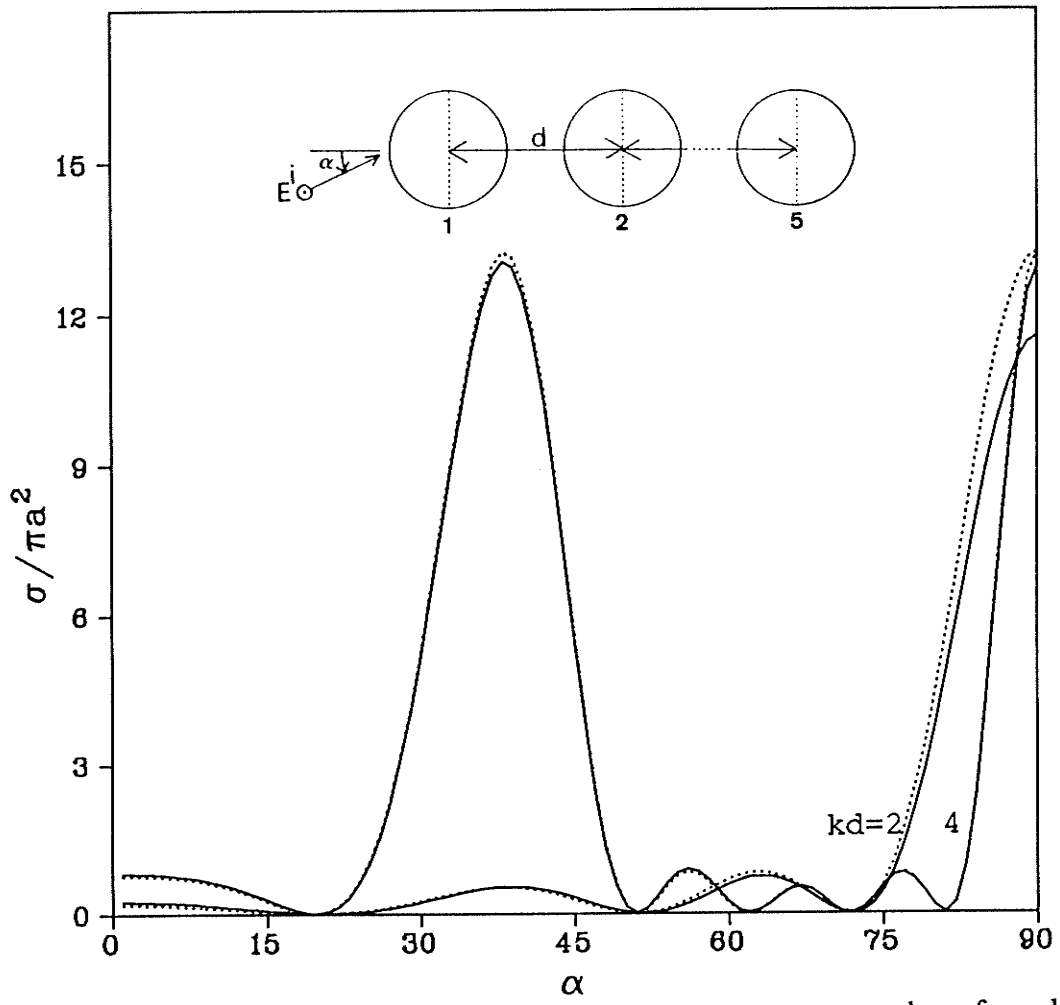

Fig.5-11. Normalized backscattering cross section versus aspect angle α for a linear array of five spheres with ka=0.5. (—analytic, ...approximate)

tion versus the angle of incidence α for an array of three and five identical spheres with ka=0.5, and different values of kd [46-47]. Due to the symmetry in the angle of incidence α it is sufficient to get the backscattering cross section pattern for the interval from α=0 to α=90^o. In the case of the larger separation, kd=4, there is a pronounced maximum at about α=38^o, as well as more minima than for kd=2. It can be seen that the agreement is good for kd=4 at all the values of α and also for kd=2 when α<75^o. The results show that by increasing the number of spheres and kd the backscattering cross section vanishes at more angles of incidence. This is partly due to the increase of the interaction between the spheres.

Table 5-1 compares the endfire and broadside backscattering cross sections for a linear array of system of spheres, corresponding to ka=0.5 where the results are rounded off to 4 decimal places. For the endfire touching case, the result does not show significant change in the magnitude of the backscattering cross section for the scattering by one or two spheres, while a significant change (drop) occurs after adding the third or sixth sphere, due to resonance and multiple scattering phenomena. In the broadside touching case, the magnitude of the backscattering cross section increases with the number of spheres (since the fields scattered by each sphere are in phase), while it changes insignificantly after adding the eighth sphere and so on. This is due to the weak coupling between the outer spheres.

5.4.2 Radar cross section of arrays of dielectric spheres

In this section, we present numerical results for systems of dielectric spheres. The dielectric constant ε_r is the same for all spheres and equals 3.0 in most of the results presented. Moreover, the formulation and computer program presented are

Table.5-1. Normalized backscattering cross section $\sigma/\pi a^2$ for a linear array of N identical spheres, ka=0.5

kd	N	$\alpha=0^o$(Endfire)	$\alpha=90^o$(Broadside)
1.0	1	0.5295	0.5295
	2	0.5271	1.6487
	3	0.0042	3.2492
	4	0.4598	5.3169
	5	0.6004	7.9053
	6	0.0340	11.0875
	7	0.5223	14.8951
	8	0.8230	15.2134
2.0	2	0.4229	1.9308
	3	0.0409	4.1914
	4	0.6941	7.4326
	5	0.2542	11.5377
	6	0.1870	16.4778
	7	0.7485	22.4026
	8	0.0863	24.0329

valid for arrays containing a mixture of conducting and dielectric spheres.

Examination of the geometry indicates that an array of dielectric spheres could have a lower normalized backscattering and bistatic cross sections and weaker sphere to sphere coupling than a similar array of perfectly conducting spheres. On the other hand, the forward scattering cross section could be significantly enhanced with an increase in the number of spheres.

Figure 5-12 presents the normalized backscattering cross section for a linear array of three dielectric spheres with different radii, namely ka_1=0.5, ka_2=0.25, and ka_3=0.1, as a function of kd ($1 \leq kd \leq 11$) for endfire incidence, and compares the exact (solid curve) and approximate (doted curve) solutions. The discrepancy between the two curves occurs at kd<2.5, and decreases as kd increases relative to the electrical size of the spheres. On the other hand, the magnitude of the backscattering cross section varies between a minimum of 0.0283 and a maximum of 0.0481 which is about 76% more than the normalized backscattered field of a single dielectric sphere of the same size (Table 5-2), while there is a reduction of about 6.9% relative to a similar array of conducting spheres. The curve behaves sinusoidaly as in the case of conducting spheres with approximately half wavelength periods. Figure 5-13 is another example for the same array except the second sphere is perfectly conducting. This leads to a better agreement between the two methods, even for small kd, along with an increase in the magnitude of the backscattering cross section. Figure 5-14 consists of five spheres of equal radii ka=0.5. We observe that the high peaks occur at specific electrical distances, *i. e.* kd=π, 2π, 3π, which is approximately every kd= π as in the case of conducting spheres. Again, very good agreement between the exact

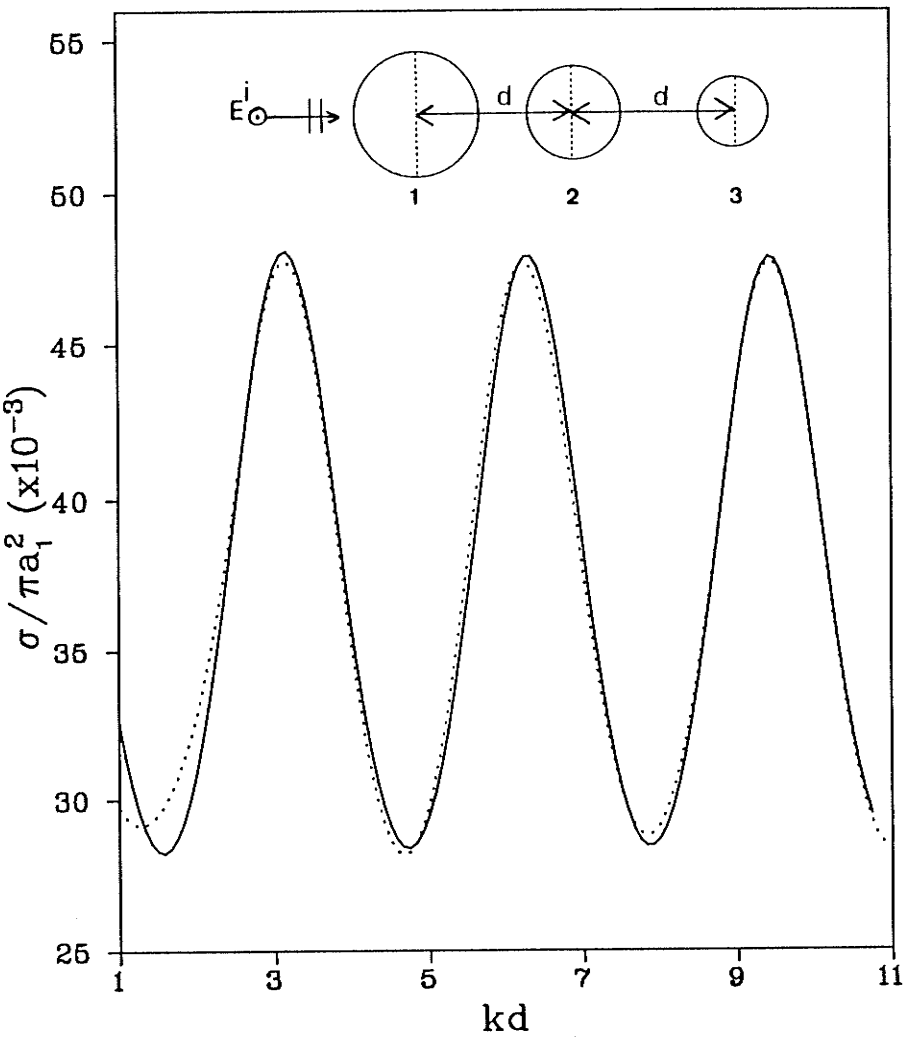

Fig.5-12. Normalized backscattering cross section versus kd for three unequal spheres of ε_r=3.0 and k a_1=0.5, ka_2=0.25, ka_3=0.1. (—analytic, ...approximate)

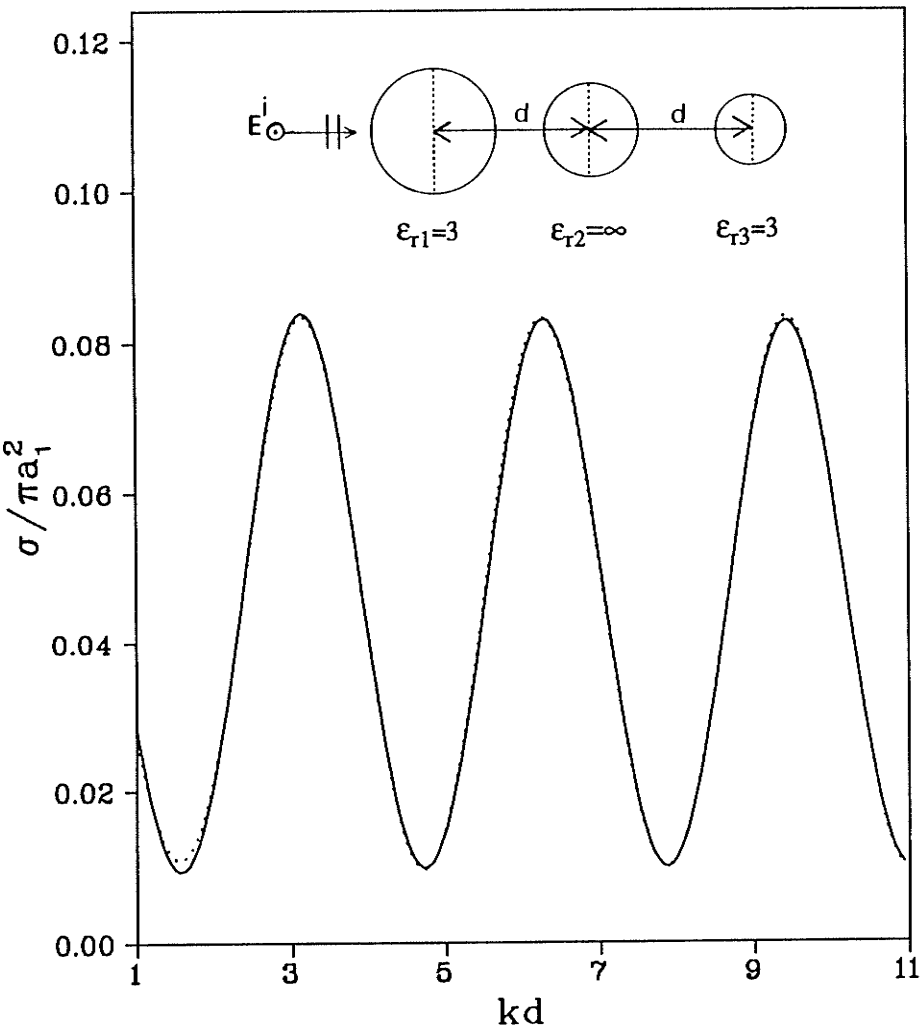

Fig.5-13. Normalized backscattering cross section versus kd for three unequal spheres of $\varepsilon_{r1}=3.0$, $\varepsilon_{r2}=\infty$, $\varepsilon_{r3}=3.0$, and $ka_1=0.5$, $ka_2=0.25$, $ka_3=0.1$. (—analytic, ...approximate)

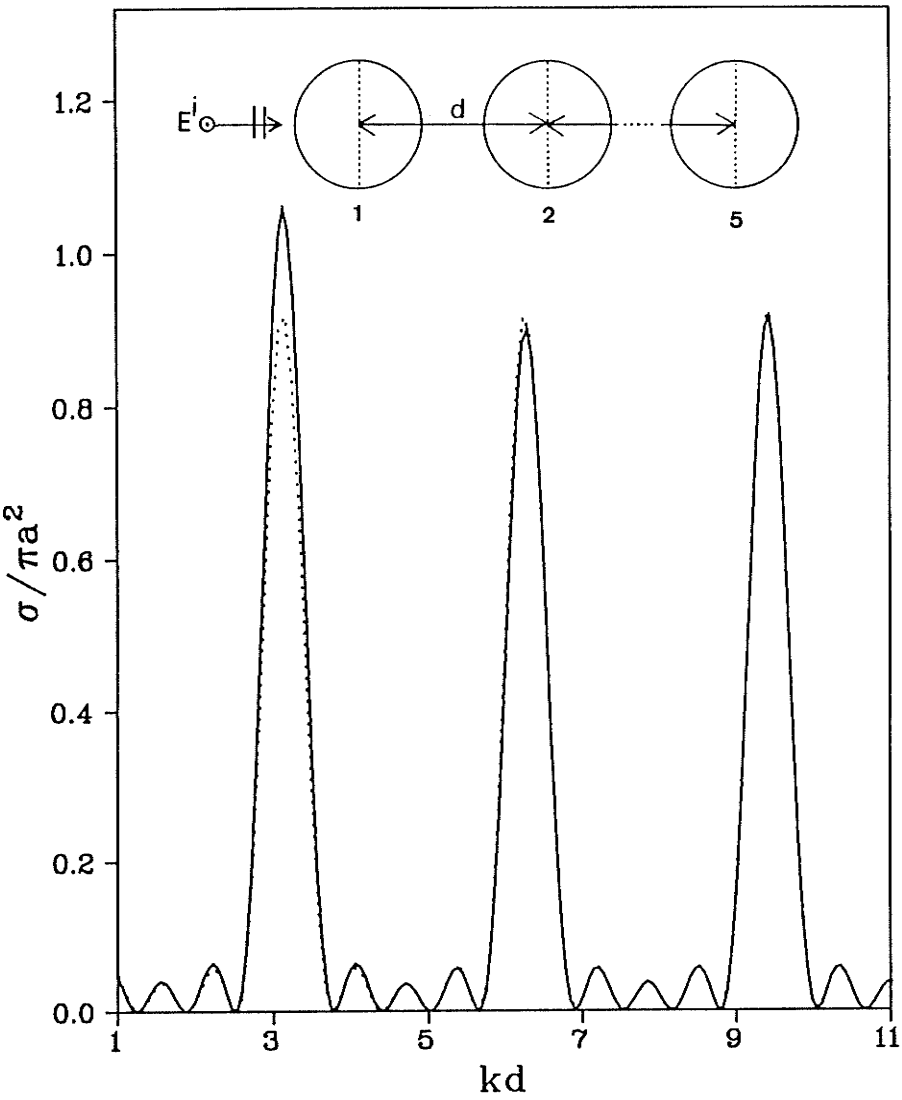

Fig.5-14. Normalized backscattering cross section versus kd for five equal spheres of ε_r=3.0 and ka=0.5. (—analytic, ...approximate)

and approximate solutions is obtained even when the spheres are in contact. Figure 5-15 consists of five dielectric spheres of unequal radii, where the larger sphere has an electrical radius $ka_1=0.5$ and the other radii decrease from the largest towards the smallest sphere by an increment of 0.1. It is interesting to note that the small ripples in Fig. 5-14 disappear by changing the electrical radii of the spheres in Fig. 5-15 while the high peaks remain at the same locations.

By comparing the above examples with similar ones for the conducting spheres, we see that the resonances occur in both cases at the same locations and hence independent from material characteristics.

Figure 5-16 shows the normalized bistatic cross section versus scattering angle θ for an equispaced linear array of three identical dielectric spheres at endfire incidence. The radius and separation between the successive spheres are ka=0.5 and kd=4.0, respectively. The agreement between the exact and approximate solutions is satisfactory except for a small variation in the forward scattering, and it can be seen that the back and forward scattering cross sections are equal in the E and H planes, as expected. In addition, a reduction of about 7.1% in the backscattering is obtained relative to a similar array of conducting spheres. Figure 5-17 shows the same array with the second sphere being perfectly conducting. It can be seen from the latter case that the ripple disappears over the range $60^o \leq \theta \leq 120^o$ by replacing the dielectric sphere with a conducting sphere.

Figure 5-18 consists of an array of five dielectric spheres where there is no significant change in the shape of the bistatic cross section relative to Fig. 5-16, except for an increase in the number of ripples. Figure 5-19 shows an array of eight

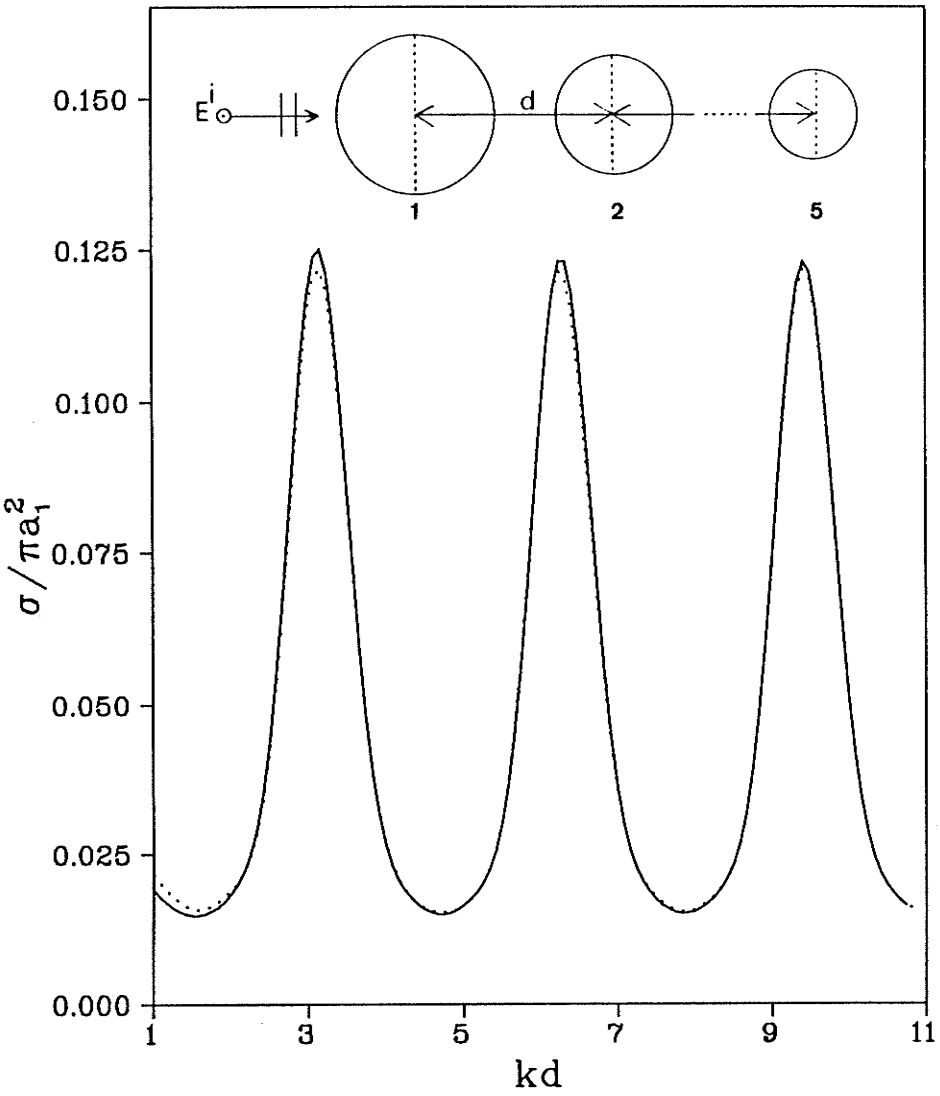

Fig.5-15. Normalized backscattering cross section versus kd for five unequal spheres of ε_r=3.0 and ka_1=0.5, ka_2=0.4, ka_3=0.3, ka_4=0.2, ka_5=0.1. (—analytic, ...approximate)

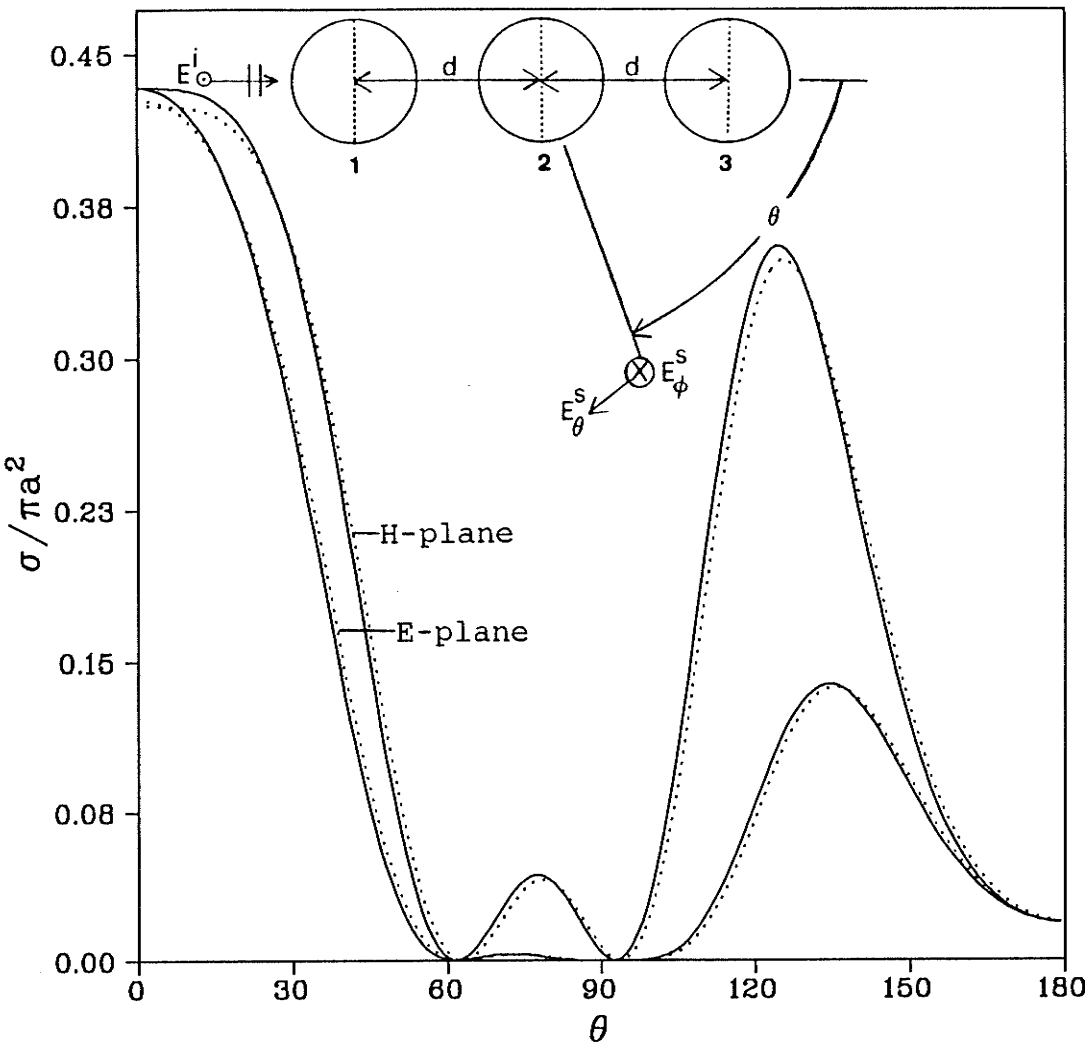

Fig.5-16. Normalized bistatic cross section versus scattering angle θ for a linear array of identical three spheres: ka=0.5, kd=4.0, ε_r=3.0. (—analytic, ...approximate)

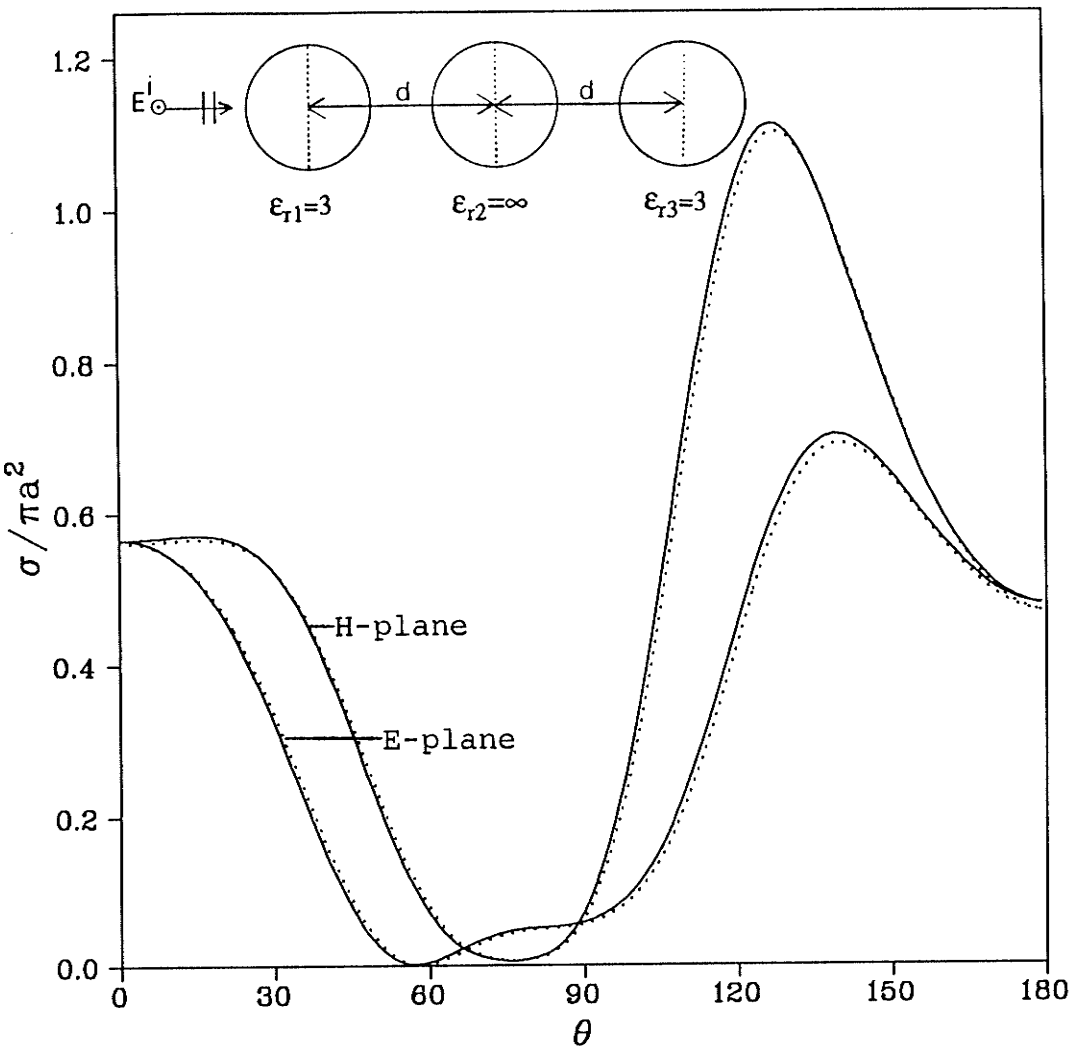

Fig.5-17. Normalized bistatic cross section versus scattering angle θ for a linear array of identical three spheres: ka=0.5, kd=4.0, ε_{r1}=3.0 , ε_{r2}=∞, ε_{r3}=3.0. (—analytic, ...approximate)

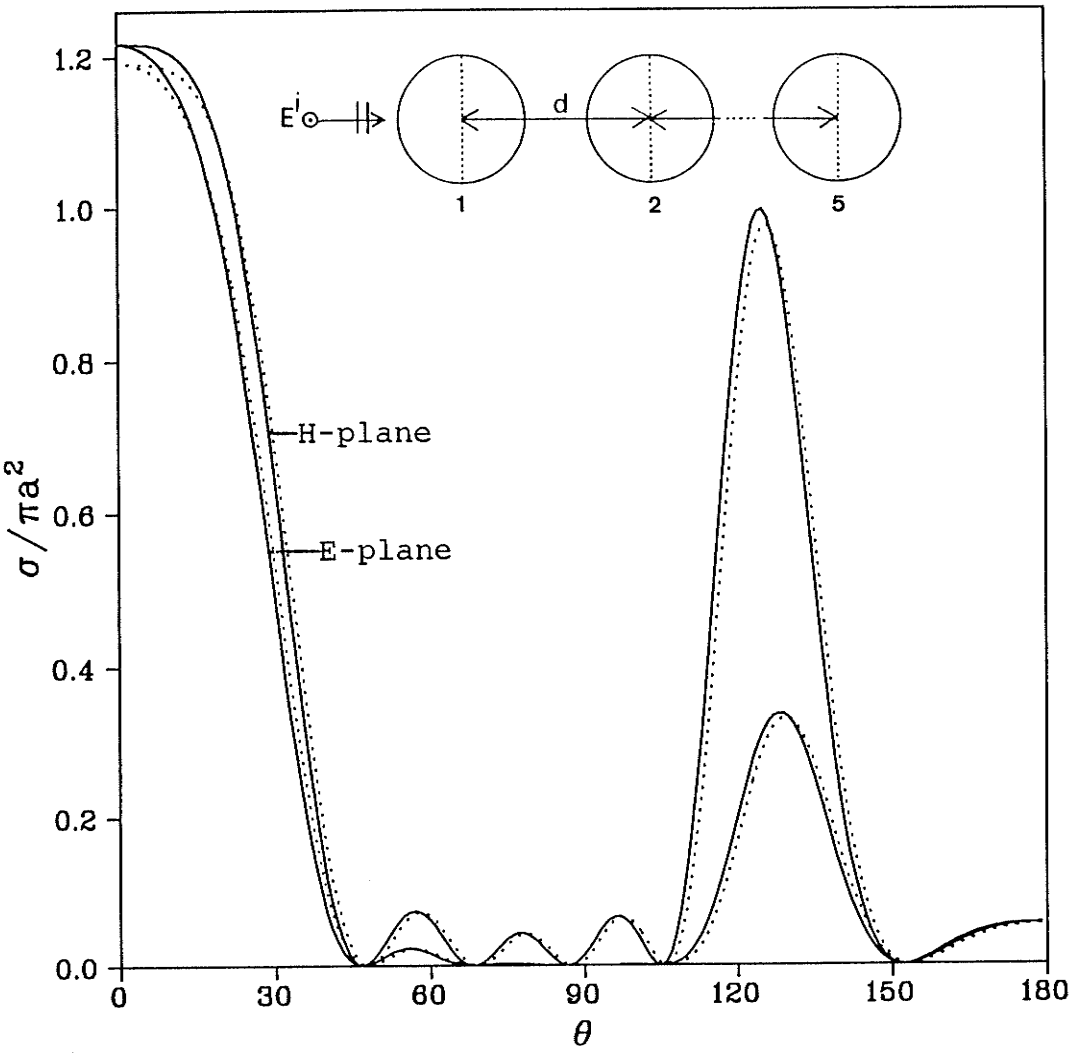

Fig.5-18. Normalized bistatic cross section versus scattering angle θ for a linear array of identical five spheres: ka=0.5, kd=4.0, ε_r=3.0. (—analytic, ...approximate)

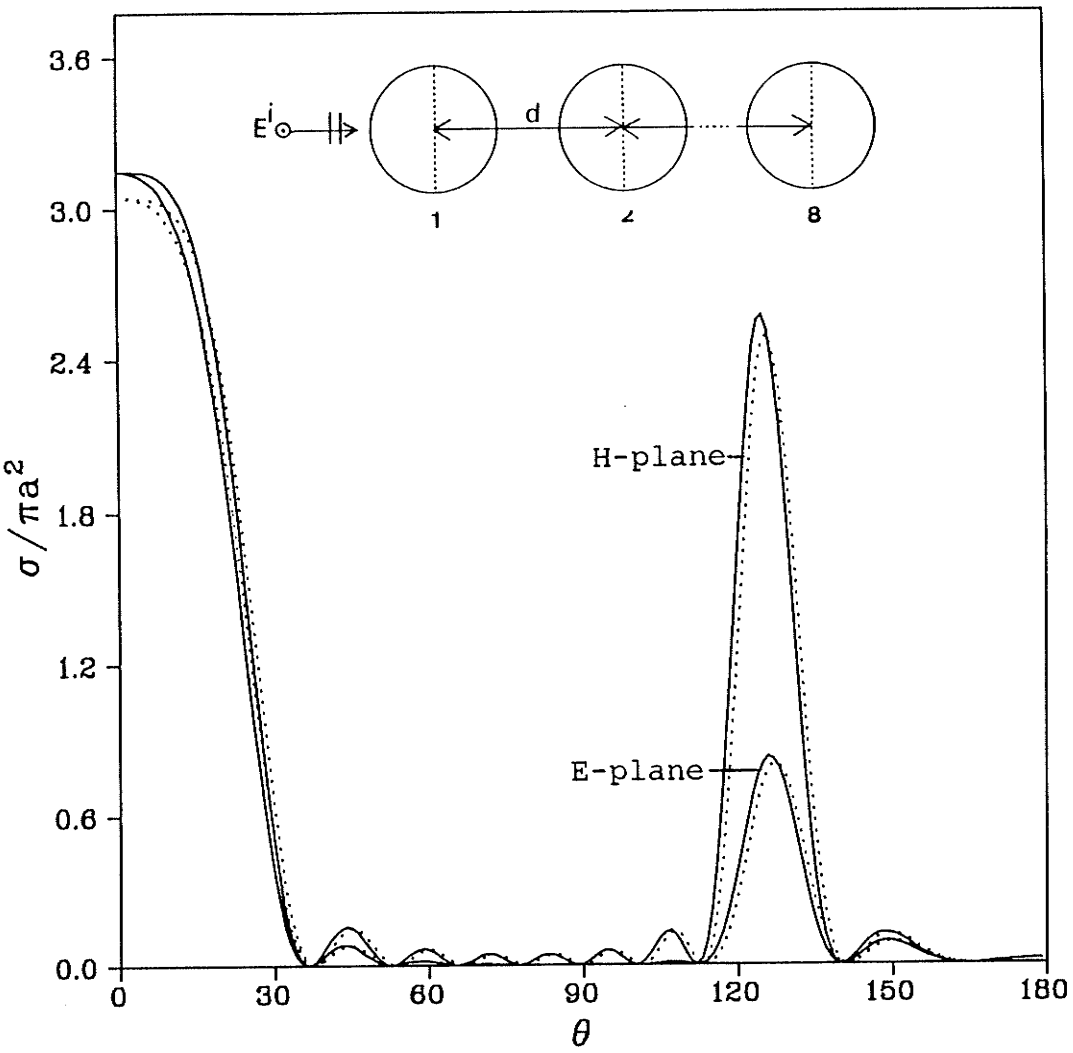

Fig.5-19. Normalized bistatic cross section versus scattering angle θ for a linear array of identical eight spheres: ka=0.5, kd=4.0, ε_r=3.0. (—analytic, ...approximate)

spheres, the two planes are virtually very close for θ less than 35^o, and the magnitude of the backscattering drops from 0.06 in Fig. 5-16 to 0.02 in this case.

In Figs. 5-20 and 5-21 we have plotted the normalized backscattering cross section versus angle of incidence (α) for an array of three and five identical dielectric spheres with ka=0.5 for different values of kd. We observe a significant increase in the oscillations of the curves by varying kd. Once again, the location of the oscillations is independent of the material characteristics when compared with those for conducting spheres.

Figures 5-22 and 5-23 show the backscattering plotted as a function of the dielectric constant ($1 \leq \varepsilon_r \leq 30$) for various values of kd. The magnitude of the backscattering is zero at ε_r=1.0 and 30.0 and maximum at ε_r=13.0 for the arrays considered.

The normalized forward scattering cross section is plotted in Figs. 5-24 and 5-25 as a function of kd ($1 \leq kd \leq 9$) for various numbers of dielectric spheres, namely N=3,5 and 8, with ka=0.5. The magnitude of the forward scattering is enhanced by increasing the number of spheres and also by changing the relative dielectric constant (ε_r) from 3 to 5, respectively. However, the forward scattering does not change significantly by varying the electrical separation and converges rapidly for large kd. It can be seen from the two presented cases that the resonance occurs approximately every kd= π.

Table 5-2 presents results for the special cases of endfire and broadside backscattering cross sections for a linear array of dielectric spheres, corresponding to ka=0.5, kd=1.0 and 2.0. The magnitude of the backscattering cross section for endfire

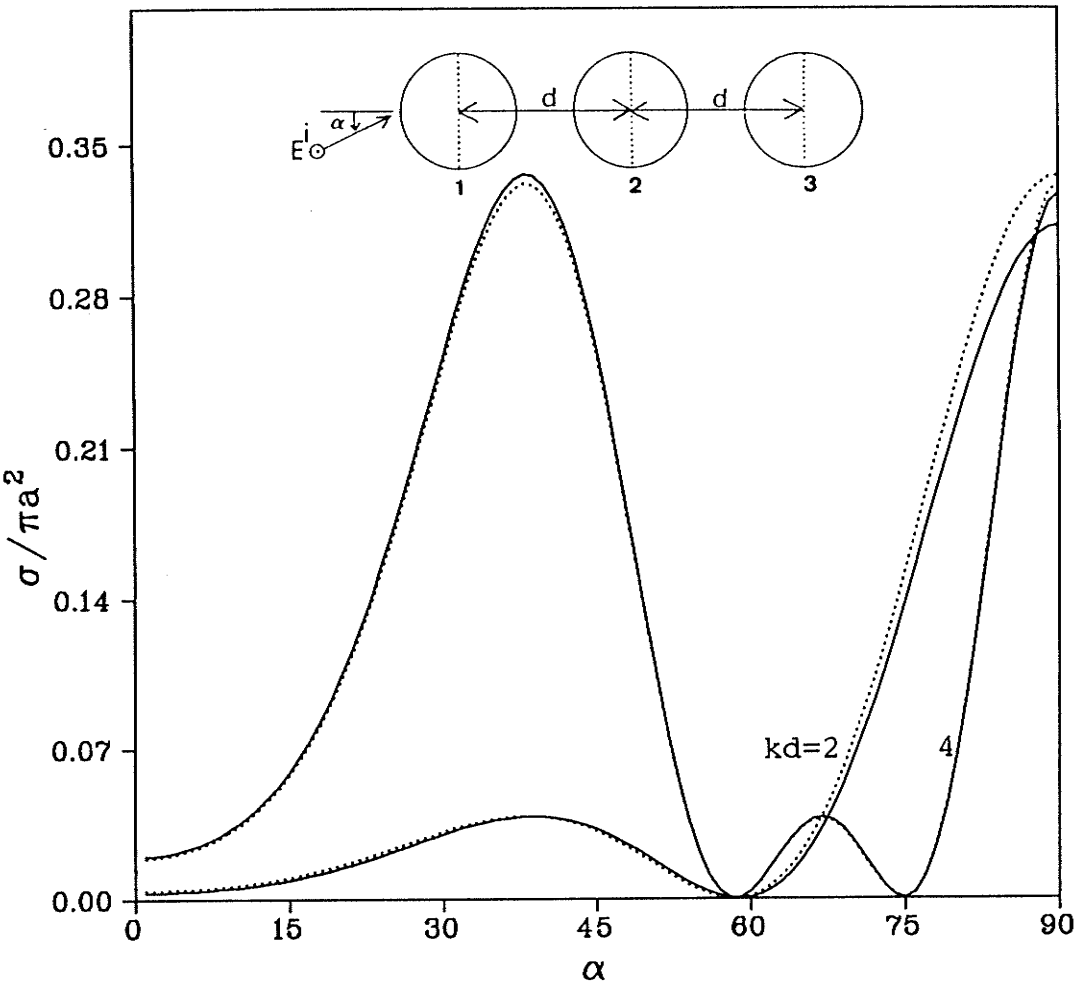

Fig.5-20. Normalized backscattering cross section versus aspect angle α for a linear array of three spheres with ka=0.5 and ε_r=3.0. (—analytic, ...approximate)

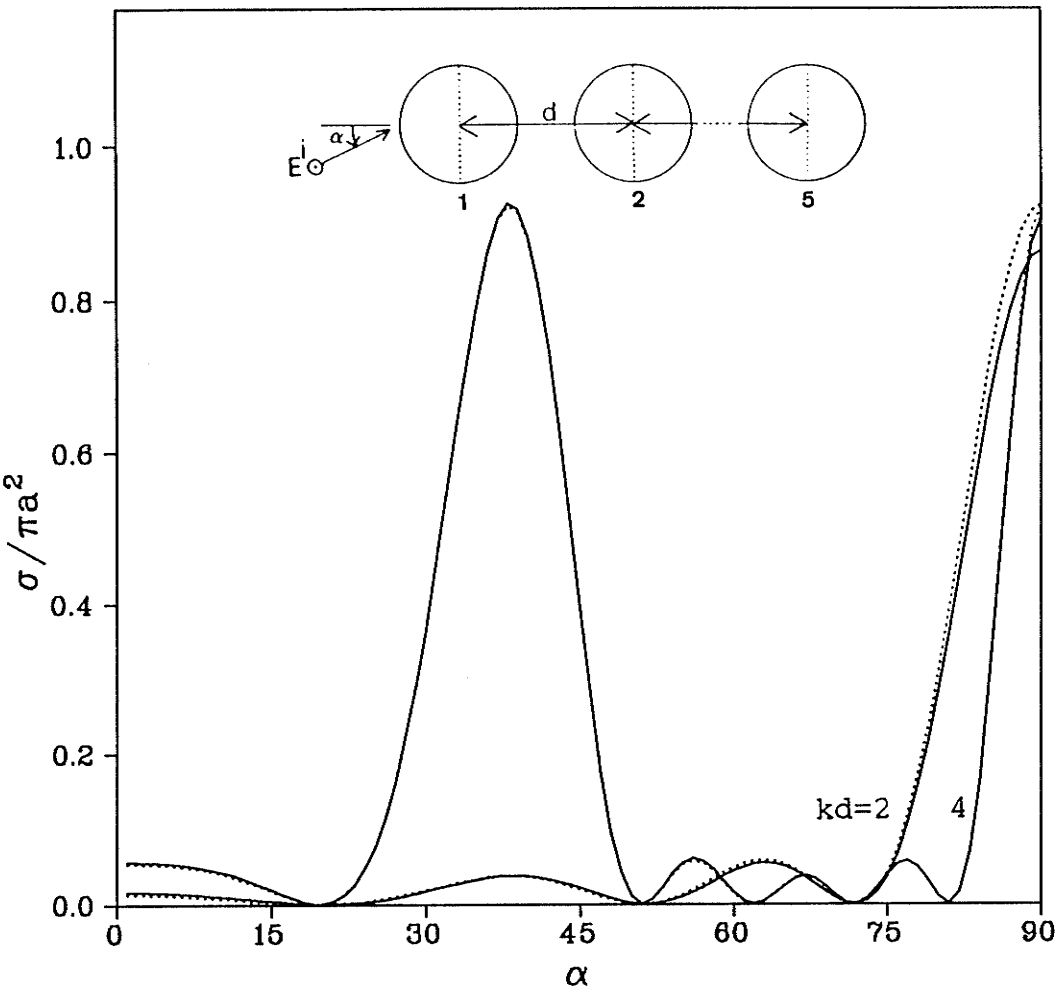

Fig.5-21. Normalized backscattering cross section versus aspect angle α for a linear array of five spheres with ka=0.5 and ε_r=3.0. (—analytic, ...approximate)

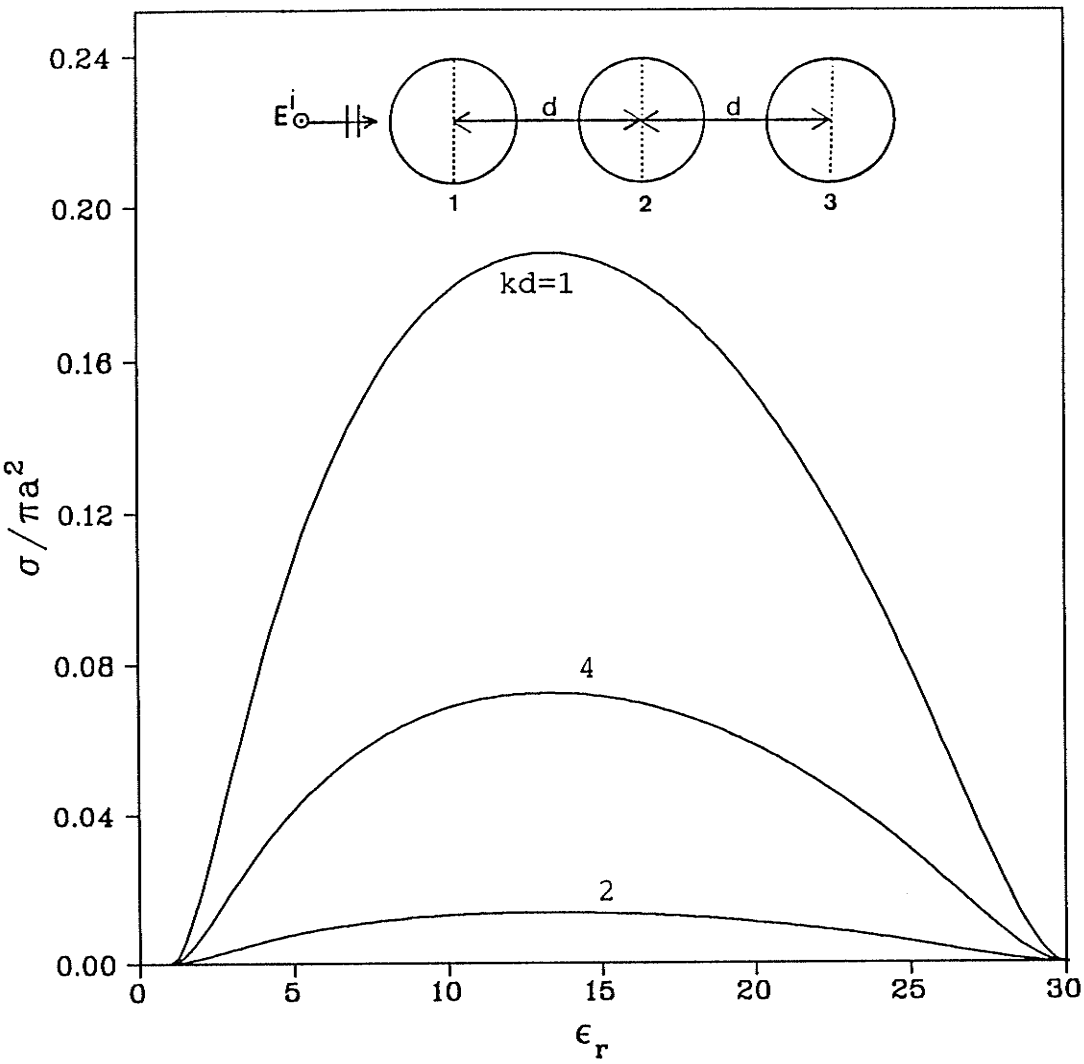

Fig.5-22. Normalized backscattering cross section versus dielectric constant ε_r for a linear array of three spheres with ka=0.5.

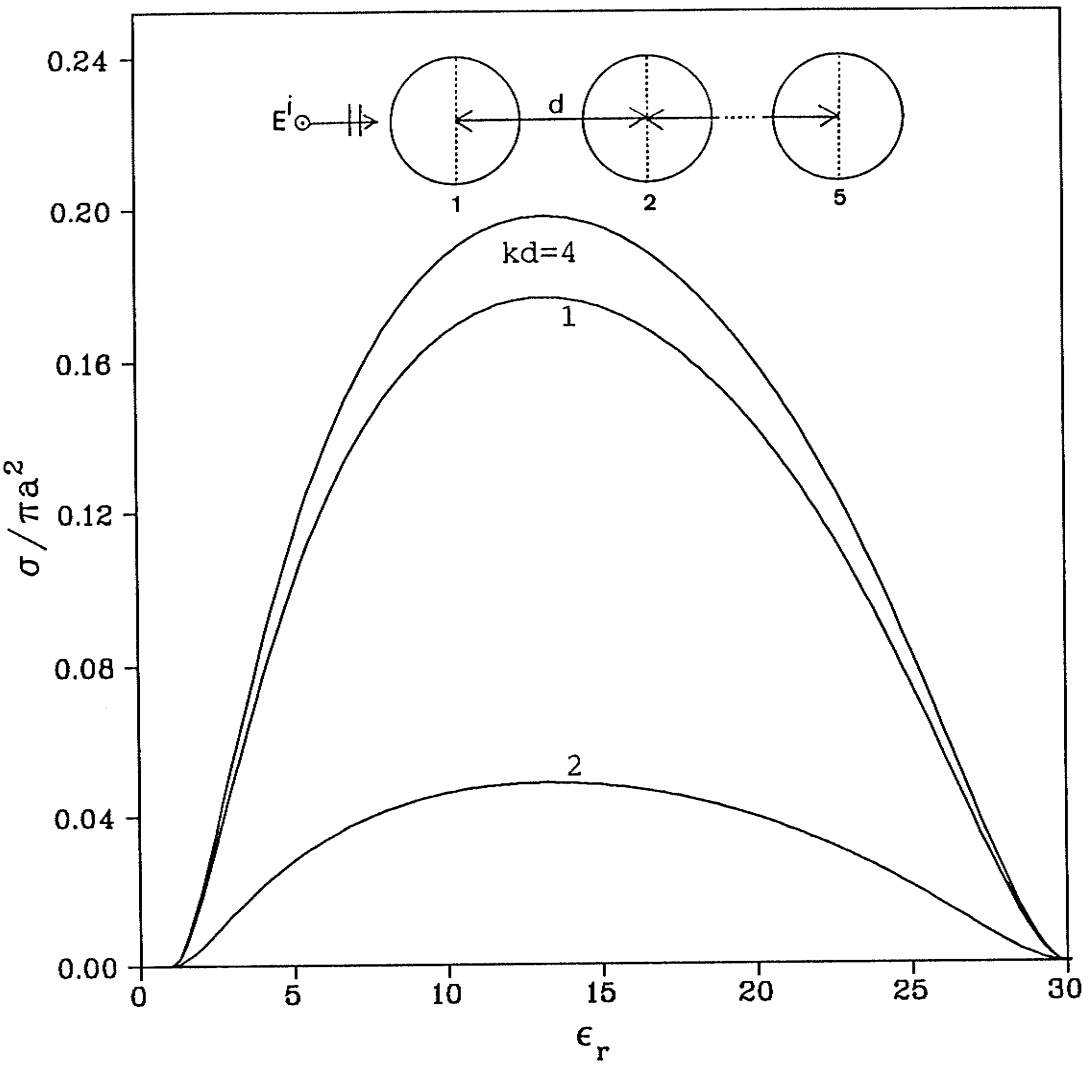

Fig.5-23. Normalized backscattering cross section versus dielectric constant ε_r for a linear array of five spheres with ka=0.5.

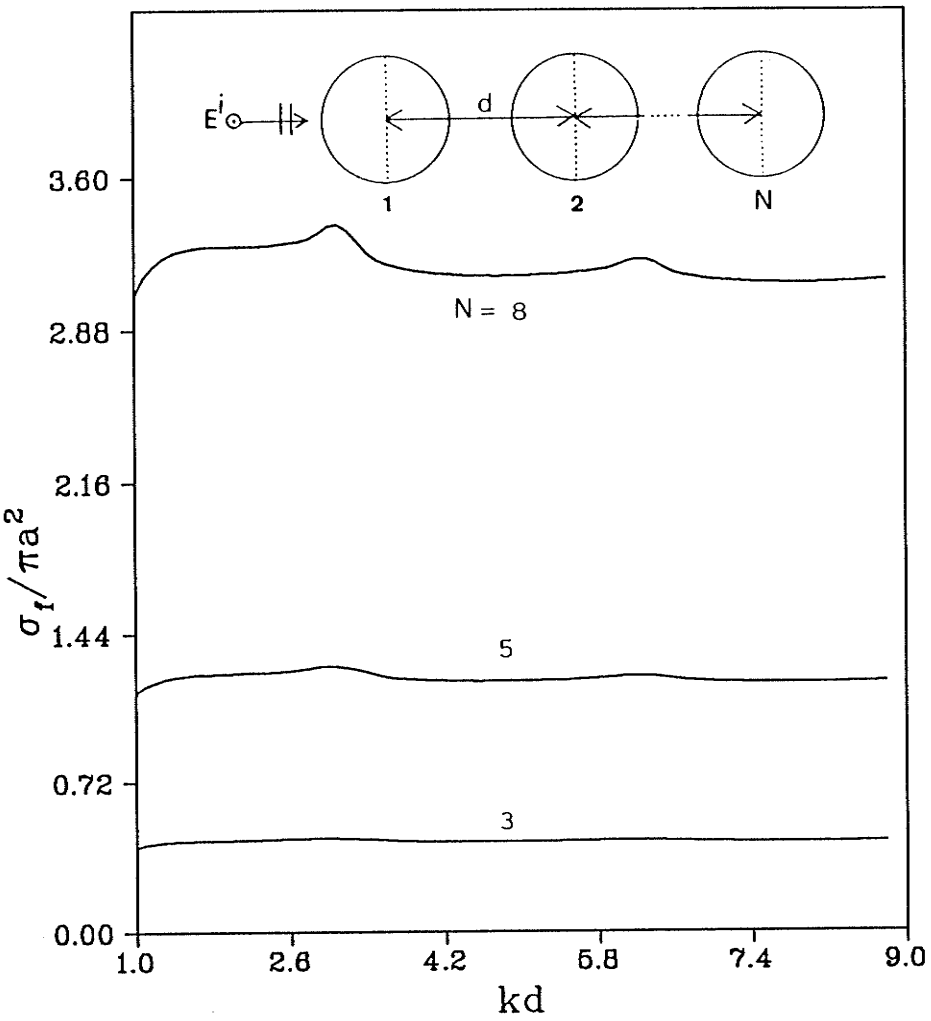

Fig.5-24. Normalized forward scattering cross section versus kd with ka=0.5 and ε_r=3.0.

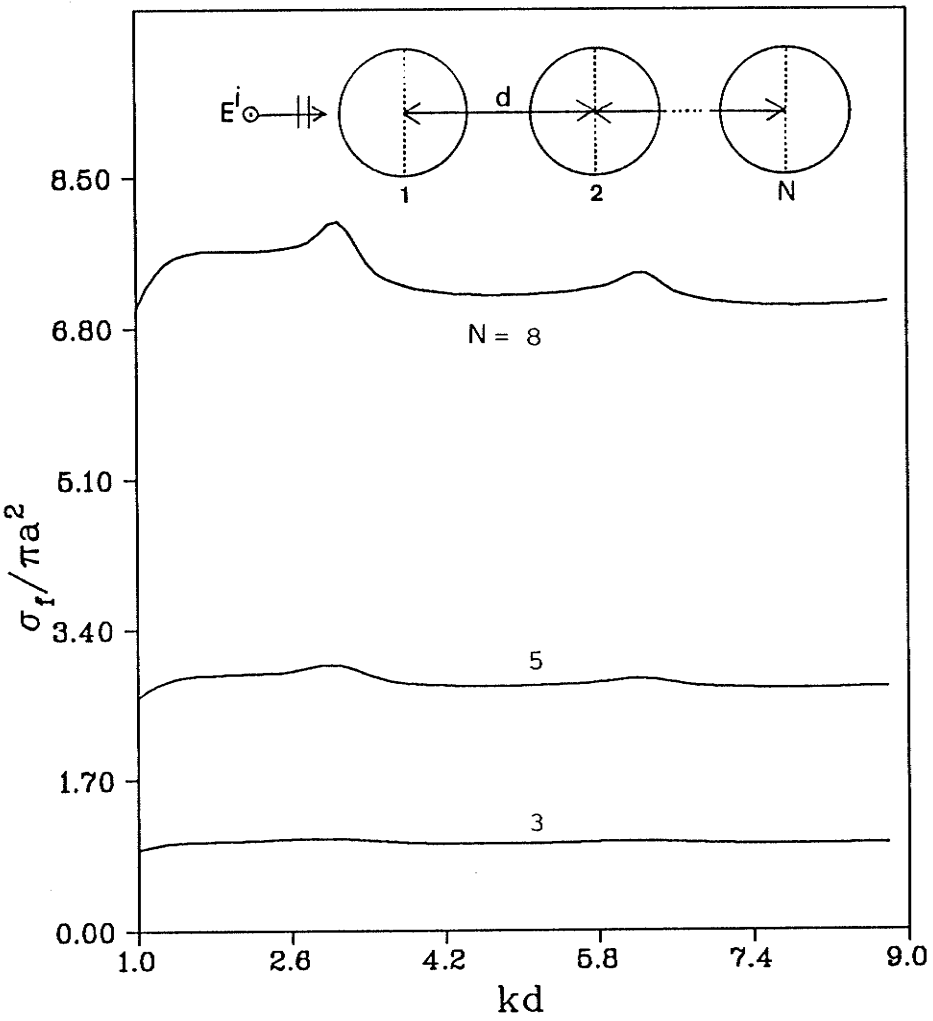

Fig.5-25. Normalized forward scattering cross section versus kd with ka=0.5 and ε_r=5.0.

Table.5-2. Normalized backscattering cross section $\sigma/\pi a^2$ for a linear array of N identical spheres with ka=0.5, ε_r=3.0.

kd	N	$\alpha=0^o$ (Endfire)	$\alpha=90^o$ (Broadside)
1.0	1	0.0369	0.0369
	2	0.0365	0.1355
	3	0.0003	0.2881
	4	0.0362	0.4905
	5	0.0456	0.7443
	6	0.0019	1.0554
	7	0.0312	1.4274
	8	0.0529	1.5734
2.0	2	0.0283	0.1414
	3	0.0029	0.3116
	4	0.0471	0.5534
	5	0.0163	0.8623
	6	0.0128	1.2360
	7	0.0494	1.6812
	8	0.0055	1.7385

incidence and kd=1.0 drops from 0.0369 (N=1) to 0.0003 (N=3). For broadside incidence, the magnitude of the backscattering cross section increases for the cases considered with kd and number of spheres as already encountered in the case of conducting spheres.

CHAPTER 6

SCATTERING FROM TWO DIELECTRIC COATED CONDUCTING SPHERES

In this chapter the formulation is extended to the problem of scattering of a plane electromagnetic wave by conducting spheres covered with a dielectric layer. In addition to the incident and scattered fields in the region surrounding the spheres, we have also the fields existing in the dielectric layers. The latter fields are expressed in terms of the vector spherical wave functions of the first and third kinds to satisfy the boundary conditions at the various interfaces [48].

Previous work on scattering by one sphere covered with a dielectric layer has been studied by many authors. Aden and Kerker [49] obtained analytic expressions to the scattering of plane electromagnetic waves by a dielectric sphere coated with a concentric spherical shell of a different dielectric material, while Scharfman [50] presented numerical values for the special case of a small ($ka<1$) dielectric-coated conducting sphere.

In section 6.1, the scattered fields are expressed in terms of the vector wave functions of the third kind which are similar to those used in the case of conducting or dielectric spheres. In addition, the transmitted fields inside the dielectric layers are presented by the vector wave functions of the first and third kinds. In section 6.2, application of the boundary conditions require continuity of the tangential electric and magnetic fields at the surface of each dielectric layer, and also the tangential transmitted electric field components must vanish at the metal surface of each sphere. Finally, numerical results are presented in section 6.3 to show the effects of the dielectric coating on the scattering cross section behaviour.

6.1 Expansion of the fields

Fig. 6-1 shows the system geometry. Spheres A and B are spaced along the z-axis and centered at the origins O and O′, respectively. The separation distance between the centers of the spheres is d.

The incident field in the region surrounding the spheres may be expressed in terms of the coordinate system attached to sphere A as

$$\overline{E}_A^i = \sum_{n=1}^{\infty} \sum_{m=-n}^{m=n} [P(m,n)\overline{N}_{mn}^{(1)}(r,\theta,\phi) + Q(m,n)\overline{M}_{mn}^{(1)}(r,\theta,\phi)] \tag{6-1}$$

The scattered field form sphere A ($r>a_1$) can be written in terms of the spherical vector wave functions as

$$\overline{E}_A^s = \sum_{n=1}^{\infty} \sum_{m=-n}^{m=n} [A_E^s(m,n)\overline{N}_{mn}^{(3)}(r,\theta,\phi) + A_M^s(m,n)\overline{M}_{mn}^{(3)}(r,\theta,\phi)] \tag{6-2}$$

Here A_E^s, A_M^s are the scattering coefficients of sphere A for transverse magnetic (TM) and transverse electric (TE) waves.

The fields in region 1 ($b_1 \le r \le a_1$) are expressed in terms of the vector spherical wave functions of the first and third kinds. Hence the electric field can be written as

$$\begin{aligned}\overline{E}_A^c = \sum_{n=1}^{\infty} \sum_{m=-n}^{m=n} [&A_E'(m,n)\overline{N}_{mn}^{(1)}(r,\theta,\phi) + A_E''(m,n)\overline{N}_{mn}^{(3)}(r,\theta,\phi) \\ &+ A_M'(m,n)\overline{M}_{mn}^{(1)}(r,\theta,\phi) + A_M''(m,n)\overline{M}_{mn}^{(3)}(r,\theta,\phi)]\end{aligned} \tag{6-3}$$

6.2 Application of the boundary conditions

The scattered field from sphere A in the presence of sphere B is due to the incident field and to the outgoing scattered field from sphere B. In order to impose the boundary conditions at $r=a_1$ the latter scattered field is transformed into an incoming field with respect to the sphere A, expressed in terms of the coordinates attached to this

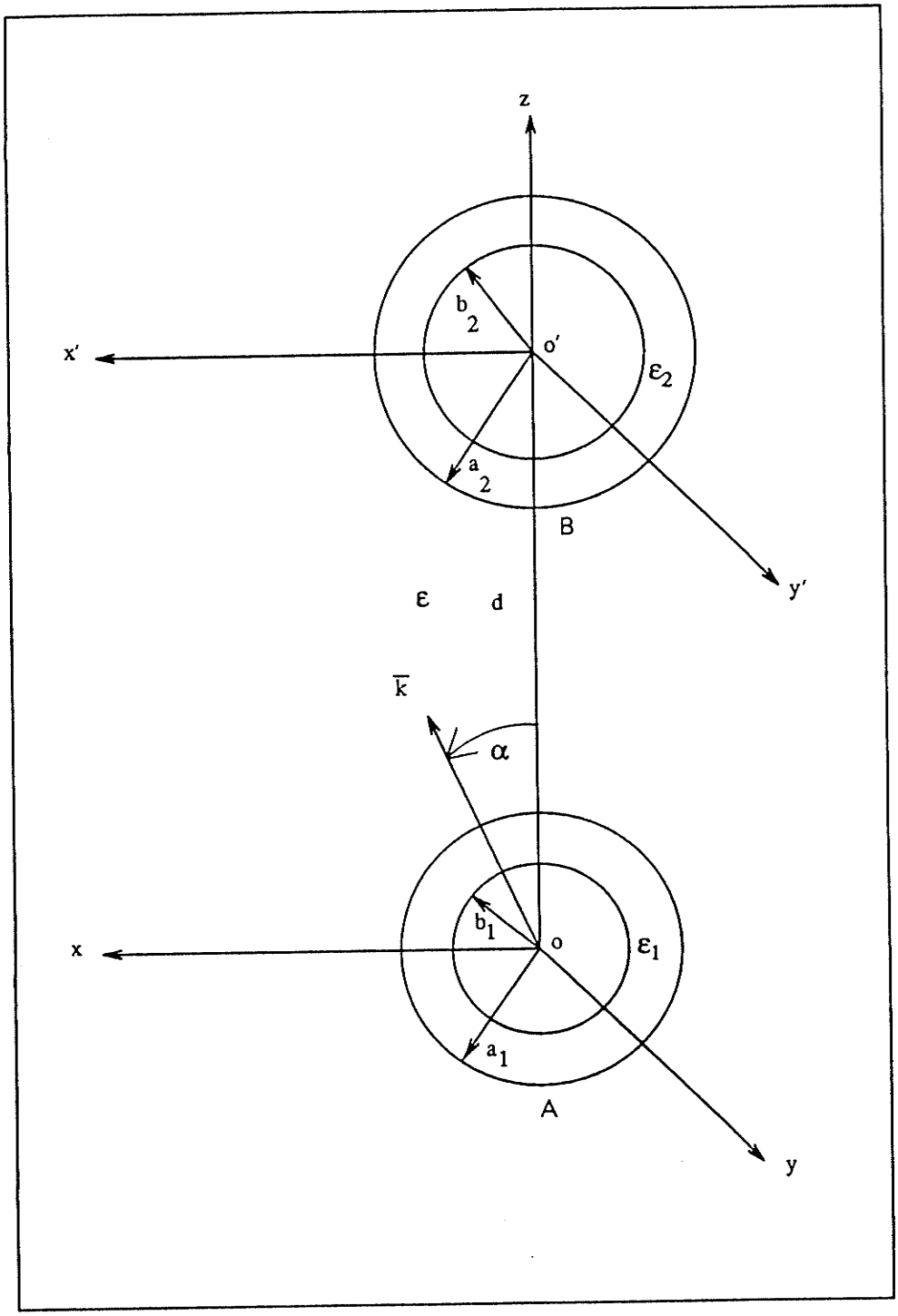

Fig.6-1. A system of two dielectric-coated spheres.

sphere. The boundary conditions require continuity of the tangential components (along θ and ϕ) of the electric and magnetic fields, *i. e.*,

$$\bar{r} \times [\, \bar{E}_A^i + \bar{E}_A^s + \bar{E}_{BA}^s \,] = \bar{r} \times \bar{E}_A^c \qquad \text{for } r = a_1 \tag{6-4}$$

$$\bar{r} \times [\, \bar{H}_A^i + \bar{H}_A^s + \bar{H}_{BA}^s \,] = \bar{r} \times \bar{H}_A^c \qquad \text{for } r = a_1 \tag{6-5}$$

The tangential electric field components at $r=b_1$ must be zero, i.e.,

$$\bar{r} \times \bar{E}_A^c = 0 \tag{6-6}$$

$\bar{E}_{BA}^s$ represents the scattered field from sphere B which is expressed in terms of the coordinate system of sphere A by using the translation addition theorem. This yields

$$\bar{E}_{BA}^s = \sum_{n=1}^{\infty} \sum_{m=-n}^{m=n} \{ B_E^s(m,n) \sum_{\nu=1}^{\infty} [A_{m\nu}^{mn}(d) \bar{N}_{m\nu}^{(1)}(r,\theta,\phi) + B_{m\nu}^{mn}(d) \bar{M}_{m\nu}^{(1)}(r,\theta,\phi)]$$
$$+ B_M^s(m,n) \sum_{\nu=1}^{\infty} [A_{m\nu}^{mn}(d) \bar{M}_{m\nu}^{(1)}(r,\theta,\phi) + B_{m\nu}^{mn}(d) \bar{N}_{m\nu}^{(1)}(r,\theta,\phi)] \} \tag{6-7}$$

$A_{m\nu}^{mn}$ and $B_{m\nu}^{mn}$ are the translation coefficients in the addition theorem, while B_E^s and B_M^s are the scattering coefficients of sphere B. The boundary conditions at $r=a_2$ and $r=b_2$ are implemented in a similar way.

Since we are mainly interested in the field outside the spheres, we present here expressions for the scattered field coefficients. Using the orthogonality properties of the vector wave functions leads to a system of coupled linear equations for the unknown scattered field coefficients in the form

$$A_E^s(m,n) = v_{An} \{ P(m,n) + \sum_{\nu=1}^{\infty} [A_{mn}^{m\nu}(d) B_E^s(m,\nu) + B_{mn}^{m\nu}(d) B_M^s(m,\nu)] \}$$

$$A_M^s(m,n) = u_{An} \{ Q(m,n) + \sum_{\nu=1}^{\infty} [A_{mn}^{m\nu}(d) B_M^s(m,\nu) + B_{mn}^{m\nu}(d) B_E^s(m,\nu)] \}$$

$$B_E^s(m,n) = v_{Bn} \{ P'(m,n) + \sum_{\nu=1}^{\infty} (-1)^{n+\nu}$$
$$\cdot [A_{mn}^{m\nu}(d) A_E^s(m,\nu) - B_{mn}^{m\nu}(d) A_M^s(m,\nu)] \}$$

$$B_M^s(m,n) = u_{Bn}\{Q'(m,n) + \sum_{\nu=1}^{\infty}(-1)^{n+\nu} \cdot [A_{mn}^{m\nu}(d)A_M^s(m,\nu) - B_{mn}^{m\nu}(d)A_E^s(m,\nu)]\} \tag{6-8}$$

where P' and Q' are the incident field expansion coefficients relative to the sphere B, which differ form those relative to the sphere A by the phase factor $e^{jkd\cos\alpha}$. Furthermore, v_{An} and u_{An} are the scattering coefficients corresponding to the conducting sphere A covered with a dielectric layer, assumed to be alone in the incident field, which are given by

$$v_{An} = -\frac{\rho_A\, j_n(\rho_A) - jY_{An}[\rho_A j_n(\rho_A)]'}{\rho_A\, h_n^{(1)}(\rho_A) - jY_{An}[\rho_A\, h_n^{(1)}(\rho_A)]'} \tag{6-9}$$

$$u_{An} = -\frac{\rho_A\, j_n(\rho_A) - jZ_{An}[\rho_A j_n(\rho_A)]'}{\rho_A\, h_n^{(1)}(\rho_A) - jZ_{An}[\rho_A\, h_n^{(1)}(\rho_A)]'} \tag{6-10}$$

and the coefficients Z_{An} and Y_{An} are

$$Z_{An} = j\rho_A \frac{j_n(\xi_A)h_n^{(1)}(\beta_A) - j_n(\beta_A)\, h_n^{(1)}(\xi_A)}{j_n(\beta_A)[\xi_A\, h_n^{(1)}(\xi_A)]' - h_n^{(1)}(\beta_A)[\xi_A\, j_n(\xi_A)]'} \tag{6-11}$$

$$Y_{An} = j\rho_A N_A^2 \frac{h_n^{(1)}(\xi_A)\,[\beta_A j_n(\beta_A)]' - j_n(\xi_A)\,[\beta_A h_n^{(1)}(\beta_A)]'}{[\xi_A j_n(\xi_A)]'\,[\beta_A h_n^{(1)}(\beta_A)]' - [\beta_A j_n(\beta_A)]'\,[\xi_A h_n^{(1)}(\xi_A)]'} \tag{6-12}$$

Here $k_1 = N_A k$, $\rho_A = ka_1$, $\xi_A = k_1 a_1$, $\beta_A = k_1 b_1$, $N_A = \sqrt{\varepsilon_1/\varepsilon}$, while ε_1 and ε are the permittivities of sphere A and of the medium surrounding the spheres. The coefficients v_{Bn} and u_{Bn} can be written similarly by replacing a_1 , b_1 by a_2, b_2. In the case of lossy dielectric-coated spheres, N_A and N_B are complex.

The series in equation (6-8) are infinite and must therefore be truncated to a finite number of terms $\nu = n$. Hence the system of equations may be written in a matrix form as

$$A = L + T\,A \tag{6-13}$$

where A and L are column matrices while T is a square matrix representing the cou-

pling between the spheres and depends on the separation distance between the spheres.

The total scattered field in the far zone can be obtained after taking the asymptotic form of the vector spherical wave functions. Thus the total far scattered field can be written as

$$\bar{E}^s = \frac{e^{jkr}}{kr}[F_\theta(\theta,\phi)\,\hat{\theta} + F_\phi(\theta,\phi)\,\hat{\phi}] \tag{6-14}$$

where

$$F_\theta(\theta,\phi) = F_{\theta A}(\theta,\phi) + F_{\theta B}(\theta,\phi) \tag{6-15}$$

$$F_\phi(\theta,\phi) = F_{\phi A}(\theta,\phi) + F_{\phi B}(\theta,\phi) \tag{6-16}$$

and

$$F_{\theta A}(\theta,\phi) = \sum_{n=1}^{\infty}\sum_{m=0}^{n} j^{-n+1}\varepsilon_m [A_E^s(m,n)\frac{\partial}{\partial\theta}P_n^m(\cos\theta) + A_M^s(m,n)\frac{m}{\sin\theta}P_n^m(\cos\theta)]\,\sin m\phi \tag{6-17}$$

$$F_{\phi A}(\theta,\phi) = \sum_{n=1}^{\infty}\sum_{m=0}^{n} j^{-n+1}\varepsilon_m [A_E^s(m,n)\frac{m}{\sin\theta}P_n^m(\cos\theta) + A_M^s(m,n)\frac{\partial}{\partial\theta}P_n^m(\cos\theta)]\,\cos m\phi \tag{6-18}$$

with ε_m being the Neumann number (1 for $m=0$ and 2 for $m>0$). The expressions for $F_{\theta B}$ and $F_{\phi B}$ are obtained from those $F_{\theta A}$ and $F_{\phi A}$ by replacing A_E^s, A_M^s by B_E^s, B_M^s and multiplying each expression by the phase factor $e^{-jkd\cos\theta}$.

The normalized bistatic cross section is given by

$$\frac{\sigma(\theta,\phi)}{\lambda^2} = \frac{1}{\pi}\left[\,|F_\theta(\theta,\phi)|^2 + |F_\phi(\theta,\phi)|^2\right] \tag{6-19}$$

6.3 Numerical results

Typical numerical results are presented graphically in Fig. 6-2 for the normalized bistatic cross section patterns of two identical dielectric-coated spheres with ka=2, kb=1, kd=4, with $\varepsilon_{r1}=\varepsilon_{r2}=5$, as a function of the scattering angle θ and with endfire plane wave incidence ($\alpha=0$). Fig. 6-3 shows the same geometry except kd is increased to 8. It can be seen that by increasing kd from 4 to 8 the magnitude of the forward scattering cross section ($\theta=0$) is increased from 11.3 to 27.6, and the bistatic cross section patterns vanish at more scattering angles. Figs. 6-4 and 6-5 present the same geometry and electrical separations as in the above example except the dielectric-coatings have permittivities $\varepsilon_{r1}=5$ and $\varepsilon_{r2}=2$. By reducing ε_{r2} from 5 to 2 the ripples are substantially reduced and the magnitude of the backscattering cross section ($\theta=\pi$) increases from 0.2 to 5.5. This is in contrast with Fig. 6-3 which shows reduction in the forward scattering cross section and only a slight change in the backscattering cross section.

In the cases considered, the system of matrices is solved only for the azimuthal mode $m=1$ due to the symmetry with respect to the z-axis, with $n=14$ in the case when the spheres are in contact (kd=4).

In this chapter we have obtained an exact solution of the problem of multiple scattering by two dielectric-coated conducting spheres with arbitrary size, and angle of incidence. The boundary conditions are imposed on the outer surface of each dielectric layer by using the translation addition theorem for the spherical wave functions. The resultant system of equations is written in a matrix form and therefore the desired field scattering coefficients are obtained by matrix inversion. Some numerical

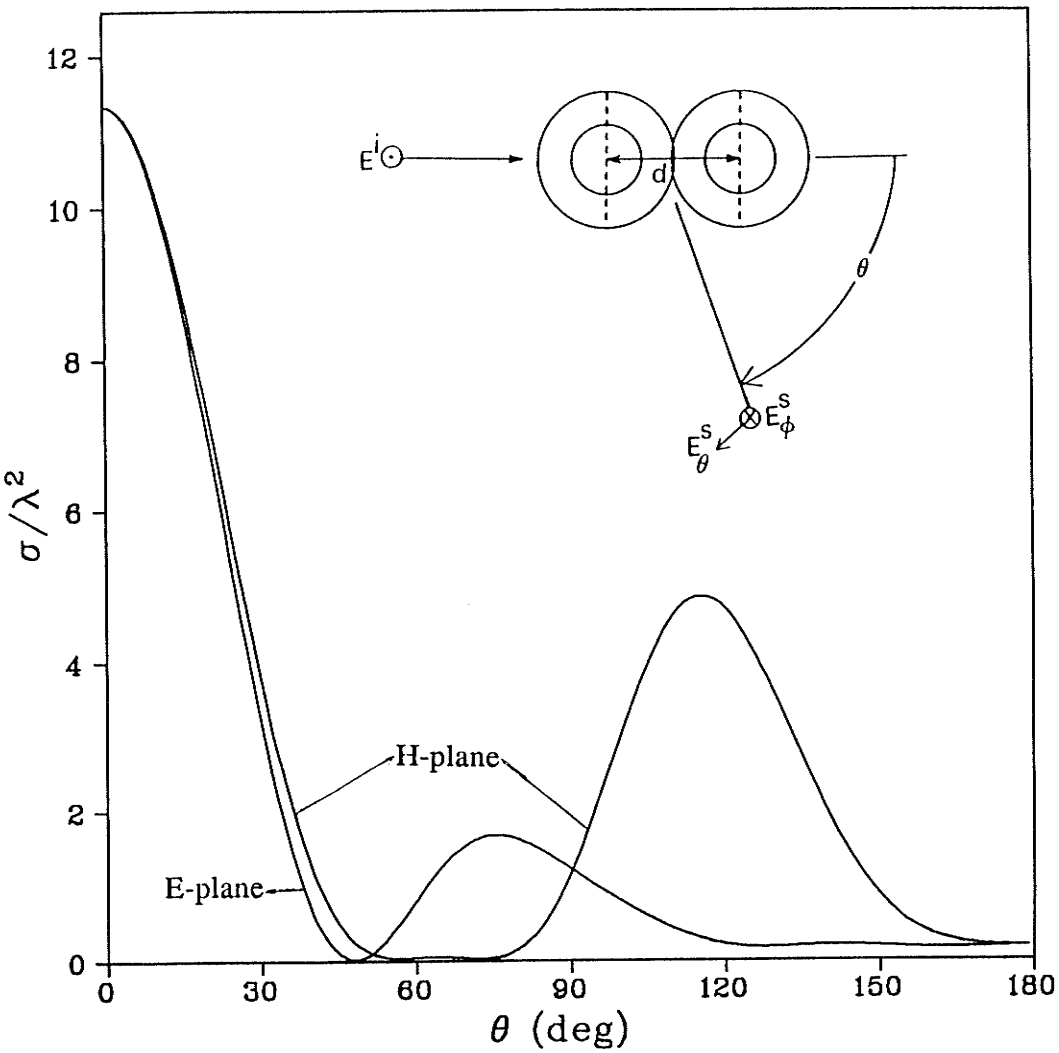

Fig.6-2. Normalized bistatic cross section patterns for two identical dielectric-coated spheres with ka=2, kb=1, $\varepsilon_{r1}=\varepsilon_{r2}=5$, kd=4.

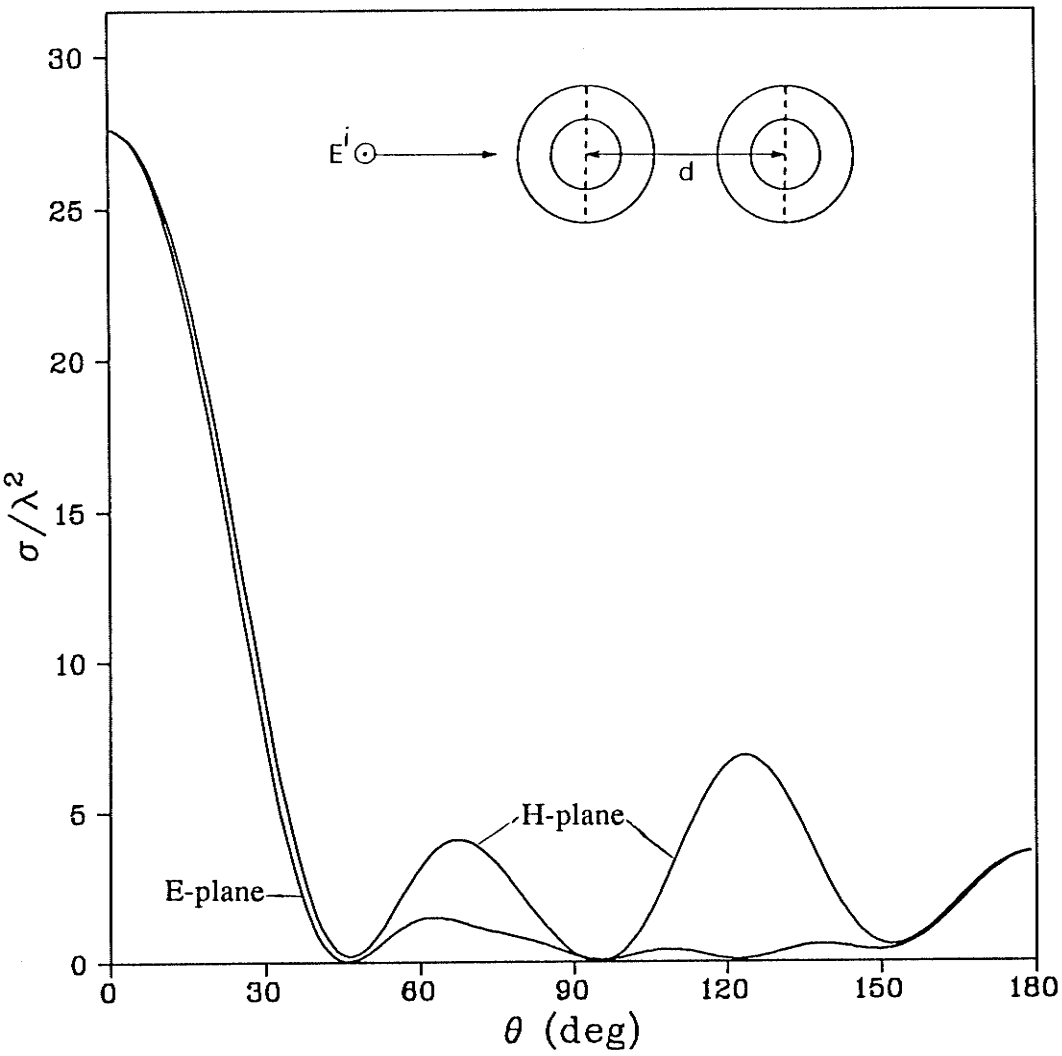

Fig.6-3. Normalized bistatic cross section patterns for two identical dielectric-coated spheres with ka=2, kb=1, $\varepsilon_{r1}=\varepsilon_{r2}=5$, kd=8.

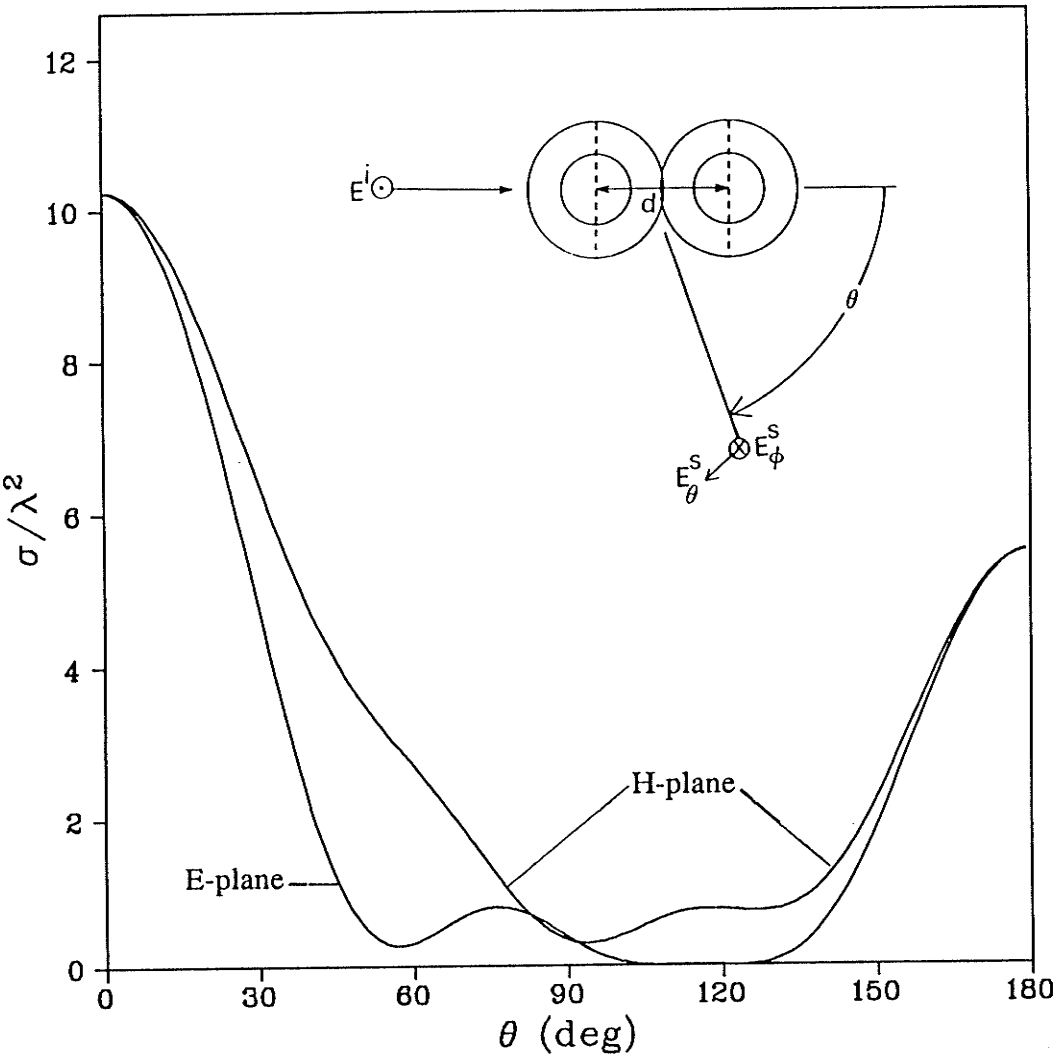

Fig.6-4. Normalized bistatic cross section patterns for two identical dielectric-coated spheres with ka=2, kb=1, ε_{r1}=5, ε_{r2}=2, kd=4.

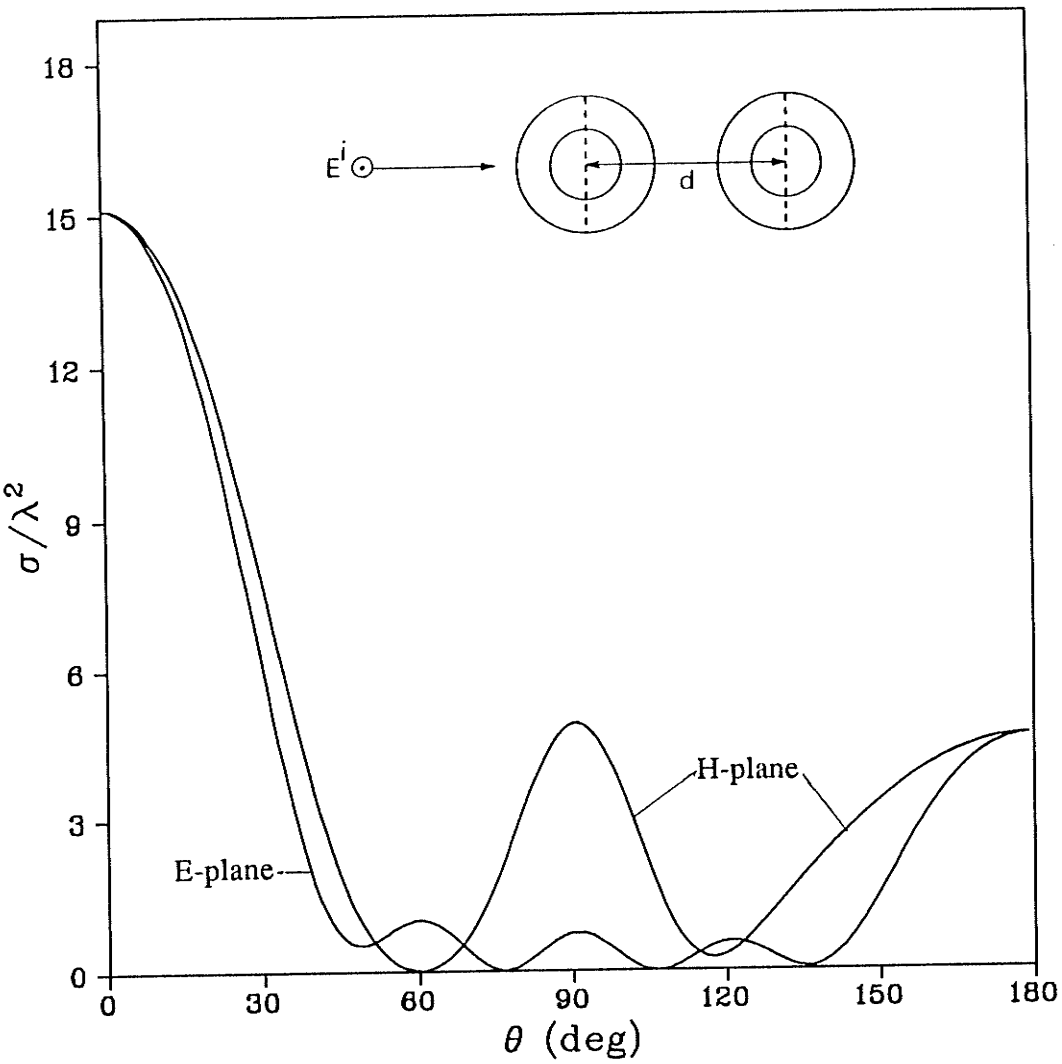

Fig.6-5. Normalized bistatic cross section patterns for two identical dielectric-coated spheres with ka=2, kb=1, ϵ_{r1}=5, ϵ_{r2}=2, kd=8.

results are presented for the normalized bistatic cross section patterns for the special case of endfire incidence on two identical spheres with ka=2, kb=1 for various kd and ε_r.

CHAPTER 7

DISCUSSION AND OUTLINE OF SUGGESTIONS FOR FUTURE RESEARCH

7.1 Discussion

The problem of scattering of a plane electromagnetic wave by an arbitrary configuration of conducting, dielectric or a mixture of conducting and dielectric spheres has been formulated analytically. The incident, transmitted and scattered fields have been expressed in chapter 2 in terms of the vector spherical wave functions of the first and third kind, respectively. The boundary conditions require continuity of the tangential electric and magnetic fields on the surface of each dielectric sphere, and have been imposed by using the translation addition theorem for the vector spherical wave functions in order to express the outgoing scattered fields from one sphere in terms of incoming fields incident on the remaining spheres. Using the orthogonality properties of the vector spherical wave functions, a system of equations for the unknown scattered field coefficients is obtained. This system of equations has been written in a matrix form and solved by matrix inversion for the scattered field coefficients from which the electric and magnetic fields can be computed everywhere.

The special case of perfectly conducting spheres has been obtained from the dielectric case by letting the relative dielectric constant of each dielectric sphere in section 2.6 become very high. We have noticed that the resulting system of equations for perfectly conducting spheres is similar to that for dielectric spheres with the scattered field coefficients of a single dielectric sphere replaced by the perfectly conducting ones.

The required computer time and memory to invert the resulting system of matrices increases rapidly with the number and dimensions of the spheres. Therefore, in chapter 3 we have presented a novel iterative solution for the scattering by an arbitrary configuration of conducting or dielectric spheres. The first order scattered field (first iteration) requires the solution of the scattered field by each sphere, assumed to be alone in the incident field. The second order scattered field results from the excitation of each sphere due to the sum of all first order scattered fields. Finally a general expression for the i th order scattered fields is obtained and written in a matrix form.

The validity of this technique has been verified numerically by comparing the numerical results with those obtained by the simultaneous boundary conditions solution (chapter 2). The results show that the iterative solution converges as the number of iterations increases. However, for the particular cases considered in chapter 4, the results show that the first and second order scattered fields are needed to obtain the backscattering cross section patterns with endfire incidence, while four orders of scattered fields are needed for an arbitrary angle of incidence and contacting linear array of spheres.

One of the main advantages of employing the iterative solution is that of handling each iteration separately and then summing over all previous iterations to obtain the total scattered field. Another advantage is that of saving computer time and memory by avoiding the inversion of the system matrix. For example in Fig. (4-6) the required computer time to obtain the normalized bistatic cross section patterns using the iterative solution for a system of five spheres with ka=1.5 and kd=4.0 is about 50% less than using the simultaneous solution.

In chapter 4 we have presented for the first time numerical results for a one-dimensional array of more than two spheres, and also a two-dimensional array of four spheres located at the vertices of a square. The results show that the required number of iterations to obtain the normalized bistatic cross section patterns for a system of dielectric spheres is less when compared with a system of conducting spheres of the same dimensions and separations. Moreover, it is worth mentioning that the results in chapter 4 are too difficult to obtained by numerical methods such as the moment method since the latter requires a large memory compared with the exact solutions.

As mentioned previously, one of the most useful applications of the scattering by N spheres is that it can be used to simulate the scattering by three-dimensional bodies, since we know that most of these bodies do not have analytic solution available in the literature. Three spheres were used in Figs. (4-14) and (4-15) to simulate a spheroid with a major axis ka=1.0 and axial ratio of 2.0.

In principle, the analytic solutions are valid for any number of spheres, electrical sizes and separation distances. However, due to the computational time and storage required, the presented numerical results are hence given to one and two-dimensional array of spheres.

For electrically small and non conducting spheres, a novel approximate method has been derived in chapter 5. The approximate solution is based on the assumption that the scattered field from each sphere is due to the incident field and the fields from the other spheres approximated by plane waves of unknown magnitudes.

It should be pointed out that the approximate solution gives excellent agree-

ments with the exact numerical results for the backscattering cross section patterns with ka<1.0 and kd>1.5 which means that the assumption of the far field interaction between the spheres is adequate once these conditions are met. In addition, It has proven that the approximate method has computational advantages over the exact solutions, since there is no need to compute the series resulting from application of the translation addition theorem for the vector wave functions. This approach does not require large computer storage and leads to fast convergence.

The practical relevance of the numerical results in Figs. (5-24) and (5-25) is their potential application in studying aperture antennas loaded with a linear array of dielectric spheres in order to enhance the gain along preferred directions. Figure (5-24) shows that the forward scattering is equal to 0.45 for three spheres and increases to 3.38 by increasing the number of spheres to 8 where the incident plane wave is assumed to be due to the far field of an aperture antenna whose main lobe along the line joining the centers of the spheres.

One of the most interesting results in chapter 5 is the deviation of the peak value of the bistatic cross section from $\theta=180^o$ for a single sphere to $\theta=127^o$ for the particular case of N=8, ka=0.5 and kd=4.0, and other values of θ for other arrangements of spheres. The physical justifications for these variations are due to the multiple scattering phenomena and the resulting interference by the collection of spheres.

We have shown in chapter 5 that the resonances in the normalized backscattering cross section patterns occur at the same locations for a system of conducting and dielectric spheres and hence are independent of material characteristics.

Examination of the presented numerical results for an array of dielectric spheres

shows lower backscattering and bistatic cross sections for some cases with respect to those for the conducting spheres. This is partly due to the fields transmitted into the spheres and also due to the weaker sphere to sphere coupling.

7.2 Future research

Although we have already investigated the scattering of a plane electromagnetic wave by conducting, dielectric, and dielectric-coated conducting spheres, the analysis can be extended to the scattering by systems of two and more dielectric spheres covered with a concentric spherical shell of a different dielectric material. In addition to the incident and scattered fields in the region surrounding the spheres, we have the fields existing in the spherical shells and inside the dielectric spheres. The fields inside the spherical shells are expressed in terms of the vector wave functions of the first and third kinds, while the fields inside the dielectric spheres are expressed in terms of the first kind of the vector wave functions. The special case of dielectric coated conducting spheres can be obtained by letting the relative dielectric constant of each dielectric sphere become very large.

A potential study is how to generalize the approximate solution to an arbitrary configuration of conducting or dielectric sphere since the approximate solution has proven to have computational advantages over the analytical solutions for small spheres.

Another possible study is that of getting numerical results for three-dimensional arrays of spheres and using these results to simulate complex three-dimensional bodies.

From the formulation given in section 2.1 for the *TE* case, where the incident electric field is perpendicular to the z-axis, the *TM* case, where the electric field is parallel to the z-axis, can be easily obtained through an appropriate change in the incident field coefficients.

APPENDIX A

ORTHOGONALITY PROPERTIES OF THE SPHERICAL WAVE FUNCTIONS

The following orthogonality properties of the spherical wave functions are used throughout the report [37],

$$(\overline{M}_{mn}^{(i)}, \overline{M}_{mv}^{(i)}) = \int_0^{2\pi}\int_0^{\pi} \overline{M}_{mn}^{(i)} \cdot \overline{M}_{mv}^{(i)} \sin\theta \, d\theta \, d\phi$$
$$= 4\pi \frac{(n+1)}{(2n+1)} \frac{(n+m)!}{(n-m)!} [Z_n^{(i)}(kr)]^2 \ \delta_{nv} \qquad \text{(A-1)}$$

$$(\overline{N}_{mn}^{(i)}, \overline{N}_{mv}^{(i)}) = \int_0^{2\pi}\int_0^{\pi} \overline{N}_{mn}^{(i)} \cdot \overline{N}_{mv}^{(i)} \sin\theta \, d\theta \, d\phi$$
$$= 4\pi \frac{(n+1)}{(2n+1)} \frac{(n+m)!}{(n-m)!} [kr \, Z_n^{(i)}(kr)]'^2 \ \delta_{nv} \qquad \text{(A-2)}$$

where $i=1$ and 2 represent the spherical Bessel and Hankel functions, respectively. The following associated Legendre integrals are applied in the above equations

$$\int_0^{\pi} P_n^m \cdot P_v^m \sin\theta d\theta = \frac{2}{(2n+1)} \frac{(n+m)!}{(n-m)!} \ \delta_{nv} \qquad \text{(A-3)}$$

$$\int_0^{\pi} \left(\frac{dP_n^m}{d\theta} \frac{dP_v^m}{d\theta} + \frac{m^2 P_n^m P_v^m}{\sin^2\theta} \right) \sin\theta \, d\theta = \frac{2}{2n+1} \frac{(n+m)!}{(n-m)!} n(n+1) \delta_{nv} \qquad \text{(A-4)}$$

APPENDIX B

TRANSLATION ADDITION THEOREM FOR VECTOR SPHERICAL WAVE FUNCTIONS

In this Appendix, the general vector translation addition theorem for a translation between arbitrarily located two spherical points are cited and discussed. Boundary value solutions involving the scattering by two or more bodies usually require the use of the translation addition theorem to transform the outgoing scattered field from one sphere into incoming field (finite at the origin) on the remaining spheres for the application of the boundary condition on the surface of each sphere.

So far the translation addition theorem is given in the literature for a translation between two spherical points: one located at the origin while the other is in space. In this Appendix we express this theorem for an arbitrary two points located in spherical coordinates in space, say p and q as shown in Fig B-1, since this form can be easily used in the solution of scattering by an arbitrary configuration of N spheres.

The formulation of the scalar addition theorem for spherical wave functions was first done by Friedman and Russek [51]. Later, Stein [26] obtained a solution for the vector translation addition theorem, while Cruzan [27] put the vector addition theorem in appropriate forms by deriving new recursion formulas. Recently, Bruning and Lo [52] obtained more efficient recursion formulas to reduce the computation time required to evaluate the series resulting from applying the addition theorem.

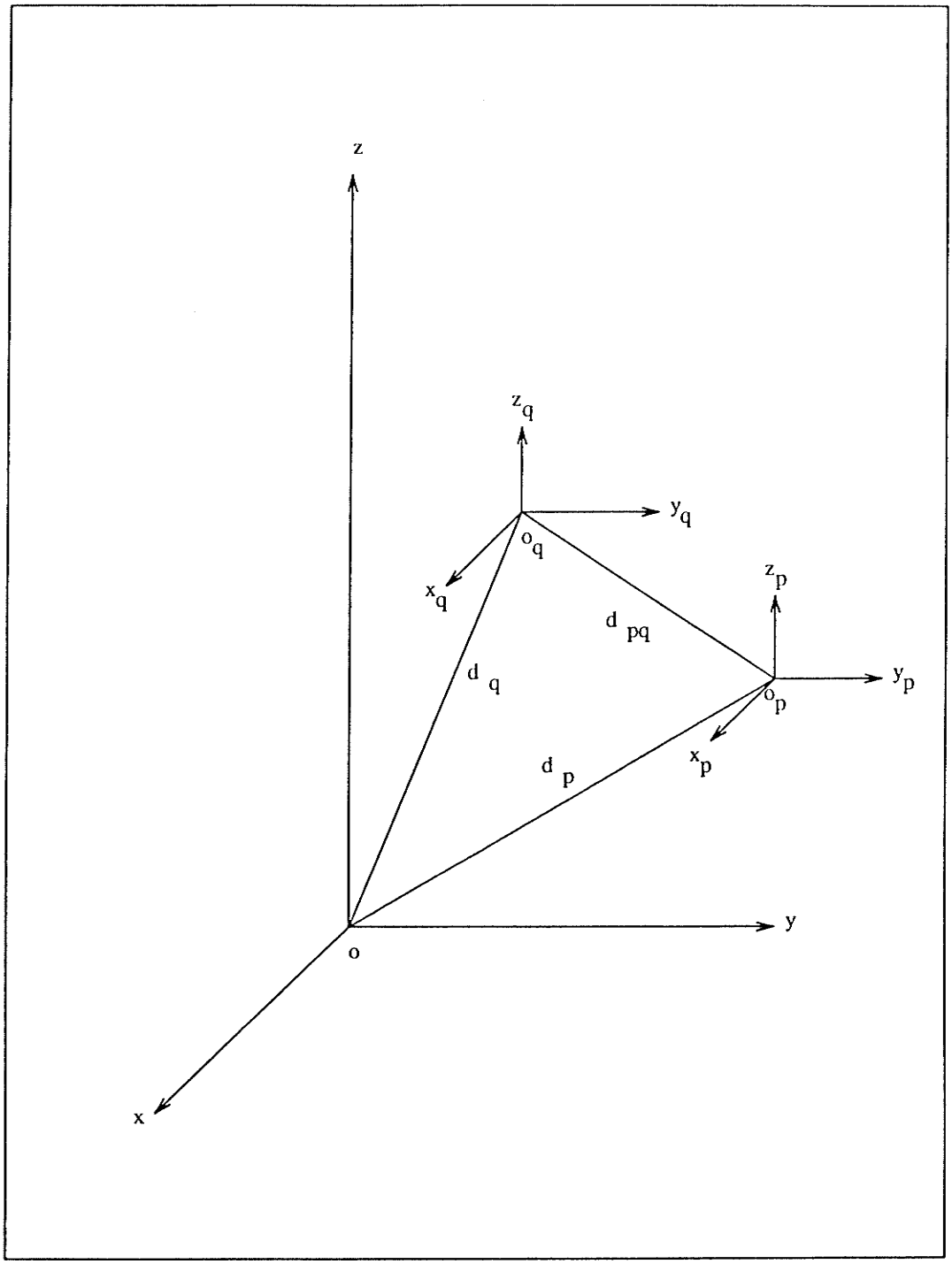

Fig.B-1 Translation of the Cartesian coordinate system (x_q, y_q, z_q) to the system (x_p, y_p, z_p) a distance d_{pq}.

B.1 Scalar translation addition theorem

A derivation of the scalar addition theorem for the scalar spherical wave functions was given by Friedman and Russek [51], and then pursued by Stein [26].

We start by the scalar Helmholtz wave equation which has the following form

$$\nabla^2 u + k^2 u = 0 \tag{B-1}$$

where a solution for the above differential equation in spherical coordinates can be written as

$$u_{mn}(r_p,\theta_p,\phi_p) = Z_n^{(i)}(kr_p)\,P_n^m(\cos\theta_p)\,e^{jm\phi_p}, \quad 0 \le n \le \infty,\ -n \le m \le n \tag{B-2}$$

Here i =1 and 2 represent the spherical Bessel and Hankel functions, respectively. The translation of the scalar spherical wave functions from the spherical coordinates (r_q,θ_q,ϕ_q) to (r_p,θ_p,ϕ_p) a separation distance d_{pq} is given by

$$u_{mn}^{(3)}(r_q,\theta_q,\phi_q) = \sum_{\nu=0}^{\infty} \sum_{\mu=-\nu}^{\mu=\nu} \alpha_{\mu\nu}^{mn}(d_{pq},\theta_{pq},\phi_{pq})\,u_{\mu\nu}^{(1)}(r_p,\theta_p,\phi_p) \tag{B-3}$$

with

$$\alpha_{\mu\nu}^{mn}(d_{pq},\theta_{pq},\phi_{pq}) = (-1)^{\mu} j^{\nu-n}\,(2\nu+1) \sum_{p'} j^{-p'}\,a(m,n,-\mu,\nu,p')\,h_{p'}^{(1)}(kd_{pq}) \cdot P_{p'}^{m-\mu}(\cos\theta_{pq})\,e^{j(m-\mu)\phi_{pq}} \qquad r \le d_{pq} \tag{B-4}$$

or

$$\alpha_{\mu\nu}^{mn}(d_{pq},\theta_{pq},\phi_{pq}) = (-1)^{m-\mu} j^{\nu-n} \sum_{p'} j^{-p'}\,(2p'+1)\,a(m,n,\mu-m,p',\nu)\,j_{p'}(kd_{pq}) \cdot P_{p'}^{m-\mu}(\cos\theta_{pq})\,e^{j(m-\mu)\phi_{pq}} \qquad r \ge d_{pq} \tag{B-5}$$

The coefficient $a(m,n,\mu,\nu,p')$ can be expanded in terms of the product of two associated Legendre functions, *i.e.*,

$$P_n^m P_\nu^\mu = \sum_{p'} a(m,n,\mu,\nu,p')\,P_{p'}^{m+\mu} \tag{B-6}$$

where $p' = n+\nu, n+\nu-2, \cdots, |n-\nu|$. To obtain a simpler form for (B-5), the fol-

lowing identity is used:

$$a(m,n,\mu-m,p',\nu)=(-1)^m\frac{2\nu+1}{2p'+1}a(m,n,-\mu,\nu,p') \tag{B-7}$$

Substituting equation (B-7) into (B-5), we obtain

$$\alpha_{\mu\nu}^{mn}(d_{pq},\theta_{pq},\phi_{pq})=(-1)^{\mu}j^{\nu-n}(2\nu+1)\sum_{p'}j^{-p'}a(m,n,-\mu,\nu,p')\,j_{p'}(kd_{pq})$$
$$\cdot P_{p'}^{m-\mu}(\cos\theta_{pq})e^{j(m-\mu)\phi_{pq}} \qquad r\geq d_{pq} \tag{B-8}$$

B.2 Vector translation addition theorem

To transform the outgoing vector spherical wave functions which are expressed in terms of the spherical coordinates (r_q,θ_q,ϕ_q) into incoming vector spherical wave functions in terms of the coordinates (r_p,θ_p,ϕ_p), we employ the following vector translation addition theorem [27],

$$\overline{M}_{mn}^{(3)}(r_q,\theta_q,\phi_q)=\sum_{\nu=1}^{\infty}\sum_{\mu=-\nu}^{\mu=\nu}[A_{\mu\nu}^{mn}(d_{pq},\theta_{pq},\phi_{pq})\overline{M}_{\mu\nu}^{(1)}(r_p,\theta_p,\phi_p)$$
$$+B_{\mu\nu}^{mn}(d_{pq},\theta_{pq},\phi_{pq})\overline{N}_{\mu\nu}^{(1)}(r_p,\theta_p,\phi_p)\,] \tag{B-9}$$

$$\overline{N}_{mn}^{(3)}(r_q,\theta_q,\phi_q)=\sum_{\nu=1}^{\infty}\sum_{\mu=-\nu}^{\mu=\nu}[A_{\mu\nu}^{mn}(d_{pq},\theta_{pq},\phi_{pq})\overline{N}_{\mu\nu}^{(1)}(r_p,\theta_p,\phi_p)$$
$$+B_{\mu\nu}^{mn}(d_{pq},\theta_{pq},\phi_{pq})\overline{M}_{\mu\nu}^{(1)}(r_p,\theta_p,\phi_p)\,] \tag{B-10}$$

where $A_{\mu\nu}^{mn}$ and $B_{\mu\nu}^{mn}$ are the translation addition theorem coefficients given as

$$A_{\mu\nu}^{mn}(d_{pq},\theta_{pq},\phi_{pq})=(-1)^{\mu}\sum_{p'}a(m,n\mid-\mu,\nu\mid p')\,a(n,\nu,p')$$
$$\cdot h_{p'}^{(1)}(kd_{pq})P_{p'}^{m-\mu}\cos(\theta_{pq})\,e^{j(m-\mu)\phi_{pq}} \tag{B-11}$$

$$B_{\mu\nu}^{mn}(d_{pq},\theta_{pq},\phi_{pq})=(-1)^{\mu+1}\sum_{p'}a(m,n\mid-\mu,\nu\mid p',p'-1)\,b(n,\nu,p')$$
$$\cdot h_{p}^{(1)}(kd_{pq})P_{p'}^{m-\mu}\cos(\theta_{pq})\,e^{j(m-\mu)\phi_{pq}} \tag{B-12}$$

with

$$a(m,n\mid\mu,\nu\mid p')=(-1)^{m+\mu}(2p'+1)\left[\frac{(n+m)!\,(\nu+\mu)!\,(p'-m-\mu)!}{(n-m)!\,(\nu-\mu)!\,(p'+m+\mu)!}\right]^{1/2}$$

$$\cdot \begin{bmatrix} n & \nu & p' \\ m & \mu & -(m+\mu) \end{bmatrix} \begin{bmatrix} n & \nu & p' \\ 0 & 0 & 0 \end{bmatrix} \tag{B-13}$$

$$a(m,n \mid \mu,\nu \mid p',q) = (-1)^{m+\mu}(2p'+1)\left[\frac{(n+m)!\,(\nu+\mu)!\,(p'-m-\mu)!}{(n-m)!\,(\nu-\mu)!\,(p'+m+\mu)!}\right]^{1/2}$$
$$\cdot \begin{bmatrix} n & \nu & p' \\ m & \mu & -(m+\mu) \end{bmatrix} \begin{bmatrix} n & \nu & q \\ 0 & 0 & 0 \end{bmatrix} \tag{B-14}$$

$$a(n,\nu,p') = \frac{j^{\nu-n+p'}}{2\nu(\nu+1)}[2\nu(\nu+1)(2\nu+1) + (\nu+1)(n+\nu-p')(n+p'-\nu+1)$$
$$-\nu(n+\nu+p'+2)(\nu+p'-n+1) \tag{B-15}$$

$$b(n,\nu,p') = -\frac{(2\nu+1)}{2\nu(\nu+1)} j^{\nu+p'-n}[(n+\nu+p'+1)(\nu+p'-n)(n+p'-\nu)(n+\nu-p'+1)]^{1/2} \tag{B-16}$$

and

$$\begin{bmatrix} j_1 & j_2 & j_3 \\ m_1 & m_2 & m_3 \end{bmatrix} \tag{B-17}$$

is the Wigner 3-j symbol [53].

B.3 Asymptotic forms of the addition theorem

For large electrical separation distances between the spheres, the previous addition theorems may reduce to simpler forms which are fast for computations. If the argument $kd_{pq} > 0(p'^2)$ where $p' \le n+\nu$, the Hankel function may reduce to its large argument asymptotic form as

$$h_p^{(1)}(kd_{pq}) \simeq j^{p'-1}\frac{e^{jkd_{pq}}}{kd_{pq}} \tag{B-18}$$

Substituting equation (B-18) into (B-4) leads to the asymptotic form of the scalar addition theorem coefficient, *i.e.*,

$$\alpha_{\mu\nu}^{mn}(d_{pq},\theta_{pq},\phi_{pq}) = (-1)^{\mu} j^{\nu-n}(2\nu+1)\frac{e^{jkd_{pq}}}{jkd_{pq}}\sum_{p'}(-1)^{-p'}a(m,n,-\mu,\nu,p')$$
$$\cdot P_{p'}^{m-\mu}(\cos\theta_{pq})e^{j(m-\mu)\phi_{pq}} \qquad r \le d_{pq} \tag{B-19}$$

Using the identity in (B-6), equation (B-19) reduces to a simpler form, *i.e.*,

$$\alpha_{\mu\nu}^{mn}(d_{pq},\theta_{pq},\phi_{pq}) = (-1)^{\mu} j^{n-\nu-1}(2\nu+1)\frac{e^{jkd_{pq}}}{kd_{pq}} P_n^m(\cos\theta_{pq})$$
$$\cdot P_\nu^{-\mu}(\cos\theta_{pq}) e^{j(m-\mu)\phi_{pq}} \qquad kd_{pq} > 0\,(n+\nu)^2 \qquad \text{(B-20)}$$

While in the case of the vector wave function, the translation coefficients become

$$A_{\mu\nu}^{mn}(d_{pq},\theta_{pq},\phi_{pq}) = (-1)^{\mu} j^{n-\nu-1}\frac{2\nu+1}{2\nu(\nu+1)}\frac{e^{jkd_{pq}}}{kd_{pq}} e^{j(m-\mu)\phi_{pq}} \sum_{p'} a(m,n,-\mu,\nu,p')$$
$$\cdot [\, n(n+1)+\nu(\nu+1)-p'(p'+1)\,] P_{p'}^{m,-\mu}(\cos\theta_{pq}) \qquad \text{(B-21)}$$

To remove the summation from equation (B-21), the following identity is introduced

$$\sum_{p'} [\, n(n+1)+\nu(\nu+1)-p'(p'+1)\,] a(m,n,-\mu,\nu,p') P_{p'}^{m,-\mu} = 2\mu m P_n^m P_\nu^{-\mu}$$
$$-(\nu-\mu)(\nu+\mu+1)P_n^{m+1}P_\nu^{-\mu-1} - (n+m)(n-m+1)P_n^{m-1}P_\nu^{-\mu+1} \qquad \text{(B-22)}$$

Substituting the above relation into equation (B-21), we obtain

$$A_{\mu\nu}^{mn}(d_{pq},\theta_{pq},\phi_{pq}) = (-1)^{\mu} j^{n-\nu-1}\frac{2\nu+1}{2\nu(\nu+1)}\frac{e^{jkd_{pq}}}{kd_{pq}} e^{j(m-\mu)\phi_{pq}} [\, 2\mu m P_n^m(\cos\theta_{pq})$$
$$\cdot P_\nu^{-\mu}(\cos\theta_{pq}) - (\nu-\mu)(\nu+\mu+1)P_n^{m+1}(\cos\theta_{pq}) P_\nu^{-(\mu+1)}(\cos\theta_{pq})$$
$$-(n+m)(n-m+1)P_n^{m-1}(\cos\theta_{pq}) P_\nu^{-\mu+1}(\cos\theta_{pq})] \qquad \text{(B-23)}$$

For higher order expansion of the Hankel function, equation (B-18) becomes

$$h_{p'}^{(1)} \approx j^{-(p'+1)}\frac{e^{jkd_{pq}}}{kd_{pq}} [\, 1 + \frac{j}{2kd_{pq}} p'(p'+1)\,] \qquad \text{(B-24)}$$

With equation (B-24), the final asymptotic form of the scalar addition theorem coefficient may be written as

$$\alpha_{\mu\nu}^{mn}(d_{pq},\theta_{pq},\phi_{pq}) \approx (-1)^{\mu} j^{n-\nu-1}(2\nu+1)\frac{e^{jkd_{pq}}}{kd_{pq}} e^{j(m-\mu)\phi_{pq}}$$
$$\cdot \left[P_n^m P_\nu^{-\mu} + \frac{j}{2kd_{pq}} \{ [\, n(n+1)+\nu(\nu+1)-2\mu m\,] P_n^m P_\nu^{-\mu} \right.$$
$$\left. + (\nu-\mu)(\nu+\mu+1)P_n^{m+1} P_\nu^{-(\mu+1)} + (n+m)(n-m+1)P_n^{m-1} P_\nu^{-\mu+1} \} \right] \qquad \text{(B-25)}$$

APPENDIX C

TRANSLATION ADDITION ALONG THE Z-AXIS

For translation along the z-axis, the coefficient $\alpha_{\mu\nu}^{mn}$ vanishes for all values of μ except for $\mu=m$. Thus equations (B-4) and (B-8) become

$$\alpha_{m\nu}^{mn}(d_{pq}) = (-1)^m j^{\nu-n} (2\nu+1) \sum_{p'} j^{-p'} a(m,n,-m,\nu,p') h_{p'}^{(1)}(kd_{pq}) \quad r \le d_{pq} \tag{C-1}$$

$$\alpha_{m\nu}^{mn}(d_{pq}) = (-1)^m j^{\nu-n} (2\nu+1) \sum_{p'} j^{-p'} a(m,n,-m,\nu,p') j_{p'}^{(1)}(kd_{pq}) \quad r \ge d_{pq} \tag{C-2}$$

While in the case of the vector translation addition theorem along the z-axis, we have

$$\overline{M}_{mn}^{(3)}(r_q,\theta_q,\phi_q) = \sum_{\nu=1}^{\infty} [A_{m\nu}^{mn}(d_{pq}) \overline{M}_{m\nu}^{(1)}(r_p,\theta_p,\phi_p) + B_{m\nu}^{mn}(d_{pq}) \overline{N}_{m\nu}^{(1)}(r_p,\theta_p,\phi_p)] \tag{C-3}$$

$$\overline{N}_{mn}^{(3)}(r_q,\theta_q,\phi_q) = \sum_{\nu=1}^{\infty} [A_{m\nu}^{mn}(d_{pq}) \overline{N}_{m\nu}^{(1)}(r_p,\theta_p,\phi_p) + B_{m\nu}^{mn}(d_{pq}) \overline{M}_{m\nu}^{(1)}(r_p,\theta_p,\phi_p)] \tag{C-4}$$

where $A_{m\nu}^{mn}(d_{pq})$ and $B_{m\nu}^{mn}(d_{pq})$ are the translation coefficients for a separation distance d_{pq} along the z-axis given as

$$A_{m\nu}^{mn}(d_{pq}) = (-1)^m j^{\nu-n} \frac{2\nu+1}{2\nu(\nu+1)} \sum_{p'} j^{-p'} [n(n+1)+\nu(\nu+1)-p'(p'+1)] \cdot a(m,n,-m,\nu,p') h_{p'}^{(1)}(kd_{pq}) \quad r \le d_{pq} \tag{C-5}$$

$$A_{m\nu}^{mn}(d_{pq}) = (-1)^m j^{\nu-n} \frac{2\nu+1}{2\nu(\nu+1)} \sum_{p'} j^{-p'} [n(n+1)+\nu(\nu+1)-p'(p'+1)] \cdot a(m,n,-m,\nu,p') j_{p'}(kd_{pq}) \quad r \ge d_{pq} \tag{C-6}$$

and

$$B_{mn}^{mn}(d_{pq}) = -\frac{jmkd_{pq}}{\nu(\nu+1)} \alpha_{m\nu}^{mn}(kd_{pq}) \tag{C-7}$$

The asymptotic forms of the scalar and vector additions theorems are

$$\alpha_{\mu\nu}^{mn}(d_{pq}) \approx j^{n-\nu-1} (2\nu+1) \frac{e^{jkd_{pq}}}{kd_{pq}} \delta_{m,0} \delta_{\mu,0} \tag{C-8}$$

and

$$A_{\mu\nu}^{mn}(d_{pq}) = -B_{\mu\nu}^{mn}(d_{pq}) \approx j^{n-\nu-1} \frac{2\nu+1}{2\nu(\nu+1)} \frac{e^{jkd_{pq}}}{kd_{pq}} \delta_{m\mu} [\nu(\nu+1)\delta_{m,-1} + n(n+1)\delta_{m,1}]$$

(C-9)

APPENDIX D

ELEMENTS OF THE MATRICES $\bar{A}^s_{pE}, \bar{A}^s_{pM}, \bar{P}_p, \bar{Q}_p, [v_p], [u_p], [A^{pq}], [B^{pq}]$

Elements of the scattered field coefficients column matrices $\bar{A}^s_{PE}$ and $\bar{A}^s_{PM}$ are written as

$$\bar{A}^s_{pE} = \begin{bmatrix} A^s_{pE}(1,m) \\ \cdot \\ \cdot \\ \cdot \\ \cdot \\ \cdot \\ A^s_{pE}(n,m) \end{bmatrix} \tag{D-1}$$

$$\bar{A}^s_{pM} = \begin{bmatrix} A^s_{pM}(1,m) \\ \cdot \\ \cdot \\ \cdot \\ \cdot \\ \cdot \\ A^s_{pM}(n,m) \end{bmatrix} \tag{D-2}$$

For p=1,2,...,N. The elements of the incident field expansion coefficients column matrices $\bar{P}_p$ and $\bar{Q}_p$ are given in the form

$$\bar{P}_p = \begin{bmatrix} P_p(1,m) \\ \cdot \\ \cdot \\ \cdot \\ \cdot \\ \cdot \\ P_p(n,m) \end{bmatrix} \tag{D-3}$$

$$\bar{Q}_p = \begin{bmatrix} Q_p(1,m) \\ \cdot \\ \cdot \\ \cdot \\ \cdot \\ \cdot \\ Q_p(n,m) \end{bmatrix} \tag{D-4}$$

Elements of the diagonal submatrices $[v_p]$ and $[u_p]$ are written in the following form

$$[v_p] = \begin{bmatrix} v_1(\rho_p) & & 0 \\ \vdots & \ddots & \vdots \\ 0 & & v_n(\rho_p) \end{bmatrix} \tag{D-5}$$

$$[u_p] = \begin{bmatrix} u_1(\rho_p) & & 0 \\ \vdots & \ddots & \vdots \\ 0 & & u_n(\rho_p) \end{bmatrix} \tag{D-6}$$

Elements of the submatrices resulting from the translation addition theorem coefficients for the vector wave functions are

$$[A^{pq}] = \begin{bmatrix} A_{m1}^{m1}(d_{pq}) & \cdots & A_{m1}^{mv}(d_{pq}) \\ \vdots & & \vdots \\ A_{mn}^{m1}(d_{pq}) & \cdots & A_{mn}^{mv}(d_{pq}) \end{bmatrix}, \quad p \neq q \tag{D-7}$$

$$[B^{pq}] = \begin{bmatrix} B_{m1}^{m1}(d_{pq}) & \cdots & B_{m1}^{mv}(d_{pq}) \\ \vdots & & \vdots \\ B_{mn}^{m1}(d_{pq}) & \cdots & B_{mn}^{mv}(d_{pq}) \end{bmatrix}, \quad p \neq q \tag{D-8}$$

REFERENCES

[1] G. Mie, Ann. Physik, vol. 22, pp. 377, 1908.

[2] T. B. A. Senior and R. F. Goodrich,"Scattering by a single sphere", Proc. IEE, vol. 3, no. 5, pp. 907-916, May 1964.

[3] J. W. Young and J. C. Bertrand,"Multiple scattering by two conducting circular cylinders", J. Acoust. Soc. Am., vol. 58, pp. 1190-1195, 1975.

[4] A. Z. Elsherbeni and M. Hamid,"Novel cylindrical wave spectrum for analysis of scattering by multiple bodies", IEE Proc., vol. 43 Pt. H, no.1, pp. 35-44, Feb. 1987.

[5] V. Twersky,"On scattering of waves by the infinite grating of circular cylinders", IRE Trans. Antennas and Propagat., vol. AP-10, pp. 737-743. 1962.

[6] H. A. Ragheb and M. Hamid,"Scattering by N parallel conducting circular cylinders", International J. of Electronics, vol. 59, pp. 407-421, 1985.

[7] G. N. Watson, Bessel Functions, Cambridge University Press, London, pp. 359-361, 1948.

[8] V. Twersky,"Multiple scattering of radiation by an arbitrary planar configuration of parallel cylinders and by two parallel cylinders", J. of Appl. Phys., vol. 23, no.4, pp. 407-412, 1952.

[9] R. H. Ragheb,"Simulation of cylindrical reflector antennas", Ph.D. Thesis, Department of Electrical Engineering, University of Manitoba, Winnipeg, Manitoba, Canada, 1987.

[10] V. Twersky,"Multiple scattering of radiation by an arbitrary configuration of parallel cylinders", J. Acoust. Soc. Am., vol. 24, no.1, pp. 42-46, Jan. 1952.

[11] C. Liang and Y. T. Lo,"Scattering by two spheres", Radio Sci., vol. 2, no.1, pp. 1481-1495, 1967.

[12] J. H. Bruning and Y. T. Lo,"Multiple scattering of EM wave by spheres: Parts I and II", IEEE Trans. on Antennas and Propagat., vol. AP-19, pp. 378-400, 1971.

[13] A-K. Hamid, I.R. Ciric, and M. Hamid,"Iterative technique for scattering by a linear array of spheres", Proc. of IEEE AP-S International Symposium, London, Ontario, Canada, June 1991.

[14] A-K. Hamid, I.R. Ciric, and M. Hamid,"Iterative solution of the scattering by an arbitrary configuration of conducting or dielectric spheres", submitted to Proc. IEE Pt. H., 1991.

[15] W. Trinks,"Zur vielfachstreuung an kleinen kugeln", Ann. Phys. (Leipzing), vol. 22, pp. 561-590, 1935.

[16] O. A. Germogenova,"The scattering of a plane electromagnetic wave by two spheres", Izv. Akad. Nauk. SSR. Ser. Geofiz., no.4, pp. 648-635, 1963.

[17] N. Zitron and S. Karp,"Higher order approximations in multiple scattering, I: Two dimensional case", J. Math. Phys., vol. 2, pp. 394-402, 1961.

[18] N. Zitron and S. Karp,"Higher order approximations in multiple scattering, II: Three dimensional case", J. Math. Phys., vol. 2, pp. 402-406, 1961.

[19] V. Twersky,"On multiple scattering of waves", J. Res. Nat. Bur. Stand., vol. 640, no.6, pp. 715-730, 1960.

[20] D. J. Angelakas and K. Kumagai,"High frequency scattering by multiple spheres", IEEE Trans. on Antennas Propagat., vol. AP-12, pp. 105-109, Jan. 1964.

[21] P. Bhartia, R. A. Ross, and M. Hamid,"Ray Optical scattering by two spheres", Archiv. der Elect. Ubertragung., vol. 24, pp. 215-222, 1970.

[22] L. Tsang and J. A. Kong,"Efficient propagation constants for coherent electromagnetic wave propagation in media embedded with dielectric scatterers", J. Appl. Phys., vol. 53, pp. 7162-7173, 1983.

[23] J. F. Hunka and K. K. Mei,"Electromagnetic scattering by two bodies of revolution", Electromagnetics, vol. 1, pp. 329-347, 1981.

[24] J. R. Mautz and R. F. Harrington,"Electromagnetic scattering from a homogeneous material body of revolution", Tech. Report, Department of Electrical and Computer Engineering, Syracuse University, Syracuse, N.Y., 1978.

[25] A. A. Kishk and L. Shafai,"Different formulations for numerical solution of single or multibodies of revolution with mixed boundary conditions", IEEE Trans. on Antennas and Propagat., vol. AP-34, pp. 666-673, 1986.

[26] S. Stein,"Addition theorems for spherical wave functions", Quart. Appl. Math., vol. 19, no. 1, pp. 15-24, 1961.

[27] O. R. Cruzan,"Translation addition theorem for spherical vector wave functions ", Quart. Appl. Math., vol. 20, no. 1, pp. 33-40, 1962.

[28] B. P. Sinha and R. H. MacPhie,"Electromagnetic plane wave scattering by a system of two parallel conducting prolate spheroids", IEEE Trans. Antennas Propagat., vol. AP-31, no. 2, pp. 294-304, 1983.

[29] M. F. R. Cooray and I. R. Ciric,"Electromagnetic wave scattering by a system of two spheroids of arbitrary orientation", IEEE Trans. Antennas Propag., vol. 37, no. 37, 1989.

[30] J. S. Chatterjee and W. F. Croswell,"Waveguide excited dielectric spheres as feeds", IEEE Trans. Antennas Propagat. (commun)., vol. AP-20, pp. 206-208, March 1972.

[31] P. S. Neelakantaswamy and D. K. Banerjee,"Radiation characteristics of a waveguide excited dielectric sphere backed by a metallic hemisphere", IEEE Trans. Antennas Propagat., vol. AP-21, pp. 384-385, May 1973.

[32] A-K. Hamid, I. R. Ciric, and M. Hamid,"Scattering by a system of dielectric spheres", Symposium on Antenna Technology and Applied Electromagnetics (ANTEM), Winnipeg, Manitoba, Canada, August 1990.

[33] A-K. Hamid, I. R. Ciric, and M. Hamid,"Electromagnetic scattering by an arbitrary configuration of dielectric spheres", Can. J. Phys., vol. 68, 1990, pp. 1419-1428.

[34] R. W. P. King and C. W. Harisson,"Scattering by imperfectly conducting spheres", IEEE Trans. Antennas Propagat., vol. AP-19, no. 2, pp. 197-207, March 1971.

[35] S. B. Adler and R. S. Johnson,"New backscattering computation and tables for dielectric and metal spheres", Appl. Optics, vol. 1, no. 5, pp. 655-660, Sept. 1962.

[36] J. R. Mautz and R. Harrington,"Electromagnetic scattering from a homogeneous material body of revolution", Arch. Elek. Ubertragung., vol. 33, pp. 71-80, 1979.

[37] J. A. Stratton, Electromagnetic theory. New York, McGraw Hill, 1946.

[38] A-K. Hamid, I. R. Ciric, and M. Hamid,"Analytic solution of scattering by an array of conducting spheres", Proc. of IEEE AP-S International Symposium and USRI Science Meeting, Dallas, Texas, U.S.A., pp. 1256-1259, May 1990.

[39] A-K. Hamid, I. R. Ciric, and M. Hamid,"Multiple scattering by a linear array of conducting spheres", Can. J. Phys., vol. 68, pp. 1157-1165, 1990.

[40] A-K. Hamid, I. R. Ciric, and M. Hamid,"Radar cross section of an array of dielectric spheres", Symposium on Antenna Technology and Applied Electromagnetics (ANTEM), Winnipeg, Manitoba, Canada, August 1990.

[41] B. P. Sinha and R. H. MacPhie,"Electromagnetic scattering from prolate spheroid for axial incidence", IEEE Trans. Antennas Propagat., vol. AP-23, pp. 676-679, Sept. 1975.

[42] S. N. Karp and A. Russek,"Diffraction by a wide slit", J. Appl. Phys., vol. 27, pp. 886-894, 1956.

[43] A. Z. Elsherbeni,"Diffraction by two conducting wedges", Ph.D. Thesis, Department of Electrical Engineering, University of Manitoba, Winnipeg, Manitoba, Canada, 1986.

[44] J. Bruning and Y. T. Lo,"Electromagnetic scattering by two spheres", Proc. of IEEE, vol. 57, pp. 119-120, 1968.

[45] P. Bhartia,"Scattering by imperfectly conducting bodies", Ph.D. Thesis, Department of Electrical Engineering, University of Manitoba, Winnipeg, Manitoba, Canada, 1971.

[46] A-K. Hamid, I. R. Ciric, and M. Hamid,"Scattering by systems of small conducting spheres", Proc. of Progress In Electromagnetics Research Symposium (PIERS 91), Cambridge, Massachusetts, U.S.A., July 1991.

[47] A-K. Hamid, I. R. Ciric, and M. Hamid,"Backscattering cross section of many-sphere systems", Proc. of Progress In Electromagnetics Research Symposium (PIERS 91), Cambridge, Massachusetts, U.S.A., July 1991.

[48] A-K. Hamid, I. R. Ciric, and M. Hamid,"Scattering from two conducting spheres covered with a dielectric layer", Proc. of the Seventh IEE International Conference on Antennas and Propagation (ICAP 91), University of York, U.K., April 1991.

[49] A. L. Aden and M. Kerker,"Scattering of electromagnetic waves from two concentric spheres", J. Appl. Phys., vol. 22, pp. 1242-1246, 1951.

[50] H. Scharfman,"Scattering from dielectric coated spheres in the region of first resonance", J. Appl. Phys., vol. 25, pp. 1352-1356, 1954.

[51] B. Friedman and J. Russek,"Addition theorems for spherical waves", Quart. Appl. Math., vol. 12, no. 1, pp. 13-23, April 1954.

[52] J. Bruning and Y. T. Lo,"Multiple scattering by spheres", Tech. Report, Antenna Lab., University of Illinois, Urbana, Illinois, U.S.A., 1969.

[53] A. R. Edmonds, Angular Momentum in Quantum Mechanics. Princeton University Press, Princeton, N.J., U.S.A., 1957.